CENTRO DE INVESTIGACIÓN Y DE ESTUDIOS AVANZADOS

DEL INSTITUTO POLITÉCNICO NACIONAL

UNIDAD ZACATENCO

DEPARTAMENTO DE CONTROL AUTOMÁTICO

Controlador Adaptable Neuro-Difuso para el Seguimiento de Trayectorias de un Vehículo Submarino Autónomo

Tesis que presenta

Jorge Said Cervantes Rojas

Para obtener el grado de

Doctor en Ciencias

En la especialidad de

Control Automático

Directores de tesis:

Dr. Wen Yu Liu

Dr. Sergio Rosario Salazar Cruz

Ciudad de México **Diciembre 2016**

Contents

List of Figures

Abstract

The problem of control uncertain nonlinear systems is a widely studied problem in modern control theory. This kind of problem considers parameter uncertainties, non-modeled dynamics and external disturbances in the system structure. In this thesis this control problem is solved applying an adaptive approach in order to identify the uncertainties of the nonlinear system by using Takagi-Sugeno (T-S) fuzzy modeling and differential neural network (DNN) theory. In consequence, an adaptive controller based on neuro-fuzzy identifier of the nonlinear system can be designed. Finally in order to validate the proposed algorithms in this study an Autonomous Underwater Vehicle (AUV) system is used to reach a desired trajectory. In the AUV control field the most common problems treated are: vertical and horizontal plane control, position and attitude control, trajectory tracking and path following control. The trajectory tracking control refers to the problem of steering a vehicle to follow a given route. In general this problem are not easy to solve because of the highly nonlinear dynamic behaviour of the vehicle, uncertainties in hydrodynamic coefficients and unknown disturbances caused by ocean waves and currents.

Resumen

El problema de controlar sistemas nolineales inciertos ha sido ampliamente estudiado in la teoría de control moderna. Este tipo the problema considera incertidumbres paramétricas, dinámicas no modeladas y perturbaciones externas en la estructura del sistema. En esta tésis este problema de control es resuelto aplicando un enfoque adaptable para poder identificar las incertidumbres del sistema nolineal usando modelado difuso Takagi-Sugeno (T-S) y la teoría de redes neuronales diferenciales (DNN por sus siglas en inglés). En consecuencia, un identificador adaptable neurodifuso del sistema nolineal puede ser diseñado. Finalmente, para poder validar los algoritmos propuestos en esta tésis, un vehículo submarino autónomo (AUV por sus siglas en inglés) es usado para seguir una trayectoria deseada. En el campo del control de vehiculos submarinos los problemas mas comúnes tratados son: control en el plano vertical y horizontal, control de posición y orientación, control de seguimiento de trayectorias y control the seguimiento de una vía. El control de seguimiento de trayectorias se refiere al problema de direccionar un vehículo para seguir una ruta desada. En general este problema no es fácil de resolver debido al comportamiento dinámico altamente nolineal del vehiculo, incertidumbres en los coeficientes hidrodinámicos y perturbaciones desconocidas causadas por olas y corrientes oceánicas.

1

Introduction

The problem of control uncertain nonlinear systems is a widely studied problem in modern control theory [Jain and Bhasin, 2015], [Esfandiari et al., 2015], [Kim, 2015], [Buciakowski et al., 2015], [Teodorescu and Vandenplas, 2015], [Chen and Ge, 2015], [Chen et al., 2016]. This kind of problem considers parameter uncertainties, nonmodeled dynamics and external disturbances in the system structure. In this thesis, this control problem is solved applying an adaptive approach in order to identify the uncertainties of the nonlinear system by using Takagi-Sugeno (T-S) fuzzy modeling [Cao et al., 1997], [Joh et al., 1998], [Li and Li, 2004], [Lin et al., 2004] and differential neural network (DNN) theory [Chairez, 2013b], [Chairez, 2013a], [Viana and Chairez, 2010]. In consequence, an adaptive controller based on neuro fuzzy-identifier of the non-linear system can be designed. Regarding the controller robustness, this is included in the design by considering the worst case of perturbations effect. Finally in order to validate the proposed algorithms in this study an Autonomous Underwater Vehicle (AUV) system is used to reach a desired trajectory.

1.1 Motivation

The identification problem incorporated in feedback control of uncertain nonlinear systems exhibiting complex behaviour has been solved in different ways. Some of these solutions have used artificial intelligence methods like fuzzy logic and neural networks. Two main ideas are proposed in this work in order to solve the cited problem. First, the control problem of the uncertain system by doing an on-line identification procedure based on a standard T-S fuzzy inference system to approximate the uncertainties of the nonlinear dynamics is carried out. However, the individual implementation of the T-S systems suffers from certain drawbacks, such as the problem of finding suitable membership functions for fuzzy systems and the corresponding set of matrices A_i, B_i for the $i-th$ consequent local linear system. These weaknesses can be avoided by implementing a hybrid structure combining fuzzy and neural network approaches, the so-called neuro-fuzzy systems. So, a second part of this work is devoted to a neuro-fuzzy system identification methodology that implements differential neural networks as consequences of T-S fuzzy inference rules. The DNNs substitute the local linear systems that are used in the common T-S method to approximate the uncertain nonlinear system dynamics. In this thesis, DNNs are used to provide an effective tool for dealing with the identification of the uncertain nonlinear system while the T-S rules is used to provide the framework of previous knowledge of the system. The main idea is to carry out an on-line identification process of an uncertain nonlinear system with the aim to design a close-loop adaptive trajectory tracking controller.

1.2 Objectives

Within the scope of this investigation work the following particular objectives are stated:

- Trajectory tracking of an uncertain system using a T-S fuzzy identifier to design a controller assuming the state is available,

- Trajectory tracking of an uncertain system using a T-S neuro-fuzzy identifier to design a controller assuming the state is available,

- Trajectory tracking of an uncertain system using a neuro-fuzzy identifier to design a controller assuming the state is not available,

- Design and construction of an AUV experimental platform,

- Trajectory tracking of a 2 dimension route using the real-time AUV platform applying a proportional derivative controller.

1.3 Antecedents of Autonomous Underwater Vehicles

An autonomous underwater vehicle (AUV) is a robot which moves underwater without an operator command. Autonomous underwater vehicles (AUVs) are equipped with an embedded electronic system composed by a computer and an independent power source. In the literature this type of vehicles are also known as Remotely Operated Vehicles (ROVs), Unmanned Underwater Vehicles (UUVs), etc. The main advantage of an AUV is that it does not need a human operator to execute underwater maneuvers. This characteristic make AUVs suitable to work in conditions where humans cannot effectively complete difficult tasks or represents dangerous risks [Smallwood and Whitcomb, 2004], [Horgan and Toal, 2006], [Gaccia and Veruggio, 2000].

The United States Navy [Wernli, 2001] built an underwater device in the 1960's which was required to perform deep sea rescue and salvage operations. In the next decade, the government and some universities performed their own research with AUVs producing significant advances in the following years. The last AUV technology studies motivate the oil and gas industrial sector to implement underwater vehicles for the development of off shore oil fields [Williams, 2004]. In the 1980's, AUVs was built to

dive to depths greater than the limits reached by a deep diver. However, due to a global depression occurred in the middle of the decade that affected the oil industry the AUV development remained without progress the following years. Once again in the 90's decade, a new interest arised about AUV systems in the academic research. That was reflected in the development of new designs of AUVs by many universities. The previous research culminated in the construction of the first commercial AUVs in 2000 [von Alt, 2003], [Blidberg, 2001]. From this moment, AUVs have been developed rapidly [Smallwood et al., 1999], [Griffiths and Edwards, 2003]. Nowadays AUVs are being used for a large number of applications, for example locating ship wrecks like the Titanic [Ballard, 1987], mapping the sea floor [Tivey et al., 1998]. Other applications consist of object tracing [Kondoa and Ura, 2004], monitoring harbours, searching for sea mines [Willcox et al., 2001], and scientific projects [Curtin and Bellingham, 2001], [Rife and Rock, 2002], [Lygouras et al., 1998]. Recently, battery design development have helped to increment the time AUVs can be autonomously be sourced [Wilson and Bales, 2006]. Also new advanced technologies have improved the efficiency on the AUVs. From a technological point of view, the development of algorithms to automate an underwater vehicle also have had a progress over the years.

In the AUV control field the most common problems treated are: vertical and horizontal plane control, position and attitude control, trajectory tracking and path following control [Nakamura and Savant, 1992], [Egeland and Dalsmo, 1996], [Kinsey and Whitcomb, 2007], [Husa and Fossen, 1997], [Refsnes et al., 2008], [Aguiar and Pascoal, 2007]. The trajectory tracking control refers to the problem of steering a vehicle to follow a given route. In general, this problem are not easy to solve because of the highly nonlinear dynamic behaviour of the vehicle, uncertainties in hydrodynamic coefficients and unknown disturbances caused by ocean waves and currents.

Recent research in order to solve the trajectory tracking problem for AUVs applying advanced control techniques has been developed, for example: sliding mode con-

trol [Elmokadem et al., 2015], [Joe et al., 2014], nonlinear control [Bian et al., 2010], [He-ming et al., 2012], adaptive control [Kumar and Subudhi, 2014], [Rezazadegan and Shojaei, 2013], neural network control [Eski and Yildirim, 2014], [Wang and Wang, 2014], fuzzy control [Lakhekar and Waghmare, 2015], [Raimondi and Melluso, 2010].

1.4 Contributions

In this work we deal with the problem of control uncertain nonlinear systems in order to solve the trajectory tracking problem. This objective was achieved by combining Takagi-Sugeno fuzzy approach and Lyapunov stability theory.

The existence of a non conventional time-varying Lyapunov function was demonstrated in order to prove the ultimate boundedness of the tracking error between the Takagi-Sugeno representation and a reference system.

The controller design was proposed to rely on the existence of a set of Riccati differential equations and sufficient conditions were obtained to assure their positive definite solutions.

In order to analyse a control problem based on output information, a T-S fuzzy controller-observer system was studied whose solution is also based on Riccati differential equations.

A methodology to design an adaptive neuro-fuzzy scheme was proposed two accomplish identification and tracking control of uncertain nonlinear systems. This structure mixed the use of differential neural networks and Takagi-Sugeno inference rules. A set of continuous neural networks was used to approximate the dynamics of each subsystem. A controlled Lyapunov function was proposed to prove the ultimate bounded state equilibrium point for the tracking error dynamics. The same Lyapunov function was used to design the laws that adjust the weights of each neural network. This kind of solution is rarely explored and offered superior performance that linear Parallel

Distributed Compensation controller without adaptation.

Numerical simulations was carried out considering several models of an autonomous underwater vehicle.

A controller based output information for tracking a desired reference by an autonomous underwater vehicle was designed using the backstepping approach. The yaw rate was used to modify the x-y position of the vehicle. This controller was implemented using the velocity displacement provided by a super-twisting observer. Applying a set on robust exact differentiators was possible to recover the velocities using the position information of the vehicle. Obtaining better tracking error convergence results with less energy than a conventional PD controller.

Also, an experimental platform was built in order to validate the effectiveness of the proposed controllers.

1.5 Structure

In Chapter 2 a methodology to design a Takagi-Sugeno tracking controller using Riccati Differential Equations is presented. In chapter 3 a Takagi-Sugeno fuzzy control using based on Differential Neural Networks as approximators of the uncertain nonlinear system was introduced. In chapter 4 a methodology to design a tracking controller using Riccati Differential Equations considering only the system output information is designed. In chapter 5 an feedback controller using backstepping approach and a super-twisting estimator is designed. In chapter 5 the experimental platform used for real-time experiments was described.

2

Autonomous underwater vehicle modeling

This chapter is devoted to derive the AUV models used as an object of study in simulation results in the following chapters. The nonlinear models are simplifications of the general AUV model presented in [Fossen, 2002] which embrace the main nonlinearities that describes the dynamic behaviour of a vehicle travelling underwater.

2.1 Body frame 3-DOF AUV model

The AUV shown in Fig. 3.4 is equipped with two propellers to control the vehicle in x-y positions. In order to obtain a model of this AUV, two frames: the inertial reference frame X_I-Y_I, and the body frame X_B-Y_B are defined. The origin of the body frame is chosen as the center of gravity of the AUV. In the inertial reference frame, X_B can be regarded as longitudinal axis (from aft to fore), Y_B is regarded as transversal axis (starboard direction).

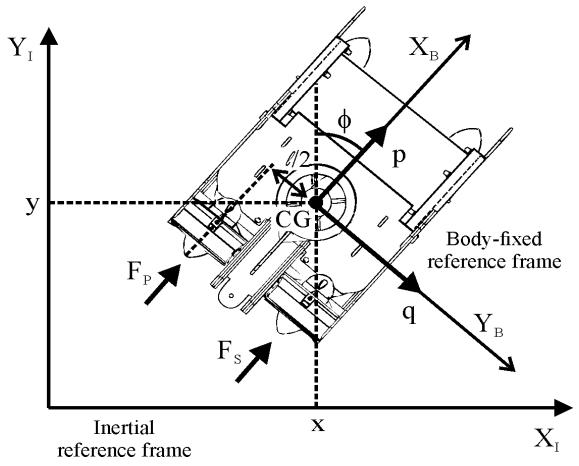

Figure 2.1: AUV coordinate system.

The body-frame nonlinear model for an underactuated AUV in the horizontal plane with two independent propellers is obtained by simplifying the surface vessel model presented in [Pettersen, 1996]. It can be noticed that F_p (N) is the port thrust, F_s is the starboard thrust (N), $X = F_p + F_s$ (N) is the total force along X_B axis and $N = (F_p - F_s)l$ (Nm) is the torque about Z_B axis. The simplified equations of motion are:

$$M\dot{\chi}(t) + C(\chi(t))\chi(t) + D(\chi(t))\chi(t) = \tau(t)$$

where

$$M = \begin{bmatrix} m_{11} & 0 & 0 \\ 0 & m_{22} & m_{23} \\ 0 & m_{32} & m_{33} \end{bmatrix}, C(\chi) = \begin{bmatrix} 0 & 0 & -f(q,w) \\ 0 & 0 & m_{11}p \\ f(q,w) & -m_{11}p & 0 \end{bmatrix},$$

$$D(\chi) = \begin{bmatrix} -X_p & 0 & 0 \\ 0 & -Y_p & -Y_w \\ 0 & -N_q & -N_w \end{bmatrix}, \tau = \begin{bmatrix} \tau_p \\ 0 \\ \tau_w \end{bmatrix},$$

$f(q,w) = m_{23}w + m_{22}q$, M is the inertia matrix. $C(\chi)$ is the Coriolis and centripetal matrix. $D(\chi)$ is the damping matrix, $\chi = [p, q, w]^\top$ is the velocity vector. p, q are linear velocities (m/s) in X_B axis and Y_B axis, respectively, w is the angular velocity (rad/s) about the vertical axis Z_B, ϕ is the yaw angle (grades) in the inertial reference frame

$X_I - Y_I$, τ is the force and torque vector, $\tau_p = F_p + F_s$ is the total force along to X_B-axis, $\tau_w = (F_p - F_s)\, l$ is the torque about Z_B axis, F_p is the port thrust, F_s is the starboard thrust, and ξ are perturbations affecting the model, for example, environmental disturbances presented in [Fossen, 2002]. As in [Fantoni and Lozano, 2002], [Pettersen and Nijmeijer, 1998b] and [Pettersen and Nijmeijer, 1998a], we have neglected hydrodynamic damping (which is not essential in controlling the system), considering that the shape of the AUV is a disc and the propellers are located at the center of mass. In order to obtain the essential nonlinearities of the AUV, we assumed the inertia matrix to be diagonal and equal to the identity matrix. Then the simplified dynamic equations with respect to the body frame are given by

$$\begin{aligned} \frac{d}{dt} p(t) &= q(t)\, w(t) + \tau_p(t) + \xi(t) \\ \frac{d}{dt} q(t) &= -p(t)\, w(t) \\ \frac{d}{dt} w(t) &= \tau_w(t) \end{aligned} \tag{2.1}$$

Also, Eq. (2.1) can be represented in a vector form

$$\frac{d}{dt}\chi(t) = f(\chi(t)) + B\tau(t) + \zeta(t) \tag{2.2}$$

where $f(\chi(t)) = \begin{bmatrix} q(t)\, w(t) \\ -p(t)\, w(t) \\ 0 \end{bmatrix}$, $B = \begin{bmatrix} 1 & 0 \\ 0 & 0 \\ 0 & 1 \end{bmatrix}$, $\zeta(t) = \begin{bmatrix} \xi(t) \\ 0 \\ 0 \end{bmatrix}$.

2.2 Body frame 3-DOF AUV model with output information

In this section the 3-DOF AUV model presented in Section 2.1 considering output information is introduced. The differential equations are the following:

$$\begin{aligned} \frac{d}{dt}p\left(t\right) &= q\left(t\right)w\left(t\right) + \tau_p\left(t\right) + \xi\left(t\right) \\ \frac{d}{dt}q\left(t\right) &= -p\left(t\right)w\left(t\right) \\ \frac{d}{dt}w\left(t\right) &= \tau_w\left(t\right) \\ y &= \left[q\ w\right]^\top \end{aligned} \tag{2.3}$$

where $y = [q, w]^\top$ is the output vector. The variables in Eq. 2.3 are the same defined in Section 2.1. Then, Eq. (2.3) can be represented in a vector form

$$\begin{aligned} \frac{d}{dt}\chi\left(t\right) &= f\left(\chi\left(t\right)\right) + B\tau\left(t\right) + \zeta\left(t\right) \\ y &= C\chi \end{aligned} \tag{2.4}$$

where $C = \begin{bmatrix} 0 & 1 & 0 \\ 0 & 0 & 1 \end{bmatrix}$

2.3 Earth frame 4-DOF AUV model

In this section, the dynamic equations of motion of an AUV equipped with five propellers: port, starboard, 2× horizontal and vertical thrusters are described. The forces and moments acting on the AUV in three dimensions and two reference frames: Earth-fixed (X_E, Y_E, Z_E), and Body-fixed (X_B, Y_B, Z_B) are presented in Fig. 2.2.

Considering the motion of the AUV in 6-DOF, the following vector is defined

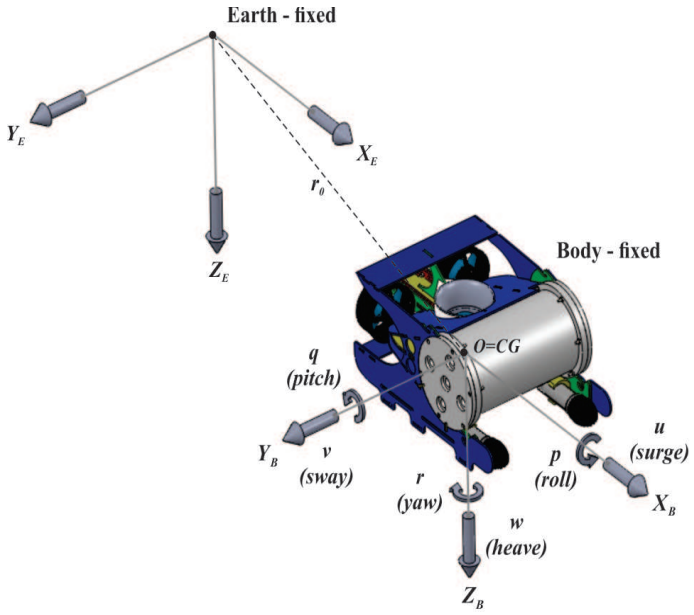

Figure 2.2: The underactuated AUV model in plane motion. Body-fixed [B] and Earth-fixed [E] reference frames.

[Fossen, 2002]:

$$\upsilon = [u, v, w, p, q, r]^\top, \quad \tau = [X, Y, Z, K, M, N]^\top$$

where υ is the velocity vector in the Body-fixed frame; u, v and w denote linear velocities of the AUV; p, q, r are angular velocities; τ is the vector of forces and moments acting on the AUV in the Body-fixed frame. X, Y, Z are forces in surge, sway and heave direction, respectively; additionally K, M, N denote torsion moments of roll, pitch and yaw, respectively. After a regular procedure of modeling [Fossen, 2002], the nonlinear dynamic equations to described the AUV behaviour as the solution of the second order system is presented as:

$$\begin{gathered} M\left(\eta\left(t\right)\right)\frac{d^2}{dt}x\left(t\right) + C\left(\eta\left(t\right), \frac{d}{dt}\eta\left(t\right)\right)\frac{d}{dt}\eta\left(t\right) + D\left(\eta\left(t\right), \frac{d}{dt}\eta\left(t\right)\right)\frac{d}{dt}\eta\left(t\right) + \\ g\left(\eta\left(t\right)\right) = \tau\left(t\right) + \tau_E\left(t\right) \end{gathered} \tag{2.5}$$

$$\frac{d}{dt}\eta\left(t\right) = J(\eta\left(t\right))\nu\left(t\right)$$

where $\eta = [x, y, z, \phi, \theta, \psi]^\top$ denotes the position and orientation vector with coordinates in the Earth-fixed reference frame, x, y, z (meters) are linear positions in X_E axis, Y_E axis and Z_E axis, respectively. ϕ, θ, ψ (radians) are angular positions with respect to X_E axis, Y_E axis and Z_E axis, respectively. In Eq, (2.5), the parameter $M : \mathbb{R}^6 \to \mathbb{R}^{6\times6}$ is the inertia matrix including the added mass, $C : \mathbb{R}^6 \to \mathbb{R}^{6\times6}$ is the matrix of Coriolis an centripetal terms including the added mass, $D : \mathbb{R}^6 \to \mathbb{R}^{6\times6}$ is the hydrodynamic damping matrix and $g : \mathbb{R}^6 \to \mathbb{R}^6$ is the forces and moments vector, $J : \mathbb{R}^6 \to \mathbb{R}^{6\times6}$ is the velocity transformation between the velocity represented in Body-fixed coordinates and the Earth-fixed coordinates. This transformation matrix is defined in the same reference.

Then the velocity matrix transformation $J(\cdot)$ [Fossen, 2002] between Body-fixed and Earth-fixed coordinate systems is

$$J(\eta_2) = \begin{bmatrix} R_{B\to E}(\eta_2) & 0_{3\times3} \\ 0_{3\times3} & T(\eta_2) \end{bmatrix}$$

where $R_{B\to E}(\eta_2)$ is the coordinate transformation matrix constructed by using the yaw-pitch-roll convention, i.e., $R_{B\to E}(\eta_2) = R_{z,\psi}R_{y,\theta}R_{x,\phi}$.

$$R_{B\to E}(\eta_2) = \begin{bmatrix} c\theta c\psi & s\phi s\theta c\psi - c\phi s\psi & c\phi s\theta c\psi + s\phi s\psi \\ c\theta s\psi & c\phi c\psi + s\phi s\theta s\psi & c\phi s\theta s\psi - s\phi c\psi \\ -s\theta & c\theta s\phi & c\phi c\theta \end{bmatrix}$$

and $T(\eta_2)$ is the angular velocity transformation between the Body-fixed and Earth-fixed coordinate

$$T(\eta_2) = \begin{bmatrix} 1 & s\phi t\theta & c\phi t\theta \\ 0 & c\phi & -s\phi \\ 0 & \frac{s\phi}{c\theta} & \frac{c\phi}{c\theta} \end{bmatrix}$$

where $s(\cdot) = sin(\cdot)$, $c(\cdot) = cos(\cdot)$, $t(\cdot) = tan(\cdot)$.

The disturbances affecting the model, for example, environmental disturbances presented in [Fossen, 2002, Perez, 2005], are represented by τ_E.

In order to apply the controller proposed in this study, the AUV dynamics can be simplified considering the following assumptions [Fossen, 2002]:

A1. Relative low speed,

A2. AUV symmetry about the three planes,

A3. The aligning moment ensures horizontal stability, then roll and pitch movement are neglected, i.e., $\phi, \theta \approx 0$,

A4. The Body-fixed frame is positioned at the center of gravity, $r_G = [0, 0, 0]^\top$.

Based on these assumptions, the following equations describing the movement dynamics of the fully actuated AUV with respect to the Earth-fixed reference frame can be obtained.

The equation used to describe the dynamics of x is

$$\begin{aligned}\frac{d^2}{dt}x(t) = \{c_1\cos^2\psi(t) + c_2\sin^2\psi(t)\}\frac{d}{dt}x(t) + \\ \{c_1\cos\psi(t)\sin\psi(t) - c_2\sin\psi(t)\cos\psi(t) - \frac{d}{dt}\psi(t)\}\frac{d}{dt}y(t) + \\ \{c_3[\frac{d}{dt}x(t)\sin\psi(t)\cos\psi(t) - \frac{d}{dt}y(t)\cos^2\psi(t)] + \\ c_4[\frac{d}{dt}x(t)\sin\psi(t)\cos\psi(t) + \frac{d}{dt}y(t)\sin^2\psi(t)]\}\frac{d}{dt}\psi(t) + \\ c_5X(t)\cos\psi(t) + c_5\tau_{E_1}(t)\cos\psi(t) - c_6\tau_{E_2}(t)\sin\psi(t)\end{aligned} \tag{2.6}$$

The corresponding nonlinear equation for the dynamic equation of y is given by

$$\begin{aligned}\frac{d^2}{dt}y(t) = \{\frac{d}{dt}\psi(t) + c_1\sin\psi(t)\cos\psi(t) - c_2\cos\psi(t)\sin\psi(t)\}\frac{d}{dt}x(t) + \\ \{c_1\sin^2\psi(t) + c_2\cos^2\psi(t)\}\frac{d}{dt}y(t) + \\ \{c_3[\frac{d}{dt}x(t)\sin^2\psi(t) - \frac{d}{dt}y(t)\sin\psi(t)\cos\psi(t)] - \\ c_4[\frac{d}{dt}y(t)\sin\psi(t)\cos\psi(t) + \frac{d}{dt}x(t)\cos^2\psi(t)]\}\frac{d}{dt}\psi(t) + \\ c_5X(t)\sin\psi(t) + c_5\tau_{E_1}(t)\sin\psi(t) + c_6\tau_{E_2}(t)\cos\psi(t)\end{aligned} \tag{2.7}$$

In the coordinate z, the nonlinear equation satisfy the following structure

$$\frac{d^2}{dt}z\left(t\right)=c_7\frac{d}{dt}z\left(t\right)+c_8+c_9Z\left(t\right)+c_9\tau_{E_3}\left(t\right) \tag{2.8}$$

In the angular velocity variable ψ, the associated nonlinear equation is

$$\begin{gathered}\frac{d^2}{dt}\psi\left(t\right)=\{c_{10}[\frac{d}{dt}x\left(t\right)\sin\psi\left(t\right)\cos\psi\left(t\right)-\frac{d}{dt}y\left(t\right)\cos^2\psi\left(t\right)]+\\ c_{11}[\frac{d}{dt}x\left(t\right)\sin\psi\left(t\right)\cos\psi\left(t\right)+\frac{d}{dt}y\left(t\right)\sin^2\psi\left(t\right)]\}\frac{d}{dt}x\left(t\right)+\\ \{c_{10}[\frac{d}{dt}x\left(t\right)\sin^2\psi\left(t\right)-\frac{d}{dt}y\left(t\right)\sin\psi\left(t\right)\cos\psi\left(t\right)]-\\ c_{11}[\frac{d}{dt}y\left(t\right)\sin\psi\left(t\right)\cos\psi\left(t\right)+\frac{d}{dt}x\left(t\right)\cos^2\psi\left(t\right)]\}\frac{d}{dt}y\left(t\right)+\\ c_{12}\frac{d}{dt}\psi\left(t\right)+c_{13}N\left(t\right)+c_{13}\tau_{E_6}\left(t\right)\end{gathered} \tag{2.9}$$

The nonlinear terms describing the effect of uncertainties on the AUV dynamics are:

$$c_1=\frac{\tau_{D_x}}{m-X_{\dot{u}}},c_2=\frac{\tau_{D_y}}{m-Y_{\dot{v}}},c_3=\frac{Y_{\dot{v}}-m}{m-X_{\dot{u}}},$$

$$c_4=\frac{m-X_{\dot{u}}}{m-Y_{\dot{v}}},c_5=\frac{1}{m-X_{\dot{u}}},c_6=\frac{1}{m-Y_{\dot{v}}},$$

$$c_7=\frac{\tau_{D_z}}{m-Z_{\dot{w}}},c_8=\frac{F_{WB}}{m-Z_{\dot{w}}},c_9=\frac{1}{m-Z_{\dot{w}}},$$

$$c_{10}=\frac{m-Y_{\dot{v}}}{I_z-N_{\dot{r}}},c_{11}=\frac{X_{\dot{u}}-m}{I_z-N_{\dot{r}}},c_{12}=\frac{\tau_{D_\psi}}{I_z-N_{\dot{r}}},c_{13}=\frac{1}{I_z-N_{\dot{r}}}$$

where m is the vehicle mass, $F_{WB}=W-B\ (N)$ is the difference of buoyancy (B) and gravity (W) forces in the Z_B-axis (this AUV has positive buoyancy, i.e., $B>W$), τ_{D_x}, τ_{D_y}, τ_{D_z} (kg/m) and τ_{D_ψ} $(kg\ m^2/rad^2)$ are elements of the hydrodynamic damping matrix, $X_{\dot{u}}$, $Y_{\dot{v}}$, $Z_{\dot{w}}$ (kg) and $N_{\dot{r}}$ $(kg\ m^2/rad)$ are elements of the added mass inertia matrix and I_z is the inertial tensor about the Z_B-axis.

2.4 Fully-actuated earth frame 4-DOF AUV model

In this section a variation of the model treated in Section 2.3 adding two horizontal thrusters are described. The forces and moments acting on the AUV in three dimensions and two reference frames: Earth-fixed (X_E, Y_E, Z_E), and Body-fixed (X_B, Y_B, Z_B) are presented in Fig. 2.3.

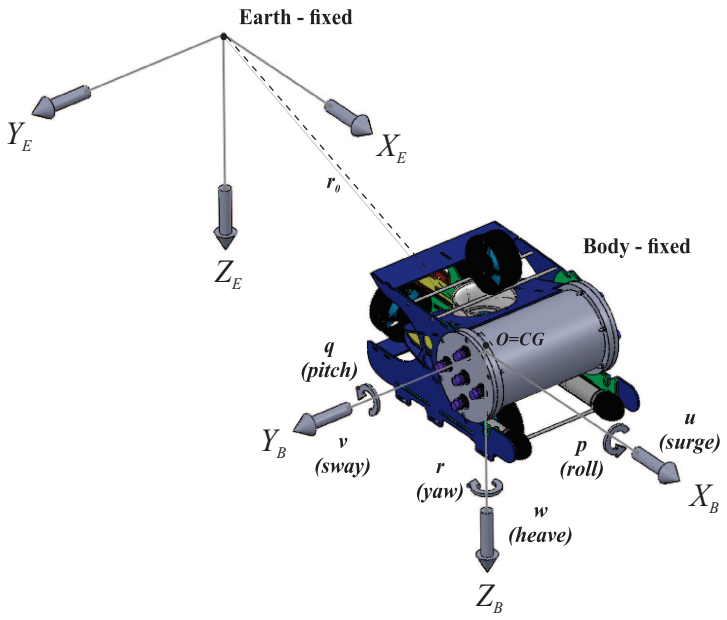

Figure 2.3: The fully actuated AUV model in plane motion. Body-fixed [B] and Earth-fixed [E] reference frames.

The difference respect to the model presented in Section 2.3 is we considered a fully-actuated AUV model, that is the control vector is defined as $\tau = [X, Y, Z, N]^\top$ where Y is a force is sway direction. The same procedure to obtain the dynamic equations as in Section 3 is carried out. The equations are the same as in the under-actuated case of previous section, only the dynamic equations in x and y are modified as follows:

The equation used to describe the dynamics of x is

$$\begin{aligned}
\frac{d^2}{dt}x\left(t\right) &= \{c_1\cos^2\psi\left(t\right)+c_2\sin^2\psi\left(t\right)\}\frac{d}{dt}x\left(t\right)+\\
&\{c_1\cos\psi\left(t\right)\sin\psi\left(t\right)-c_2\sin\psi\left(t\right)\cos\psi\left(t\right)-\frac{d}{dt}\psi\left(t\right)\}\frac{d}{dt}y\left(t\right)+\\
&\{c_3[\frac{d}{dt}x\left(t\right)\sin\psi\left(t\right)\cos\psi\left(t\right)-\frac{d}{dt}y\left(t\right)\cos^2\psi\left(t\right)]+\\
&c_4[\frac{d}{dt}x\left(t\right)\sin\psi\left(t\right)\cos\psi\left(t\right)+\frac{d}{dt}y\left(t\right)\sin^2\psi\left(t\right)]\}\frac{d}{dt}\psi\left(t\right)+\\
&c_5X\left(t\right)\cos\psi\left(t\right)-c_6Y\left(t\right)sin\psi\left(t\right)+c_5\tau_{E_1}\left(t\right)\cos\psi\left(t\right)-c_6\tau_{E_2}\left(t\right)\sin\psi\left(t\right)
\end{aligned} \tag{2.10}$$

The corresponding nonlinear equation for the dynamic equation of y is given by

$$\begin{aligned}
\frac{d^2}{dt}y\left(t\right) &= \{\frac{d}{dt}\psi\left(t\right)+c_1\sin\psi\left(t\right)\cos\psi\left(t\right)-c_2\cos\psi\left(t\right)\sin\psi\left(t\right)\}\frac{d}{dt}x\left(t\right)+\\
&\{c_1\sin^2\psi\left(t\right)+c_2\cos^2\psi\left(t\right)\}\frac{d}{dt}y\left(t\right)+\\
&\{c_3[\frac{d}{dt}x\left(t\right)\sin^2\psi\left(t\right)-\frac{d}{dt}y\left(t\right)\sin\psi\left(t\right)\cos\psi\left(t\right)]-\\
&c_4[\frac{d}{dt}y\left(t\right)\sin\psi\left(t\right)\cos\psi\left(t\right)+\frac{d}{dt}x\left(t\right)\cos^2\psi\left(t\right)]\}\frac{d}{dt}\psi\left(t\right)+\\
&c_5X\left(t\right)\sin\psi\left(t\right)+c_6Y\left(t\right)cos\psi\left(t\right)+c_5\tau_{E_1}\left(t\right)\sin\psi\left(t\right)+c_6\tau_{E_2}\left(t\right)\cos\psi\left(t\right)
\end{aligned} \tag{2.11}$$

2.5 Earth frame 2-DOF AUV lateral model

In this section, a simplification of the model treated in Section 2.3 considering only the x-z movement is described. The forces acting on the AUV in two dimensions and two reference frames: Earth-fixed (X_E, Z_E), and Body-fixed (X_B, Z_B) are presented in Fig. 2.4.

This AUV model is fully actuated, that is the control vector is defined as $\tau = [X, Z]^\top$. The dynamic equations of the AUV lateral model are The equation used to describe the dynamics of x is

$$\frac{d^2}{dt}x\left(t\right) = c_1\frac{d}{dt}x\left(t\right)+c_5X\left(t\right)+c_5\tau_{E_1}\left(t\right) \tag{2.12}$$

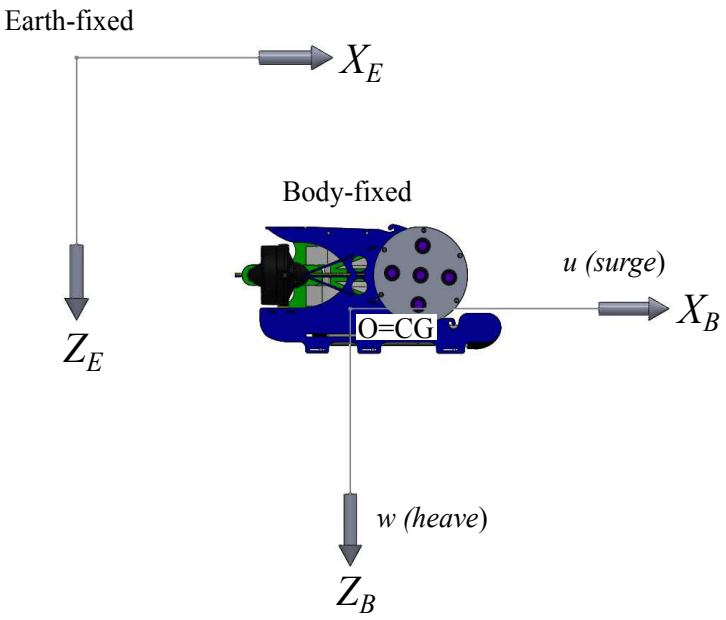

Figure 2.4: The AUV in lateral motion. Body-fixed and Earth-fixed reference frames.

The equation used to describe the dynamics of z is

$$\frac{d^2}{dt}z\left(t\right) = c_7\frac{d}{dt}z\left(t\right) + c_8 + c_9 Z\left(t\right) + c_9\tau_{E_3}\left(t\right) \tag{2.13}$$

3

Takagi-Sugeno Fuzzy Controller Design Using Riccati Differential Equation

In this chapter, we want to design a stable T-S fuzzy control without using LMIs. The locally linear time-invariant systems are transformed into a time-varying system. By using matrix RDE, we prove that the trajectory tracking error of the T-S fuzzy control is bounded. Also, for validation purposes we apply this new T-S fuzzy control to a underwater vehicle. Comparisons with LMI method are given. Experimental results show that this novel T-S fuzzy control has many advantages over the popular LMI method.

3.1 Control problem statement

The T-S system may be used to approximate uncertain nonlinear systems. The class of uncertainties may include parametric variations or nonmodeled dynamics. So, let

consider the following uncertain nonlinear system:

$$\frac{d}{dt}x\left(t\right)=f\left(x\left(t\right)\right)+g\left(x\left(t\right)\right)u\left(t\right)+\xi\left(x\left(t\right),t\right),\ x\left(0\right)=x_{0},\ \forall t\geq 0 \tag{3.1}$$

where $x \in \mathbb{R}^n$ is the state vector, $u \in \mathbb{R}^m$ is the control vector ($m < n$), and $\xi : \mathbb{R}^{n+1} \to \mathbb{R}^n$ represents parameter variations, external perturbations, unmodeled dynamics, etc. The uncertain nonlinear continuous functions $f : \mathbb{R}^n \to \mathbb{R}^n$ and $g : \mathbb{R}^n \to \mathbb{R}^{n\times m}$ each one is composed of n nonlinear functions. The function g must satisfy $\|g(x)\| \neq 0$ for all x. This condition is sufficient to ensure controllability. If possible, one may consider that $g(x)/\|g(x)\|$ is also known but this is not needed to solve the controller design proposed in this study.

The specific characterization of T-S system usually requires a non standard parameter identification to get all matrices A^i and B^i. Many studies have been proposed to resolve this problem but this aspect is beyond the scope of this article.
It is not easy to obtain exact nonlinear models for many complex physical systems. The Takagi-Sugeno (T-S) model expresses the physical systems with several local models. It has been proven that any continuous nonlinear uncertain system can be represented as the following T-S fuzzy dynamic model [Cao et al., 1997], [Joh et al., 1998], [Li and Li, 2004], [Lin et al., 2004]

$$\begin{gathered}\mathrm{R}^{k}\text{: IF } z_{1} \text{ is } F_{1}^{h_k} \text{and } z_{2} \text{ is } F_{2}^{h_k} \text{ and } \cdots\ z_{v} \text{ is } F_{v}^{h_k}\\ \text{THEN } \frac{d}{dt}x\left(t\right)=A^{i}x\left(t\right)+B^{i}u\left(t\right)+\tilde{f}^{i}\left(x\left(t\right),u\left(t\right)\right)+\xi^{i}\left(x\left(t\right),t\right)\\ k=1,\cdots,m,\ i=1,\ldots,M\end{gathered} \tag{3.2}$$

where R^k is the k-th fuzzy rule, m is the number of inference rules, M is the number of local models, $z=[z_1,z_2,\ldots,z_v]^\top$ $(v \leq n)$ are the premise variables, $F_j^{h_k}$ $(j = 1 \ldots v)$ are the fuzzy sets for the premise variables z_j, h_k is the membership function number for each premise variable j, The matrices $A^i \in \mathbb{R}^{n\times n}$ and $B^i \in \mathbb{R}^{n\times l}$ define the i-th local T-S model and $\xi^i : \mathbb{R}^{n+1} \to \mathbb{R}^n$ represents parameter variations, external perturbations

and unmodeled dynamics for each local model. The matrices $A^i \in \mathbb{R}^{n\times n}$ and $B^i \in \mathbb{R}^{n\times l}$ are designed such that the following assumption holds:

A1*:* The pairs (A^i, B^i), $i = 1, 2\cdots M$, are controllable.

The term $\tilde{f}^i(x(t), u(t)) = f(x(t)) + g(x(t))u(t) - A^i x(t) - B^i u(t)$ is named the modeling error for each local model.

Since the uncertain nonlinear functions f and g are assumed to be locally Lipschitz under the admissible control $u \in U_{adm}$, the modeling error $\tilde{f}^i(x(t), u(t))$ satisfy the following sector conditions:

$$\left\|\tilde{f}^i(x,u)\right\|^2 \leq \tilde{f}_0^i + \tilde{f}_1^i \|x\|^2 \tag{3.3}$$

where $\tilde{f}_0$, $\tilde{f}_1$ are known finite positive scalars.

Using a fuzzy standard inference method, *i.e.*, product inference, center-average and singleton fuzzifier, the m T-S models, Eq. (3.2) can be rewritten as

$$\begin{aligned}\frac{d}{dt}x(t) = &\sum_{i=1}^{M}\alpha_i(x(t))\left[A^i x(t) + B^i u(t)\right] + \sum_{i=1}^{M}\alpha_i(x(t))\tilde{f}^i(x(t), u(t)) \\ &+ \sum_{i=1}^{M}\alpha_i(x(t))\xi^i(x(t), t)\end{aligned} \tag{3.4}$$

where $\alpha_i(x)$ is defined as, $\alpha_i(x) = \prod_{j=1}^{M}\mu_j^i / \sum_{i=1}^{M}\prod_{j=1}^{M}\mu_j^i$, μ_j^i is the membership functions of the fuzzy sets F_j^i. Obviously, $0 \leq \alpha_i(x) \leq 1$, $\sum_{i=1}^{M}\alpha_i(x) = 1$.

If we define $A(t) \triangleq A(x(t)) = \sum_{i=1}^{M}\alpha^i(x(t))A^i$, $B(t) \triangleq B(x(t)) = \sum_{i=1}^{M}\alpha^i(x(t))B^i$, $\eta(x(t), u(t)) = \sum_{i=1}^{M}\alpha^i(x(t))\tilde{f}^i(x(t), u(t))$, $\bar{\xi}(x(t), t) = \sum_{i=1}^{M}\alpha^i(x(t))\xi^i(x(t), t)$, Eq, (3.4) can be simplified as

$$\frac{d}{dt}x(t) = A(t)x(t) + B(t)u(t) + \eta(x(t), u(t)) + \bar{\xi}(x(t), t) \tag{3.5}$$

where $\eta(x, u)$ is the integrated modeling error, $\bar{\xi}(x, t)$ is the integrated uncertainty

term.

Remark 1 *The parameter variations and external disturbances and can be associated only to the term $\bar{\xi}(x,t)$ and the unmodeled dynamics can be introduced in the modeling error term $\eta(x,u)$ which satisfies a sector boundary condition.*

To establish a feasible control problem, we define an admissible control set as

$$U_{adm} = \left\{ u : \|u\|^2 \leq \gamma_{u1} + \gamma_{u2} \|x\|^2 \right\} \tag{3.6}$$

where γ_{u1} and γ_{u2} are positive constants. U_{adm} guarantees the right hand side of Eq. (3.4) is locally Lipschitz. Obviously, the normal state feedback control satisfies $\gamma_{u1} = 0$ and $\gamma_{u2} > 0$.

The controller design objective is to find $u \in U_{adm}$, such that the trajectory tracking error is ultimate bounded [Khalil, 2002] as

$$\lim_{t \longrightarrow \infty} \sup \|x(t) - x_{ref}(t)\| \leq \beta_{ref} \tag{3.7}$$

where $x_{ref} \in \mathbb{R}^n$ are the reference signals and $\beta_{ref} > o$ defines the quality of the trajectory tracking control.

The desired signals are generated by a nonlinear reference model given by

$$\frac{d}{dt} x_{ref}(t) = s(x_{ref}(t), t) \tag{3.8}$$

where $x_{ref}(0) = x_{ref,0}$, $\forall t \geq 0$. The function $s : \mathbb{R}^{n+1} \rightarrow \mathbb{R}^n$ is nonlinear and Lipschitz, it satisfies

$$\|s(x_{ref}(t)), t)\|^2 \leq L_s \|x_{ref}(t)\|^2, \forall t \geq 0 \tag{3.9}$$

where $L_s > 0$. Based on the orthogonal decomposition [Poznyak et al., 2004],

[Polyakov and Poznyak, 2011], Eq. (3.8) can be rewritten as

$$s\left(x_{ref}\left(t\right),t\right)=B\left(t\right)v\left(t\right)+B\left(t\right)^{\perp}r\left(t\right) \tag{3.10}$$

where $B^{\perp}$ is the orthogonal function of B which is selected to satisfy that $Im_B \supseteq Im_g$, and v, $r \in \mathbb{R}^{n\times 1}$ are given by

$$\begin{aligned} v &= \left[B^{\top}B\right]^{-1}B^{\top}s\left(x_{ref},t\right) \\ r &= \left[\left(B^{\perp}\right)^{\top}B^{\perp}\right]^{-1}\left(B^{\perp}\right)^{\top}s\left(x_{ref},t\right) \end{aligned} \tag{3.11}$$

Define $B^{\perp}$ using the pseudo-inverse B^{+} in the sense of Moore-Penrose [Poznyak, 2008], then

$$B^{\perp}=I-BB^{+},\quad B^{+}=\left(B^{\top}B\right)^{-1}B^{\top} \tag{3.12}$$

In this work the following assumptions are considered to be satisfied:

A2: The reference $x_{ref}\left(t\right)$ is bounded as

$$\left\|x_{ref}\right\|^{2}\leq\gamma_{ref},\quad \gamma_{ref}>0 \tag{3.13}$$

A3: The perturbations are bounded as

$$\left\|\xi\left(x,t\right)\right\|^{2}\leq\gamma_{\xi},\quad \gamma_{\xi}>0 \tag{3.14}$$

Considering the sector conditions in Eq. (3.3) the integrated modeling error $\eta\left(x,u\right)$ satisfies:

A4*:*

$$\left\|\eta\left(x,u\right)\right\|^{2}\leq f_{0}+f_{1}\left\|x\right\|^{2},\ u\in U_{adm} \tag{3.15}$$

where $f_0=\sum_{i=1}^{M}\tilde{f}_0^i$, $f_1=\sum_{i=1}^{M}\tilde{f}_1^i$.

3.2 Controller design

This work does not discuss the fuzzy modeling problem, so we are not interesting in the minimization of the modeling error. We will design a fuzzy control such that the tracking error in Eq. (3.7) is ultimate bounded. We use the model in Eq. (3.5) and assumption **A4.**

Now we define the trajectory tracking error

$$\Delta = x - x_{ref} \tag{3.16}$$

The following theorem gives the main result of the chapter. It guarantees the tracking error in Eq. (3.16) is bounded. It also provides an explicit and easy design method for the T-S fuzzy control.

Theorem 2 *(Stability of the trajectory tracking error). If there exists a positive scalar* α *and symmetric positive definite matrices* $\Lambda_i \in \mathbb{R}^{n\times n}$ $(i = 1 \cdots 4)$ *and* $|\min_t\{\lambda_{min}(A(t))\}| > max(\alpha)$ *such that the following matrix RDE [Kilicaslan and Banks, 2010] have positive definite solution:*

$$\frac{d}{dt}P(t) + P(t)\bar{A}_1(t) + \bar{A}_1^{\top}(t)P(t) - P(t)R_1(t)P(t) + Q_1(t) = 0 \tag{3.17}$$

where $P(t) = P^{\top}(t) > 0$,

$$\begin{aligned} \bar{A}_1(t) &= A(t) + \frac{\alpha}{2}I, \\ R_1(t) &= 3(A(t)\Lambda_1 A^{\top}(t) + S_1(t)\Lambda_4 S_1^{\top}(t) + \Lambda_2 + \Lambda_3), \\ Q_1(t) &= 2\lambda_{\max}\left(\Lambda_2^{-1}\right) f_1 I_{n\times n} \\ S_1(t) &= B^{\perp}(t)\left[\left(B^{\perp}(t)\right)^{\top} B^{\perp}(t)\right]^{-1}\left(B^{\perp}(t)\right)^{\top}, \end{aligned} \tag{3.18}$$

f_1 *is defined in Eq. (3.15),* $B^{\perp}$ *is defined in Eq. (3.12),* $A(t)$ *and* $B(t)$ *are defined in*

Eq. (3.5), and $I_{n\times n}$ is the identity matrix of $n \times n$, and the feedback control is in the following form

$$\begin{aligned} u(t) &= -K(t)\Delta(t) + v(t), \quad K(t) \in \mathbb{R}^{m\times n}, \\ K(t) &= 2\left[B^{\top}(t) B(t)\right]^{-1} B^{\top}(t) R_1(t) P(t) \end{aligned} \tag{3.19}$$

where $v(t)$ is defined in Eq. (3.11), then the trajectory tracking error Δ satisfies

$$\lim_{t\to\infty} \sup \|\Delta(t)\|^2 \leq \frac{\beta}{\alpha * \min\limits_{t} \{\lambda_{\min}(P(t))\}} \tag{3.20}$$

where

$$\beta = \lambda_{\max}\left(\Lambda_1^{-1}\right)\gamma_{ref} + \lambda_{\max}\left(\Lambda_2^{-1}\right) f_0 + 2\lambda_{\max}\left(\Lambda_2^{-1}\right) f_1\gamma_{ref} + \lambda_{\max}\left(\Lambda_3^{-1}\right)\gamma_{\xi} + \lambda_{\max}\left(\Lambda_4^{-1}\right) L_s\gamma_{ref}$$

f_0 and f_1 are defined in Eq. (3.15), γ_{ref} is defined in Eq. (3.13), γ_{ξ} is defined in Eq. (3.14), L_s is defined in Eq. (3.9)

Proof. See Appendix A1. ■

Remark 3 *In order to prove the stability of several linear systems Eqs. (3.2) and (3.4) for T-S fuzzy control, there are two popular methods: common Lyapunov function and LMI method. Both of them try to find common stability conditions for all linear systems. This work combines all these linear system as in Eq. (3.5). However, it becomes a time-varying linear system. We use RDE to avoid the complexity of the common Lyapunov function method and LMI method.*

3.3 On the Riccati Differential Equation solution

The T-S fuzzy controller in Eq. (3.19) needs the solution $P(t)$ of the RDE (3.17). This RDE has time-varying parameters, it is not easy to discuss the existence conditions for $P(t)$. The following lemma shows how to use a RDE with time-invariant parameters to decide the solution of a RDE with time-varying parameters.

Lemma 4 *Let us consider a matrix RDE with time-varying parameters and an algebraic Riccati equation (ARE) given by*

$$\begin{gathered}\frac{d}{dt}P(t)+A^{\top}(t)P(t)+P(t)A(t)-P(t)R(t)P(t)+Q(t)=0\\ A^{\top}P_2+P_2A-P_2RP_2+Q=0\end{gathered} \tag{3.21}$$

with the initial condition

$$P(0)>P_2 \tag{3.22}$$

and with the corresponding Hamiltonians are given by

$$H(t)=\begin{bmatrix} Q(t) & A(t)^{\top} \\ A(t) & -R(t) \end{bmatrix} \quad H_2=\begin{bmatrix} Q & A^{\top} \\ A & -R \end{bmatrix}$$

If

$$H_2 \geq H(t) \geq 0 \tag{3.23}$$

and the pair (A,R) is stable, i.e., $\exists F$: $Re(\lambda_i(A-FR))<0$, then

$$P(t)>P_2>0,\ \forall t>0 \tag{3.24}$$

Proof. See Appendix A2. ■

This lemma shows that if the T-S fuzzy system is designed, such that the condition in Eq. (3.23) is satisfied, *i.e.*

$$\begin{bmatrix} Q & A^{\top} \\ A & -R \end{bmatrix} \geq \begin{bmatrix} Q(t) & \bar{A}^{\top}(t) \\ \bar{A}(t) & -R(t) \end{bmatrix}$$

where A, Q, and R are constant matrices which are chosen such that they satisfy the following conditions 1) the pair $(A, R^{1/2})$ is controllable, 2) the pair $(Q^{1/2}, A)$ is observable. These two conditions are equivalent to the following local frequency condition

[Willems, 1971]

$$A^{\top}R^{-1}A - Q \geq 0 \tag{3.25}$$

The detailed proof of Eq. (3.25) can be found in [Osorio et al., 1997]. Then, by Lemma 1, the solution of Eq. (3.17) $P(t)$ is not less than the solution of

$$A^{\top}P_2 + P_2A - P_2RP_2 + Q = 0 \tag{3.26}$$

then the initial condition of Eq. (3.17) is bigger than that of Eq. (3.26). This means if the conditions described before are fulfilled the existence condition for Theorem 1 is always satisfied.

Remark 5 *It is important to note that in Eqs. (3.17) and (3.27) $P(t)$ is just a function of time t because its parameters $A(t)$ and $B(t)$ in Eq. (3.5) also are functions of time t. They are evaluated as functions of the trajectory of $x(t)$ not only on the state value (without time evolution). The RDE is a dynamic system, its input is $x(t)$ and its state is $P(t)$. Given an initial condition for $P(t)$ namely $P(0)$, this dynamic system starts to run. This condition has been used in the control design of time-varying systems. Indeed, if P is proposed as a function of x, then is needed to propose a way to guarantee the existence of a positive definite solution. This represents completely another problem to solve. The concept of state dependent Riccati equation (SDRE) has been proposed in different articles [Banks et al., 2007], [Xie et al., 2013], [Cimen, 2008] but it is still evaluated on the current value of the state evaluated at a given time t*

3.4 Implementation issues

In order to implement the closed-loop system applying the proposed tracking controller based on the RDEs on-line solution the following procedure needs to be carried out. The schematic in Fig. 3.1 shows the architecture of the closed-loop system.

First the RDE in Eqs. (3.17) stated in Theorem 1 can be rewritten as follows:

$$\frac{d}{dt}P(t) = P(t)\,R_1(t)\,P(t) - P(t)\,\bar{A}_1 - \bar{A}_1^{\top}P(t) - Q_1(t) \tag{3.27}$$

The parameters of the RDEs was chosen to fulfil the existence conditions presented in Lemma 4.

We do not calculate the analytical solution. To solve Eq. (3.27) a simulation on MATLAB-Simulink considering initial condition $P(0) = P_0$ was implemented.

- The matrix $\frac{d}{dt}P(t)$ of Eq. (3.27) is calculated using the values of $A(t)$, $B(t)$ which depend on $\alpha^i(x)$.
- $P(t)$ are obtained by integrating $\dot{P}(t)$.
- $P(t)$ and $A(t)$ and $B(t)$ are used to calculate $K(t)$ in Eq. (3.19).

The integral operation divide the two processes in consequence there is no algebraic loop.

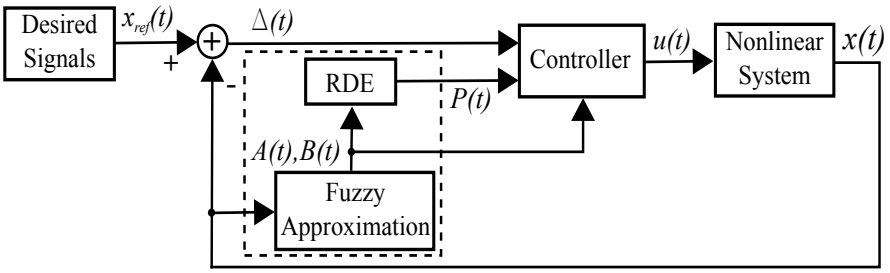

Figure 3.1: Closed-loop system architecture with on-line RDE.

3.5 Numerical results

In order to validate the performance of the RDE based on T-S fuzzy control, an AUV model in the horizontal plane is used, see Section 2.1 in Chapter 2. If one uses the method described in Section 3.1 we can use 27 T-S fuzzy rules and four local systems to approximate this AUV system:

$$\begin{aligned} &\mathrm{R}^k\text{: IF } p \in F_p^{h_k} \text{ and } q \in F_q^{h_k} \text{ and } w \in F_w^{h_k}, \\ &\text{THEN } \frac{d}{dt}\chi(t) = A^i\chi(t) + B^i\tau(t) + \tilde{f}^i(\chi(t), \tau(t)) + \zeta^i(t) \end{aligned} \tag{3.28}$$

where $k = 1 \cdots 27$, $i = 1 \cdots 4$, $A^i \in \mathbb{R}^{3\times3}$ and $B^i \in \mathbb{R}^{3\times2}$. For the fuzzification stage the sign of the measurable variables p, q and w is chosen as the fuzzy set, and the following three partitions are proposed: Negative (N), Zero (Z), and Positive (P). That is, $F_p^{h_k}, F_q^{h_k}, F_w^{h_k} \in \{N, Z, P\}$. The membership functions structure are selected as Fig. 3.2. A^i and B^i are chosen as linearizations of the nonlinear system in Eq. (3.1), and they must satisfy that the RDE in Eq. (3.17) has solution. The four local systems that were used to approximate the AUV model have the following matrices:

$$A^1 = \begin{bmatrix} 0 & 1 & 1 \\ -1 & 0 & -2 \\ 0 & 0 & 0 \end{bmatrix}, A^2 = \begin{bmatrix} 0 & 1 & 0.5 \\ -1 & 0 & -1 \\ 0 & 0 & 0 \end{bmatrix}, A^3 = \begin{bmatrix} 0 & 2 & 0.8 \\ -2 & 0 & -0.5 \\ 0 & 0 & 0 \end{bmatrix},$$

$$A^4 = \begin{bmatrix} 0 & 5.3 & 1.2 \\ -5.3 & 0 & -3.5 \\ 0 & 0 & 0 \end{bmatrix}, B^1 = ... = B^4 = B.$$

In Eq. (3.18) $\Lambda_i\,(i = 1, \cdots, 4)$ are chosen as identity matrices. For Eq. (3.26), $A_2 = diag[-1, -1, -1]$, $Q_2 = diag[0.2, 0.2, 0.2]$, $R_2 = diag[1.5, 1.5, 1.5]$ are chosen.

Based on the planning motion method, the desired reference has the same structure as the AUV, it satisfies $s(x_{ref}) = [2 + q_{ref}w_{ref}, -p_{ref}w_{ref}, 2]^\top$.

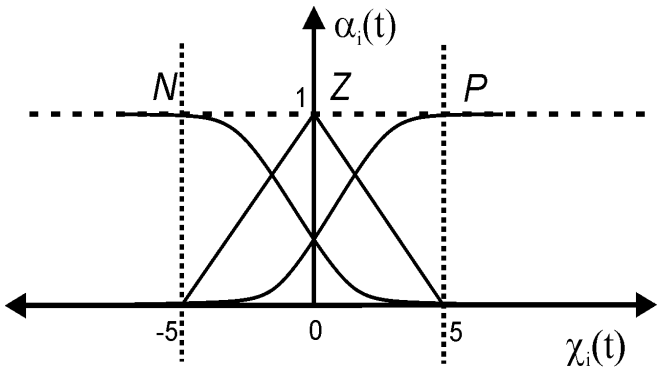

Figure 3.2: Membership functions structure of N, Z and P. .

With the initial conditions $\chi_0 = [2, -2, 4]^\top$, $s\left(x_{ref}\left(0\right)\right) = [0, 0, 0]^\top$, the final feedback control is stated in Eq. (3.19), here $P(t)$ is the numerical solution of Eq. (3.27). The norm of the time-varying controller gain $K\left(t\right)$ is shown in Fig. 3.3. This controller is applied to the original system in Eq. (3.1).

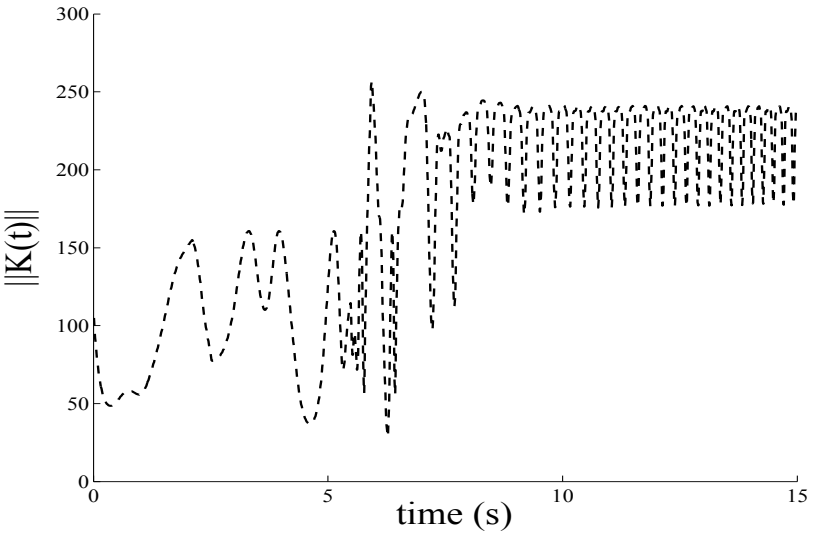

Figure 3.3: Norm of the time-varying controller gain $K\left(t\right)$ based on Riccati differential equation.

There are several results on fuzzy control for AUV one of the most common is the LMI method. We compare our method (RDE) with the popular LMI based T-S fuzzy

control [Tuan et al., 2001]. LMI method has the PDC form

$$\tau(t) = K_{LMI}(t)\,\Delta(t), \quad K_{LMI}(t) = \sum_{i=1}^{4} \alpha_i(t)\,K_i$$

The local gains K_i are

$$K_1 = \begin{bmatrix} 14.6662 & -2.5125 & 7.6231 \\ 6.5240 & -5.3162 & 9.3338 \end{bmatrix}, K_2 = \begin{bmatrix} 9.9085 & 3.6972 & 6.7541 \\ 5.8949 & -1.3966 & 6.0915 \end{bmatrix}$$

$$K_3 = \begin{bmatrix} 20.8259 & -11.8471 & 9.7919 \\ 7.4068 & -8.2994 & 11.1741 \end{bmatrix}, K_4 = \begin{bmatrix} 18.3649 & -9.4606 & 7.8695 \\ 5.7556 & -7.8510 & 11.6351 \end{bmatrix}$$

The numerical results are shown in Fig. 3.4 and Fig. 3.5. In these figures a comparison of the tracking of desired velocities in the X_B and Y_B axes implementing the proposed RDE and LMI based methods is shown. We can see that our RDE based method needs 2 seconds to converge to the reference velocities, while the LMI based method needs more than 7 seconds. Also LMI method cannot track the trajectory at the beginning. The fast speed of our RDE method may come from the dynamic system in Eq. (3.27) is more simple and faster than LMIs.

The stability analysis of T-S fuzzy system based on LMI is complex. However, it is only an off-line and analytic task. There are also many relaxing condition for LMI technique. In on-line case, we need to run the dynamic system in Eq. (3.27), while the gain of LMI is fixed. For the computation speed, LMI is better than our RDE method. However, both of them are very fast. Simulation results show our RDE has faster convergence speed than LMI, because the feedback control gain of this work is time-varying, which depends on the state $P(t)$ of the dynamic system in Eq. (3.27). $P(t)$ needs both fuzzy model $A(t)$ and $B(t)$, and the state $x(t)$. While the feedback control gain of LMIs only use the fuzzy model $A(t)$ and $B(t)$.

Although the controlled system in Eq. (3.1) is not so complex, the results of the T-S fuzzy control are not so good as the model-based control, such as feedback linearisation.

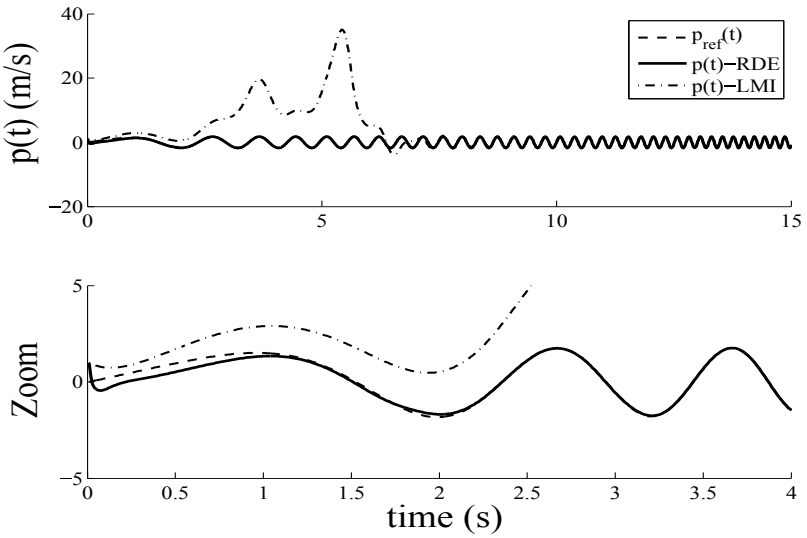

Figure 3.4: Tracking of the velocity in X_B-axis implementing the proposed RDE and LMI methods.

This because the fuzzy model in Eq. (3.28) is not exact model of the controlled system Eq. (3.1).

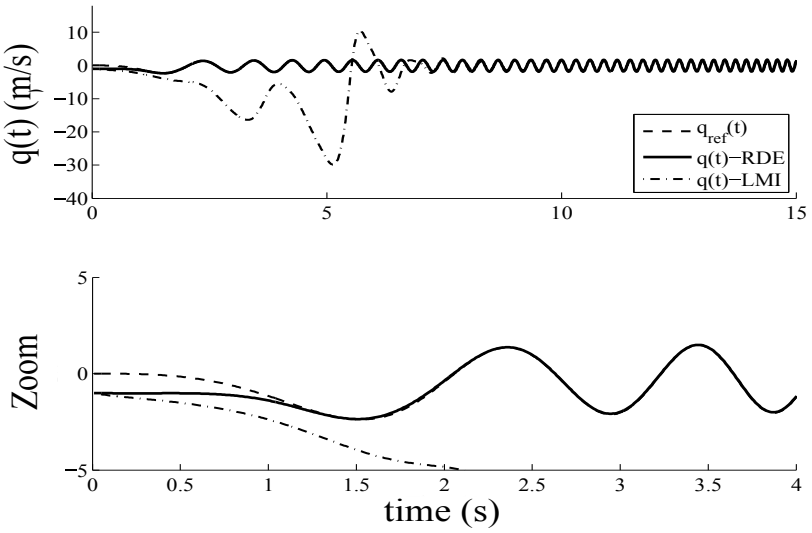

Figure 3.5: Tracking of the velocity in Y_B-axis implementing the proposed RDE and LMI methods.

3.6 Conclusions of the chapter

In this chapter a state feedback control was designed based on the Lyapunov stability analysis for a T-S fuzzy system. A nonconventional Lyapunov time-varying function was used to prove the ultimate boundedness of the tracking error between the T-S representation of an uncertain nonlinear system and a reference system. This work uses a RDE and a feedback controller with time-varying gain based on the solution of a RDE to guarantee the stability of the T-S fuzzy closed-loop system. We also propose a existence condition for the RDE. The feedback gain obtained using the LMI technique is calculated off-line and is fixed in the closed-loop system providing an stable behaviour. However, the LMI technique considers the worst case of the disturbance effect in consequence the energy used to stabilize the system is the same for small or big disturbances. Numerical simulations applying the novel controller obtained in this study for an autonomous underwater vehicle trajectory tracking was done. These simulations show the controller calculated with LMI technique consumes more energy than the one using the RED based method. This fact is due to the RDE is solved on-line providing a time-varying feeback gain which indirectly varies according to the dynamic behaviour of the system. In consequence, superiority performance of the result obtained here compared to the regular control design based on LMIs is demonstrated.

For a complete unknown nonlinear system, to obtain $A(t)$ and $B(t)$ of the T-S fuzzy system in Eq. (3.5) needs the neural training method [W. Yu, 2004]. Also is necessary to study the stability of neural networks and T-S fuzzy model [Li and Li, 2004]. In Chapter 5 a methodology to avoid the necessity to find suitable $A(t)$ and $B(t)$ based on a neuro-fuzzy identifier is developed. Also it is necessary to design an observer in order to use the state information provided by the output information of the nonlinear system. This problem is solved in Chapter 4.

4

Fuzzy Output Feedback Controller Design of Uncertain Nonlinear Systems

In this chapter, an alternative methodology based on T-S fuzzy modeling is proposed to guarantee a feasible solution of the trajectory tracking between an uncertain nonlinear perturbed system and a reference dynamics. This strategy uses the Lyapunov formalism to provide sufficient conditions that supports the control design. This output based controller structure uses the positive definite solution of two Riccati Differential Equations (RDE). Based on the assumption regarding the existence of solution for these two equations, the nonlinear system trajectories track the reference states. The internal information (unmeasurable states) used by the controller described before is provided by a T-S fuzzy observer of the nonlinear system. On opposite to the LMI based methods, only two equations must be solved instead of several LMI's. This condition simplifies the numerical algorithm because there exist well-known conditions to ensure their solution [Kilicaslan and Banks, 2012] and [Kilicaslan and Banks, 2010]. Ultimate

boundedness concept [Khalil, 2002] is used to define the stability sense that governs the tracking error.

4.1 Control problem statement

Consider the following uncertain nonlinear system:

$$\begin{gathered}\frac{d}{dt}x\left(t\right)=f\left(x\left(t\right)\right)+g\left(x\left(t\right)\right)u\left(t\right)+\xi\left(x\left(t\right),t\right),\ x\left(0\right)=x_{0},\ \forall t\geq 0\\ y\left(t\right)=h\left(x\left(t\right)\right)\end{gathered} \tag{4.1}$$

where $x \in \mathbb{R}^n$ is the state vector, $u \in \mathbb{R}^m$ is the control vector ($m < n$), $y \in \mathbb{R}^p$ ($p < n$) is the output, and $\xi : \mathbb{R}^{n+1} \to \mathbb{R}^n$ represents either parameter variations, external perturbations, unmodeled dynamics, etc. The uncertain nonlinear continuous functions $f : \mathbb{R}^n \to \mathbb{R}^n$ and $g : \mathbb{R}^n \to \mathbb{R}^{n\times m}$ each one is composed of n nonlinear functions and $h : \mathbb{R}^n \to \mathbb{R}^p$ is composed of p nonlinear continuous functions. Because of h is continuous, it is possible to recover the output information based on state information solutions, such as state observer.

The control goal is to force the system states using the output information to track desired signals, x_{ref}, generated by a nonlinear reference model given by

$$\frac{d}{dt}x_{ref}\left(t\right)=s\left(x_{ref}\left(t\right),t\right) \tag{4.2}$$

where $x_{ref} \in \mathbb{R}^n$, $x_{ref}\left(0\right) = x_{ref,0}$, $\forall t \geq 0$. The following assumption are considered to be satisfied:

A1: The reference x_{ref} is bounded as

$$\left\|x_{ref}\right\|^{2}\leq\gamma_{ref},\quad\gamma_{ref}>0 \tag{4.3}$$

The function $s : \mathbb{R}^{n+1} \to \mathbb{R}^n$ is nonlinear and Lipschitz, and considering $s\left(0\right) = 0$, the

following inequality is satisfied

$$\|s\left(x_{ref}, t\right)\|^2 \leq L_s \|x_{ref}\|^2 \tag{4.4}$$

where $L_s > 0$. Based on the orthogonal decomposition [Poznyak et al., 2004], [Polyakov and Poznyak, 2011], Eq. (4.2) can be rewritten as

$$s\left(x_{ref}\left(t\right), t\right) = T\left(t\right) v\left(t\right) + T\left(t\right)^{\perp} r\left(t\right) \tag{4.5}$$

where T is selected to satisfy that $Im_T \supseteq Im_g$, $T^{\perp}$ is the orthogonal function of T, defined as, $T^{\perp} = I_{n\times n} - TT^{+}$, and $T^{+} = \left(T^{\top}T\right)^{-1} T^{\top}$, T^{+} is the pseudo-inverse of T in the sense of Moore-Penrose [Poznyak, 2008]. Then, terms, $v\left(t\right)$ and $r\left(t\right) \in \mathbb{R}^m$, are given by

$$\begin{aligned} v\left(t\right) &= \left[T\left(t\right)^{\top} T\left(t\right)\right]^{-1} T\left(t\right)^{\top} s\left(x_{ref}\left(t\right), t\right) \\ r\left(t\right) &= \left[\left(T\left(t\right)^{\perp}\right)^{\top} T\left(t\right)^{\perp}\right]^{-1} \left(T\left(t\right)^{\perp}\right)^{\top} s\left(x_{ref}\left(t\right), t\right) \end{aligned} \tag{4.6}$$

A2: The term that contains uncertainties and perturbations are bounded as

$$\|\xi\left(x, t\right)\|^2 \leq \gamma_{\xi}, \quad \gamma_{\xi} > 0 \tag{4.7}$$

An admissible control set is defined as in equation 3.6. The controller design objective is ths same as the stated in 3.7. A fuzzy control based on state observation is designed such that the trajectory tracking error in Eq. (3.7) is minimized.

Since the T-S fuzzy model is a universal approximation function [Takagi and Sugeno, 1985], the uncertain nonlinear system Eq. (4.1) can be represented by M T-S fuzzy models with modeling error as follows.

$$\begin{aligned} &\mathrm{R}^k\text{: IF } z_1 \text{ is } F_1^{h_k} \text{and } z_2 \text{ is } F_2^{h_k} \text{ and } \cdots \ z_v \text{ is } F_v^{h_k} \\ \text{Then } \quad &\frac{d}{dt}x\left(t\right) = A^i x\left(t\right) + B^i u\left(t\right) + \tilde{f}^i(x\left(t\right), u\left(t\right)) + \xi^i\left(x\left(t\right), t\right) \\ &y\left(t\right) = C^i x\left(t\right) + \tilde{h}^i(x\left(t\right)) \\ &k = 1, \cdots, m, \ i = 1, \ldots, M \end{aligned} \tag{4.8}$$

where R^k is the k-th fuzzy rule, m is the number of inference rules, M is the number of local models, $z = [z_1, z_2, \ldots, z_v]^\top$ $(v \leq n)$ are the premise variables, $F_j^{h_k}$ $(j = 1 \ldots v)$ are the fuzzy sets for the premise variables z_j, h_k is the membership function number for each premise variable j. The matrices $A^i \in \mathbb{R}^{n\times n}$, $B^i \in \mathbb{R}^{n\times l}$ and $C^i \in \mathbb{R}^{p\times n}$ define the i-th local T-S model and $\xi^i : \mathbb{R}^{n+1} \to \mathbb{R}^n$ represents parameter variations, external perturbations and unmodeled dynamics for each local model. The matrices A^i, B^i and C^i are designed such that the following assumptions hold:

A3*:* The pairs (A^i, B^i), $i = 1, 2 \cdots M$, are controllable.

A4*:* The pairs (C^i, A^i), $i = 1, 2 \cdots M$, are observable.

The terms $\tilde{f}^i\left(x, u\right)$ and $\tilde{h}^i(x, u)$ are the modeling errors for each local model, i.e., $\tilde{f}^i\left(x, u\right) = f\left(x\right) + g\left(x\right)u - A^i x - B^i u$ and $\tilde{h}^i(x) = h^i(x) - C^i x$.

Since the uncertain nonlinear functions f, g and h are assumed to be locally Lipschitz under the admissible control $u \in U_{adm}$, the modeling errors $\tilde{f}^i\left(x, u\right)$ and $\tilde{h}^i(x)$ satisfy the following sector conditions:

$$\left\|\tilde{f}^i\left(x, u\right)\right\|^2 \leq \tilde{f}_0^i + \tilde{f}_1^i \left\|x\right\|^2, \quad \left\|\tilde{h}^i(x)\right\|^2 \leq \tilde{h}_0^i + \tilde{h}_1^i \left\|x\right\|^2 \tag{4.9}$$

where $\tilde{f}_0$, $\tilde{f}_1$, $\tilde{h}_0$, $\tilde{h}_1$ are known finite positive scalars.

Using a fuzzy standard inference method, *i.e.*, product inference, center-average and

singleton fuzzifier, the M T-S models in Eq. (4.8) can be rewritten as

$$\frac{d}{dt}x\left(t\right)=\sum_{i=1}^{M}\alpha^{i}\left(z\left(t\right)\right)\left(A^{i}x\left(t\right)+B^{i}u\left(t\right)\right)+\sum_{i=1}^{M}\alpha^{i}\left(z\left(t\right)\right)\tilde{f}^{i}(x\left(t\right),u\left(t\right))+\sum_{i=1}^{M}\alpha^{i}\left(z\left(t\right)\right)\xi^{i}\left(x\left(t\right),t\right)$$
$$y\left(t\right)=\sum_{i=1}^{M}\alpha^{i}\left(z\left(t\right)\right)C^{i}x\left(t\right)+\sum_{i=1}^{M}\alpha^{i}\left(z\left(t\right)\right)\tilde{h}^{i}(x\left(t\right)) \tag{4.10}$$

where $\alpha^{i}\left(z\right)$ is defined as $\alpha^{i}\left(z\right)=\prod_{j=1}^{v}\mu_{j}^{i}\left(z_{j}\right)/\sum_{i=1}^{M}\prod_{j=1}^{v}\mu_{j}^{i}\left(z_{j}\right)$, $\mu_{j}^{i}\left(z_{j}\right)$ is the membership functions of the fuzzy sets F_{j}^{i}. Obviously, $0\leq\alpha^{i}\left(z\right)\leq1$, $\sum_{i=1}^{M}\alpha^{i}\left(z\right)=1$.

The activation functions $\alpha^{i}\left(\cdot\right)$ depend on the decision vector $z\left(t\right)$ assumed to depend on measurable variables. It can depend on the measurable state variables, and it can be a function of the measurable outputs of the system

Considering that $A\left(t\right)=\sum_{i=1}^{M}\alpha^{i}\left(z\left(t\right)\right)A^{i}$, $B\left(t\right)=\sum_{i=1}^{M}\alpha^{i}\left(z\left(t\right)\right)B^{i}$, $C\left(t\right)=\sum_{i=1}^{M}\alpha^{i}\left(z\left(t\right)\right)C^{i}$, $\eta\left(x\left(t\right),u\left(t\right)\right)=\sum_{i=1}^{M}\alpha^{i}\left(z\left(t\right)\right)\tilde{f}^{i}\left(x\left(t\right),u\left(t\right)\right)$, $\delta\left(x\left(t\right)\right)=\sum_{i=1}^{M}\alpha^{i}\left(z\left(t\right)\right)\tilde{h}^{i}(x\left(t\right))$ and $\bar{\xi}\left(x\left(t\right),t\right)=\sum_{i=1}^{M}\alpha^{i}\left(z\left(t\right)\right)\xi^{i}\left(x\left(t\right),t\right)$, Eq. (4.10) can be simplified as

$$\frac{d}{dt}x\left(t\right)=A\left(t\right)x\left(t\right)+B\left(t\right)u\left(t\right)+\eta\left(x\left(t\right),u\left(t\right)\right)+\bar{\xi}\left(x\left(t\right),t\right)$$
$$y\left(t\right)=C\left(t\right)x\left(t\right)+\delta\left(x\left(t\right)\right) \tag{4.11}$$

where $\eta\left(x,u\right)$ and $\delta\left(x\right)$ are modeling errors, $\bar{\xi}\left(x,t\right)$ refers to as the external perturbation and uncertainty term.

Considering the sector conditions in Eq. (4.9) the integrated modeling error $\eta\left(x,u\right)$ satisfies:

A5:

$$\left\|\eta\left(x,u\right)\right\|^{2}\leq\eta_{0}+\eta_{1}\left\|x\right\|^{2},\ u\in U_{adm} \tag{4.12}$$

and the integrated modeling error $\delta\left(x\right)$ satisfies:

A6:

$$\|\delta(x)\|^2 \leq \delta_0 + \delta_1 \|x\|^2 \tag{4.13}$$

where $\eta_0 = \sum_{i=1}^{M} \tilde{f}_0^i$, $\eta_1 = \sum_{i=1}^{M} \tilde{f}_1^i$, $\delta_0 = \sum_{i=1}^{M} \tilde{h}_0^i$, $\delta_1 = \sum_{i=1}^{M} \tilde{h}_1^i$.

Remark 6 *The external disturbances can be associated only to the term $\bar{\xi}(x,t)$ and the unmodeled dynamics and uncertainties can be introduced in the modeling error term $\eta(x,u)$ which satisfies a sector boundary.*

To achieve the solution of the trajectory tracking established in Eq. (**??**) all the states of Eq. (4.11) are needed. Considering the state information of Eq. (4.11) is not available, an observer to estimate this state is proposed. Therefore, T-S fuzzy observer that do not depend on the estimated premise variables [Tanaka and Wang, 2001] is considered. This observer has the following structure:

$$\begin{gathered} \frac{d}{dt}\hat{x}(t) = A(t)\hat{x}(t) + B(t)u(t) + L(t)(y(t) - \hat{y}(t)) \\ \hat{y}(t) = C(t)\hat{x}(t) \end{gathered} \tag{4.14}$$

where $A(t)$, $B(t)$, $C(t)$ are the same as in Eq. (4.11), $L(t)$ the observation gain, and $\hat{x} \in \mathbb{R}^n$, $\hat{y} \in \mathbb{R}^p$ are the state and output of the observer, respectively.

4.2 Controller design

This work does not discuss the fuzzy modeling problem, so the minimization of the fuzzy modeling error is not of interest.

The models in equations (4.11) and (4.14), and assumptions **A1**, **A2**, **A3**, **A4**, **A5** and **A6** are used**.**

Because of the state x is supposed to be not available, then an observation error needs to be defined as

$$\Delta_1 = x - \hat{x} \tag{4.15}$$

In order to reach a desired trajectory, a trajectory tracking error is defined as

$$\Delta_2 = \hat{x} - x_{ref} \tag{4.16}$$

The following theorem gives the main result of the chapter. It guarantees that the tracking error in Eq. (4.16) is bounded. It also provides an explicit and easy design method for the T-S fuzzy control.

Theorem 7 *(Stability of the trajectory tracking error). If there exist a positive scalar* α *and symmetric positive definite matrices* Λ_i, $i = 1, \ldots, 8$ *and* $|\min_t\{\lambda_{min}(A(t))\}| > max(\alpha)$ *such that the following two RDEs [Kilicaslan and Banks, 2010] have symmetric positive definite solutions:*

$$\frac{d}{dt}P_1(t) + P_1(t)\bar{A}(t) + \bar{A}^{\top}(t)P_1(t) - P_1(t)R_1(t)P_1(t) + \tilde{Q}_1(t) = 0 \tag{4.17}$$

$$\frac{d}{dt}P_2(t) + P_2(t)\bar{A}(t) + \bar{A}^{\top}(t)P_2(t) - P_2(t)R_2(t)P_2(t) + \tilde{Q}_2(t) = 0 \tag{4.18}$$

where

$$P_1(t) \in \mathbb{R}^{n\times n}, P_2(t) \in \mathbb{R}^{n\times n}, P_1(t) = P_1^{\top}(t) > 0, P_2(t) = P_2^{\top}(t) > 0,$$

$$\begin{gathered}
\bar{A}(t) = A(t) + \frac{\alpha}{2}I_{n\times n}, R_1(t) = L(t)\Lambda_4 L^{\top}(t) + \Lambda_3 + \Lambda_6, \\
\tilde{Q}_1(t) = Q_1(t) - \frac{C^{\top}(t)\bar{R}_1^{-1}C(t)}{2}, \\
Q_1(t) = \Lambda_1^{-1} + 3\lambda_{\max}\left(\Lambda_4^{-1} + \Lambda_5^{-1}\right)\delta_1 I_{n\times n} + 3\lambda_{\max}\left(\Lambda_6^{-1}\right)\eta_1 I_{n\times n}, \\
R_2(t) = S_1(t)\Lambda_1 S_1^{\top}(t) + A(t)\Lambda_2 A^{\top}(t) + L(t)\Lambda_5 L^{\top}(t) + \\
S_2(t)\Lambda_7 S_2^{\top}(t) + S_3(t)\Lambda_8 S_3^{\top}(t), \\
\tilde{Q}_2(t) = Q_2(t) - \frac{K^{\top}(t)\bar{R}_2^{-1}K(t)}{2}, \\
Q_2(t) = 3\lambda_{\max}\left(\Lambda_4^{-1} + \Lambda_5^{-1}\right)\delta_1 I_{n\times n} + 3\lambda_{\max}\left(\Lambda_6^{-1}\right)\eta_1 I_{n\times n},
\end{gathered} \tag{4.19}$$

$$
\begin{aligned}
S_1(t) &= L(t)\, C(t), \\
S_2(t) &= T(t)\left[T^{\top}(t)\, T(t)\right]^{-1} T^{\top}(t), \\
S_3(t) &= T^{\perp}(t)\left[\left(T^{\perp}(t)\right)^{\top} T^{\perp}(t)\right]^{-1}\left(T^{\perp}(t)\right)^{\top},
\end{aligned}
\tag{4.20}
$$

η_0, η_1, δ_0, δ_1 are defined in Eq. (4.12), $T^{\perp}$ is defined in Eq. (4.5), $A(t)$, $B(t)$, $C(t)$ are defined in Eq. (4.11), $I_{n\times n}$ is the identity matrix of $n \times n$, and the feedback control is in the following form

$$
\begin{aligned}
u(t) &= -K(t)\,\Delta_2(t), \quad K(t) \in \Re^{m\times n} \\
K(t) &= 2\bar{R}_2(t)\, B^{\top}(t)\, P_2(t)
\end{aligned}
\tag{4.21}
$$

and the observation gain $L(t) \in \Re^{n\times p}$ of the form

$$
L(t) = \frac{1}{2} P_1^{-1}(t)\, C^{\top}(t)\, \bar{R}_1^{-1}(t) \tag{4.22}
$$

where

$$
\begin{aligned}
\bar{R}_1(t) &= \left[C(t)\, L(t)\right]^{-1} C(t)\, R_1(t)\, C^{\top}(t)\left[L^{\top}(t)\, C^{\top}(t)\right]^{-1}, \\
\bar{R}_2(t) &= \left[B^{\top}(t)\, B(t)\right]^{-1} B^{\top}(t)\, R_2(t)\, B(t)\left[B^{\top}(t)\, B(t)\right]^{-1},
\end{aligned}
$$

then the trajectory tracking error Δ_2 satisfies

$$
\lim_{t\longrightarrow\infty} \sup \left\|\Delta_2(t)\right\|^2 \leq \frac{\beta}{\alpha * \min\limits_{t}\left\{\lambda_{\min}\left(P_2(t)\right)\right\}} \tag{4.23}
$$

where

$$
\begin{aligned}
\beta = {} & \lambda_{\max}\left(\Lambda_2^{-1}\right)\gamma_{ref} + \lambda_{\max}\left(\Lambda_3^{-1}\right)\gamma_{\xi} + \lambda_{\max}\left(\Lambda_4^{-1}\right)\delta_0 + 3\lambda_{\max}\left(\Lambda_4^{-1}\right)\delta_1\gamma_{ref} + \\
& \lambda_{\max}\left(\Lambda_6^{-1}\right)\eta_0 + 3\lambda_{\max}\left(\Lambda_6^{-1}\right)\eta_1\gamma_{ref} + \lambda_{\max}\left(\Lambda_5^{-1}\right)\delta_0 + 3\lambda_{\max}\left(\Lambda_5^{-1}\right)\delta_1\gamma_{ref} + \\
& \lambda_{\max}\left(\Lambda_7^{-1}\right) L_s\gamma_{ref} + \lambda_{\max}\left(\Lambda_8^{-1}\right) L_s\gamma_{ref}
\end{aligned}
$$

γ_{ref} is defined in Eq. (4.3), γ_{ξ} is defined in Eq. (4.7), L_s is defined in Eq. (8.16).

Proof. See Appendix B. ■

Remark 8 *A way to relate time-varying gain $K(t)$ calculated in this section with the gains that stabilize each local system of Eq. (4.8) is using the parallel distributed compensation (Tanaka 2001)*

$$K(t) = \sum_{l=1}^{M} \alpha_l(z(t)) K_l$$

That is, if $K(t)$ is designed to stabilize the trajectory tracking error (Δ_2) of the entire system and K_l, $l = 1, \ldots, m-1$ are designed to stabilize its corresponding local system, then the gain calculated as follows

$$K_M = \frac{K(t) - \sum_{l=1}^{M-1} \alpha_l(z(t)) K_l}{\alpha_M(z(t))}$$

must stabilize the m-th local system. A similar analysis can be proposed for the observation gain $L(t)$.

4.3 On the Riccati Differential Equation solution

We have introduced two new lemmas (based on necessary conditions for the existence of the solution of RDEs presented by [Kilicaslan and Banks, 2010] and [Kilicaslan and Banks, 2012]) to support when both Riccati equations (4.17) and (4.18) can have positive definite solution. This lemmas proposed a RDE with a positive sign in the quadratic term, unlike the common RDE structure. The first lemma presents necessary conditions to ensure the existence of positive definite and continuous solution for this class of Riccati equation such as the one obtained in this chapter. The following paragraphs contains the explanation of this lemma:

Lemma 9 *Consider a linear differential equation depending on the matrix $P \in \mathbb{R}^{n \times n}$*

of the form

$$\frac{d}{dt}P(t) = P(t)A(t) + A^{\top}(t)P(t) + P(t)R(t)P(t) + Q(t) \tag{4.24}$$

where the coefficients $A \in \mathbb{R}^{n\times n}$, $Q \in \mathbb{R}^{n\times n}$ *and* $R \in \mathbb{R}^{n\times n}$ *are time-varying matrices piecewise continuous. Additionally, consider the auxiliary problem of the initial-value problem given by*

$$\begin{bmatrix} X(t) \\ Y(t) \end{bmatrix} = \begin{bmatrix} \hat{\Phi}(t,0) - \int_0^{\top} \hat{\Phi}(t,s)R(t)\check{\Phi}(s,0)\,ds\left(P_0 - \bar{P}(0)\right) \\ \bar{P}_2(t_f)\hat{\Phi}(t,0) - Y_1(t)\left(P_0 - \bar{P}(0)\right) \end{bmatrix} \tag{4.25}$$

where $Y_1(t) = \bar{P}(t_f)\int_0^{\top} \hat{\Phi}(t,s)R(t)\check{\Phi}(s,0)\,ds + \check{\Phi}(t,0)$, *and* $\hat{\Phi}(t)$, $\check{\Phi}(t)$ *are transition matrices of* $\hat{A}(t) = -A^{\top}(t) - R(t)\bar{P}(t)$ *and* $\check{A}(t) = A^{\top}(t) + \bar{P}(t)R(t)$, *respectively, and* $\bar{P}(t)$ *is the unique solution of solutions of equilibrium points of Eq. (4.24) corresponding to* $A(t)$, $R(t)$, *and* $Q(t)$ *values evaluated in the time* $t \in [0, t_f]$.

Then, equation (4.24) has a solution in the interval $[0, t_f]$ *if and only if* $X(t)$ *is invertible for all* $t \in [0, t_f]$. *Moreover, the resulting solution is unique and it is represented as* $P(t) = Y(t)X^{-1}(t)$ *where* X *and* Y *are given in Eq. (4.25).*

The following Lemma introduces a constructive way to justify if the exact solution of the Riccati equation exists.

Lemma 10 *Consider the alternative representation of* X

$$X(t) = \hat{\Phi}(t,0)(I - D(t))$$

$$D(t) = \int_0^{\top} \hat{\Phi}^{-1}(s,0)R(t)\check{\Phi}(s,0)\,ds\left(P_0 - \bar{P}(0)\right) \tag{4.26}$$

If one of the following necessary conditions presented in [Kilicaslan and Banks, 2012] and [Kilicaslan and Banks, 2010] is satisfied, the invertibility of $D(t)$ *in Eq. (4.26) is ensured (then the existence of the positive definite solution of equation (4.24) is guar-*

anteed):

a) *If the rank of* $D(t)$ *is* $n\ \forall t \geq 0$*, i.e., if the following is satisfied*

$$\int_0^{\top} \hat{\Phi}^{-1}(s,0)\, R(t)\, \check{\Phi}(s,0)\, ds \left(P_0 - \bar{P}(0)\right) < I$$

and there is a $\bar{P}(t) \in \mathbf{P}(t)$*, then Eq. (4.24) has a unique solution* $\forall t \geq 0$*. In this case,* $D(t)$ *is invertible* $\forall t \geq 0$*.*

b) *If* $R(t) = 0$*, then Eq. (4.24) has a unique solution for any initial condition and* $\forall t \geq 0$*. In this case,* $D(t) = I$ *for any* $\bar{P}(t) \in \mathbf{P}(t)$ *and* $\forall t \geq 0$*.*

c) *If* P_0 *is taken as* $\bar{P}(0)$*, then the solution of Eq. (4.24) exists* $\forall t \geq 0$*. In this case,* $D(t) = I\ \forall t \geq 0$*.*

d) *If* $R(t)$ *is symmetric positive (negative) semidefinite and if there exist a certain symmetric* $\bar{P}(t) \in \mathbf{P}(t)$ *symmetric such that* $P_0 - \bar{P}(t)$ *is positive (negative) definite, then there exists the unique solution of Eq. (4.24)* $\forall t \geq 0$*. In this case,* $rank\left(D(t)\right) = n$ $\forall t \geq 0$ *[Sasagawa, 1982].*

f) *If a bound is introduced to the integral term of Eq. (4.26), that is*

$$\int_0^{\top} \left\|\hat{\Phi}^{-1}(s,0)\right\| \|R(t)\| \left\|\check{\Phi}(s,0)\right\| \|ds\| \left\|\left(P_0 - \bar{P}(0)\right)\right\| < Z \tag{4.27}$$

and there is $\bar{P}(t) \in \mathbf{P}(t)$*, then the solution exists* $\forall t \geq 0$*. In this case,* $rank\left(D(t)\right) = n$ $\forall t \geq 0$*.*

The detailed proof of these two lemmas can be found in [Kilicaslan and Banks, 2012] and [Kilicaslan and Banks, 2010]. More explicitly the necessary conditions for the existence of the solution of Eqs. (4.17) and (4.18) make use of the transition matrices $\hat{\Phi}(t)$, $\check{\Phi}(t)$ calculated using $\hat{\mathcal{A}}_1(t) = -\bar{\mathcal{A}}_1^{\top}(t) - \bar{\mathcal{R}}_1(t)\,\bar{P}_1(t)$ and $\check{\mathcal{A}}_1(t) = \bar{\mathcal{A}}_1^{\top}(t) + \bar{P}_1(t)\,\bar{\mathcal{R}}_1(t)$, respectively, where $\bar{P}_1(t)$ is the unique solution of the AREs of Eq. (4.24),

$$0 = \bar{P}_1(t_0)\,\bar{\mathcal{A}}_1(t_0) + \bar{\mathcal{A}}_1^{\top}(t_0)\,\bar{P}_1(t_0) + \bar{P}_1(t_0)\,\bar{\mathcal{R}}_1(t_0)\,\bar{P}_1(t_0) + \bar{\mathcal{Q}}_1(t_0), \tag{4.28}$$

These AREs are calculated corresponding to $\bar{\mathcal{A}}_1$ (Hurwitz), $\bar{\mathcal{R}}_1$, and $\bar{\mathcal{Q}}_1$ (real symmetric positive definite matrices) values evaluated in the time $t_0 \in [0, t_f]$. Conditions for the existence of the solutions of (4.28) are given in [Kucera, 1972]. Finally, Lemma 8 together with any of the necessary conditions in Lemma 9 is taken into account. The same conditions apply for Eq. (4.18).

4.4 Implementation issues

In order to implement the closed-loop system applying the proposed tracking controller based on the RDEs on-line solution the following procedure needs to be carried out. The schematic in Fig. 5.1 shows the architecture of the closed-loop system.

First the coupled RDEs in Eqs. (4.17) and (4.18) stated in Theorem 1 can be rewritten as follows:

$$\frac{d}{dt}P_1(t) = -P_1(t)\bar{A}(t) - \bar{A}^\top(t)P_1(t) + P_1(t)R_1(t)P_1(t) - \tilde{Q}_1(t) \tag{4.29}$$

$$\frac{d}{dt}P_2(t) = -P_2(t)\bar{A}(t) - \bar{A}^\top(t)P_2(t) + P_2(t)R_2(t)P_2(t) - \tilde{Q}_2(t) \tag{4.30}$$

The parameters of the RDEs was chosen to fulfil the existence conditions presented in Theorem 4. To solve Eqs. (4.29) and (4.30) simultaneously a simulation on MATLAB-Simulink considering initial conditions $P_{1,0}(0) = P_{1,0}$, $P_2(0) = P_{2,0}$ was implemented

- The matrices $\frac{d}{dt}P_1(t)$ of Eq. (4.29) and $\frac{d}{dt}P_2(t)$ of Eq. (4.30) are calculated using the values of $A(t)$, $C(t)$ which depend on $\alpha^i(x)$.
- $P_1(t)$ and $P_2(t)$ are obtained by integrating $\dot{P}_1(t)$ and $\dot{P}_2(t)$, respectively.
- $P_1(t)$ and $C(t)$ are used to calculate $L(t)$ in Eq. (4.22). $L(t)$ is introduced in Eq. (4.29) and (4.30).

- $P_1(t)$ and $B(t)$ are used to calculate $K(t)$ in Eq. (4.21). $K(t)$ is introduced in Eq. (4.30).

- The observer constructed using the same $A(t)$ and $B(t)$ of the fuzzy approximation provides the estimated states used in the control law calculation.

The integral operation divide the two processes in consequence there is no algebraic loop.

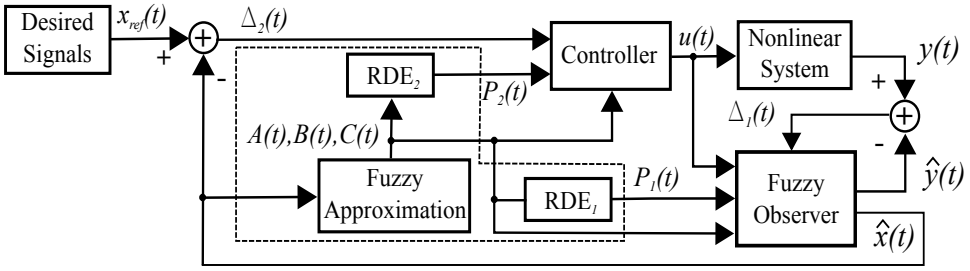

Figure 4.1: Closed-loop controller-observer system architecture based on RDEs.

4.5 Numerical results

In order to validate the performance of the RDE based on T-S fuzzy control, the AUV model presented in Section 2.2 in Chapter 2 is used. To design the T-S fuzzy observer for the nonlinear system in Eq.(2.3) of Section 2.2, it is necessary to probe that the system is observable considering $y = [q, w]^\top$ as the measurable output. In consequence, the observability rank test [Hermann and Krener, 1977] must be satisfied. The observability matrix for the nonlinear system in Eq.(2.3) is

$$(\chi) = \begin{bmatrix} 1 & 0 & 0 & -w & -w^2 & 0 \\ 0 & 0 & w & 0 & 0 & -w^2 \\ 0 & 1 & q & -p & -2pw & -2qw \end{bmatrix}^\top$$

Then, the nonlinear system is *locally observable* if neither $w = 0$ nor $p = 0$ or if neither $w = 0$ nor $q = 0$ simultaneously, or if w is different from zero.

To approximate the AUV system Eq. (2.4) by a fuzzy system, nine T-S fuzzy rules were used and the measurable states (q, w) are chosen as premise variables, that is, $z_1 = q$, $z_2 = w$. The k-th rule is:

$$\begin{aligned} R^k &: \text{If } q \in F_q^{h_k} \text{ and } w \in F_w^{h_k}, \\ \text{Then, } \frac{d}{dt}\chi(t) &= A^i\chi(t) + B^i\tau(t) + \tilde{f}^i(\chi(t)) + \zeta^i(t) \\ y(t) &= C^i\chi(t) + \tilde{h}^i(\chi(t)) \end{aligned} \tag{4.31}$$

where $i = 1 \cdots 6$, $k = 1 \cdots 9$, $A^i \in \Re^{3\times 3}$ and $B^i \in \Re^{3\times 2}$. For the fuzzification stage the sign of the measurable variables q and w is chosen as the fuzzy set, and the following three partitions are proposed: Negative (N), Zero (Z), and Positive (P). That is, $F_q^{h_k}, F_w^{h_k} \in \{N, Z, P\}$. The membership functions structure are selected as Fig. 3.2 in Chapter 3. The matrices A^i, B^i and C^i are chosen such that RDEs in Eqs. (4.17) and (4.18) have solution. The matrices that are used to represent the local dynamics are

$$A^1 = \begin{bmatrix} 0 & 3 & 2.5 \\ -3 & 0 & -2 \\ 0 & 0 & 0 \end{bmatrix}, A^2 = \begin{bmatrix} 0 & 1 & 0.5 \\ -1 & 0 & -1 \\ 0 & 0 & 0 \end{bmatrix}, A^3 = \begin{bmatrix} 0 & 2 & 0.8 \\ -2 & 0 & -0.5 \\ 0 & 0 & 0 \end{bmatrix},$$

$$A^4 = \begin{bmatrix} 0 & 1.3 & 5.2 \\ -1.3 & 0 & -4.5 \\ 0 & 0 & 0 \end{bmatrix}, A^5 = \begin{bmatrix} 0 & 3 & 2 \\ -3 & 0 & -4 \\ 0 & 0 & 0 \end{bmatrix}, A^6 = \begin{bmatrix} 0 & 1 & -0.2 \\ -1 & 0 & 0.3 \\ 0 & 0 & 0 \end{bmatrix},$$

$B^1 = ... = B^6 = B$, $C^1 = ... = C^6 = C$. In Eq. (4.20) $\Lambda_i\,(i = 1, \cdots, 6)$ are chosen as identity matrices.

First the T-S observer in (4.14) is implemented to estimate the unknown state $p(t)$ of the AUV dynamics with $\tau_p(t) = 0.1\sin(0.55t)$, $\tau_w(t) = 0.3\sin(t)$ and initial conditions $\chi_0 = [-1\ 0\ 1]^\top$, $\hat{\chi}_0 = [0\ 0\ 0]^\top$. In Fig. 4.2 the AUV trajectories against its estimates are shown

It can be seen the state $p(t)$ was closely reconstructed, however, it is important to note that this state reconstruction represents a difficult task because the T-S observer

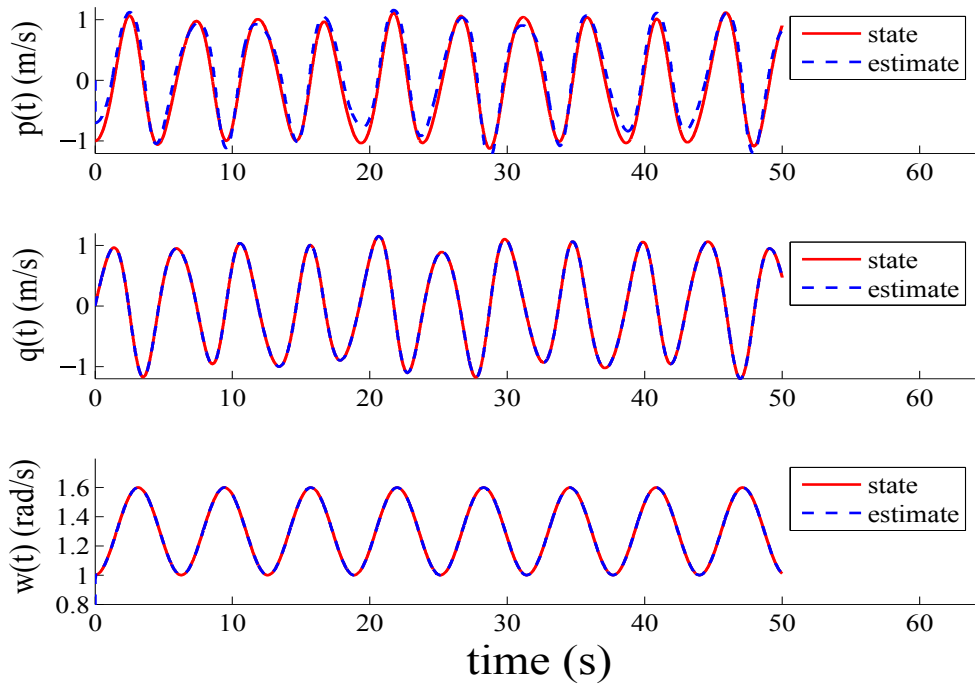

Figure 4.2: T-S observer estimation $p(t)$ vs AUV trayectories.

also carry on the identification of the AUV dynamics simultaneously. Also, it is observed the states that are measurable $q(t)$ and $w(t)$ was exactly reconstructed.

Now the controller in Eq. (4.21) and observer in Eq. (4.22) is implemented to reach a trajectory tracking of a reference dynamics, considering estimation of $p(t)$. Based on the motion planning method [Latombe, 1991], the dynamics of desired reference is chosen with the same structure as the AUV, it satisfies $s(\chi_{ref}(t)) = [2 + q_{ref}(t) w_{ref}(t), \; -p_{ref}(t) w_{ref}(t), \; 2]^\top$. Considering the initial conditions $\chi_0 = [2\ 0\ 0]^\top$, $\hat{\chi}_0 = [0\ 0\ 0]^\top$, $\chi_{ref,0} = [0\ 0\ 0]^\top$.

The time-varying feedback control gain $K(t)$ and the time-varying observer gain $L(t)$ are shown in Fig. 4.3

The control signals applied to the AUV system are shown in Fig. 4.4.

In Fig. 4.5 the reference states, the trajectories of the closed-loop system using the reconstructed states by the T-S observer, and the estimated states are shown.

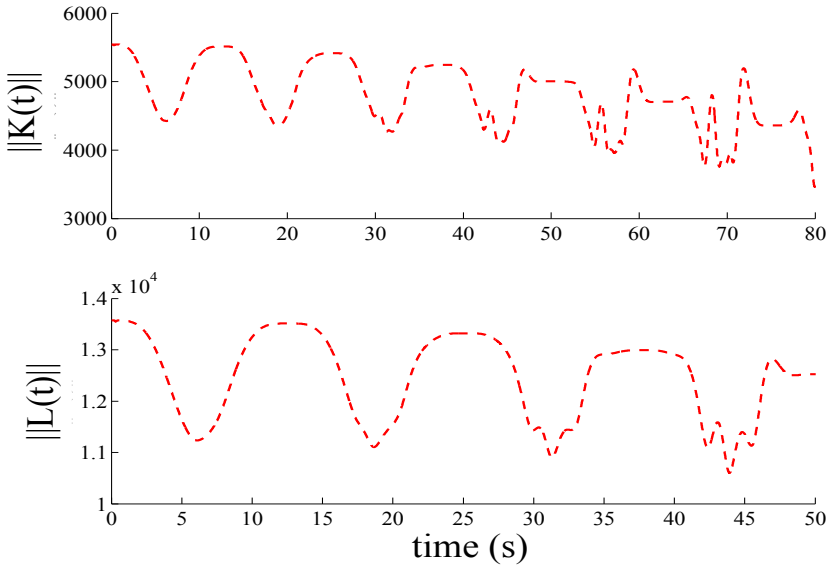

Figure 4.3: Norm of the time-varying controller and observer gains based on Riccati differential equation.

It can be seen that the state estimation is sufficient for the AUV closed-loop system to reach a trajectory tracking. It is observed the trajectories converges in approximately 2.0 seconds to the reference states.

The norm of estimation error Δ_1 and tracking error Δ_2 are shown in Fig. **??**. It can be seen that these errors belongs to a bounded region.

Now the proposed RDE based method was compared with the popular LMI based T-S fuzzy controller-observer. The LMI method use the PDC structure, so the controller has the form

$$\tau(t) = K_{LMI}(t)\,\Delta(t), \quad K_{LMI}(t) = \sum_{i=1}^{6} \alpha_i(t)\,K_i$$

where $K_1 = \begin{bmatrix} 10.0630 & -4.9061 & 5.2125 \\ 2.9012 & -5.6406 & 7.9370 \end{bmatrix}$, $K_2 = \begin{bmatrix} 8.9048 & -15.9718 & 3.4094 \\ 3.0900 & -18.0274 & 9.0952 \end{bmatrix}$,

$K_3 = \begin{bmatrix} 11.5463 & -14.1915 & 2.1965 \\ 1.7997 & -5.2276 & 6.4537 \end{bmatrix}$, $K_4 = \begin{bmatrix} 6.5180 & -1.0180 & 6.9890 \\ 1.5872 & -7.1081 & 11.4820 \end{bmatrix}$,

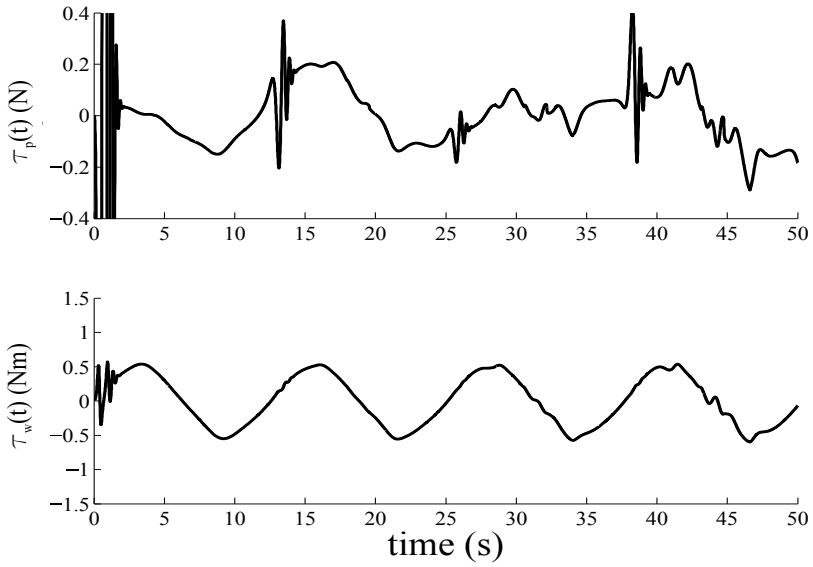

Figure 4.4: Control signals, $\tau_p(t)$ (force in the x-axis) and $\tau_w(t)$ (torque respect to the z-axis).

$$K_5 = \begin{bmatrix} 8.1665 & -1.2125 & 4.8885 \\ 2.8753 & -5.5906 & 9.8335 \end{bmatrix}, K_6 = \begin{bmatrix} 11.3898 & -30.4775 & -1.8273 \\ -2.0187 & 11.7284 & 6.6102 \end{bmatrix}$$

and, the observer gain has the form

$$L_{LMI}(t) = \sum_{i=1}^{6} \alpha_i(t) L_i$$

where

$$L_1 = \begin{bmatrix} -11.0000 & 13.0000 & 0 \\ 2.5000 & -2.0000 & 5.0000 \end{bmatrix}^\top, L_2 = \begin{bmatrix} -41.0000 & 13.0000 & 0 \\ 0.5000 & -2.0000 & 5.0000 \end{bmatrix}^\top,$$

$$L_3 = \begin{bmatrix} -19.0000 & 13.0000 & 0 \\ 0.8000 & -0.5000 & 5.0000 \end{bmatrix}^\top, L_4 = \begin{bmatrix} -31.0077 & 13.0000 & 0 \\ 5.2000 & -4.5000 & 5.0000 \end{bmatrix}^\top,$$

$$L_5 = \begin{bmatrix} -11.0000 & 13.0000 & 0 \\ 2.0000 & -4.0000 & 5.0000 \end{bmatrix}^\top, L_6 = \begin{bmatrix} -41.0000 & 13.0000 & 0 \\ -0.2000 & 0.3000 & 5.0000 \end{bmatrix}^\top$$

The simulation results are shown in Fig. 4.6. As can be seen the RDE based method has a norm of the trajectory tracking error less than the LMI based method.

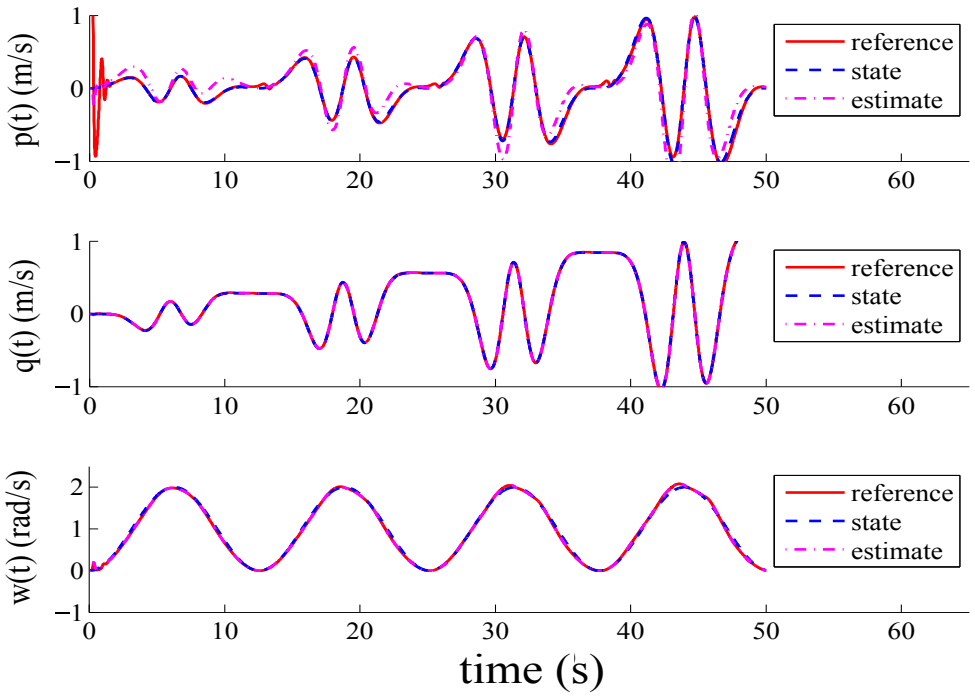

Figure 4.5: Trajectory tracking of the AUV implementing a controller using measurable states and $p(t)$ estimate, observed states and reference states.

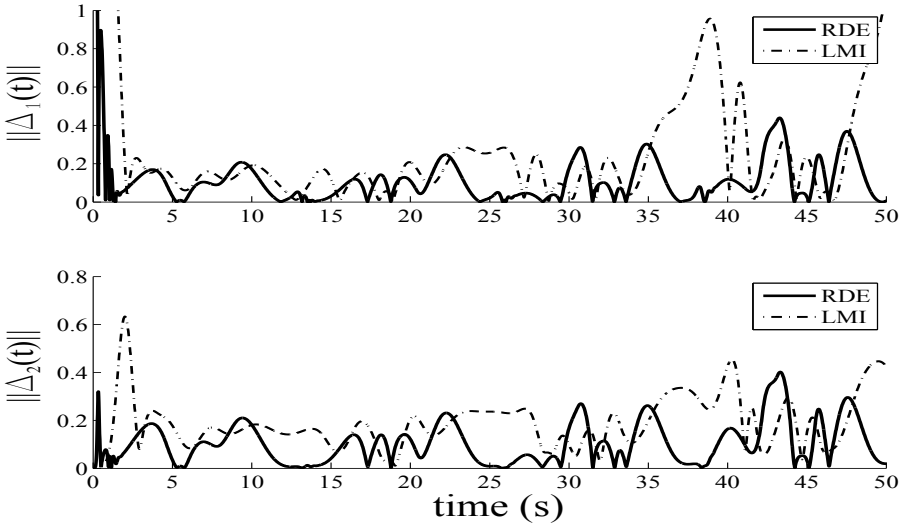

Figure 4.6: Mean-square error of estimation and trajectory tracking.

4.6 Conclusions of the chapter

A state feedback control and an state observer were designed in this study based on the Lyapunov stability analysis for a T-S fuzzy system considering an incomplete state information. The approximation of the uncertain nonlinear dynamics by the T-S fuzzy system results in a linear time-varying system. In consequence a nonconventional Lyapunov time-varying function was used to prove the ultimate boundedness of the tracking error between this linear time-varying system T-S and a reference system. The controller design was supported on the existence of two time-varying matrix RDEs. Sufficient conditions were obtained to characterize the positiveness of solutions for the RDEs. The controller-observer gains depend on the solution of the RDEs positive definite solutions. A set of numerical simulations using an AUV mathematical model with respect to rigid body-fixed frame was carried out in order to follow desired linear velocities. Also the simulations showed how to implement the results obtained in this study as well as the superiority of the result obtained here compared to the regular control design based on LMIs. The advantage of the proposed method with respect to the LMI method is that the calculation of the controller-observed gains are performed on-line while the T-S fuzzy system evolves, unlike the gains obtained using the LMI method calculated off-line.

5

Takagi-Sugeno Fuzzy Control using Differential Neural Networks

In this chapter, an alternative methodology based on a neuro-fuzzy system is proposed to guarantee feasible solutions to accomplish two goals: a) a non-parametric identification used to approximate an uncertain nonlinear perturbed system by a T-S DNN identifier, and b) design an automatic controller that must solve the trajectory tracking problem based on the identifier trajectories. In this study, we are using the Lyapunov formalism to provide sufficient conditions that supports the control design. The controller structure uses the positive definite solution of two Riccati Differential Equations (RDE). Based on the assumption regarding the existence of solution for these two equations, the uncertain nonlinear system states are identified by the estimated system trajectories. On opposite to the method proposed in [Chairez, 2013b], only two RDE equations must be solved instead of several algebraic Riccati equations (ARE). The RDE methodology simplifies the numerical algorithm because there exist well-known conditions to ensure their solution [Kilicaslan and Banks, 2012], [Kilicaslan and Banks, 2010]. Also, these RDEs are solved on-line because their solution depends on the states that evolve through

time, unlike the AREs in [Chairez, 2013b], [Chairez, 2013a], [Viana and Chairez, 2010] that are solved off-line. In order to solve the DNN problem it is necessary to implement two learning levels. First, a primary approximation of the nominal dynamics weight matrix $W_0^{[i,j]}$ is obtained by an off-line learning method. Then, an identification of the DNN nominal dynamics that represent the nonlinear system considering the approximation of $W_0^{[i,j]}$ obtained in the off-line level is carried out by the on-line identifier system. However, the methodology proposed in this chapter suppose that the off-line weight matrix $W_0^{[i,j]}$ is known. This off-line weight matrix can be obtained using the learning algorithm proposed in [Chairez, 2009]. Ultimate boundedness concept [Khalil, 2002] is used to define the stability sense that governs the identification and trajectory tracking errors.

5.1 Continuous neuro-fuzzy identifier

Consider an uncertain nonlinear system of order $2n$, that is

$$\begin{aligned} \frac{d}{dt}x_a\left(t\right) &= x_b\left(t\right) \\ \frac{d}{dt}x_b\left(t\right) &= f\left(x\left(t\right)\right) + g\left(x_a\left(t\right)\right)u\left(t\right) + \xi\left(x\left(t\right),t\right) \end{aligned} \tag{5.1}$$

where $x_a \in \mathbb{R}^n$, $x_a = \left[x_1, x_2, \ldots, x_n\right]^\top$ is the position vector and $x_b \in \mathbb{R}^n$, $x_b = \left[x_{n+1}, x_{n+2}, \ldots, x_{2n}\right]^\top$ is the velocity vector. Both vectors compose the state vector $x = \left[x_a^\top, x_b^\top\right]^\top$. Let X be an universe of discourse equivalent to $x \in X \subseteq \mathbb{R}^{2n}$. The bounded function $u \in \mathbb{R}^m$ is the control function. Throughout this study, we assume the state x is available.

The nonlinear continuous functions $f : \mathbb{R}^{2n} \to \mathbb{R}^n$ and $g : \mathbb{R}^n \to \mathbb{R}^{n\times m}$ $(m < n)$ each one is composed of n nonlinear functions that describe the system dynamics. In this study the structure of the function g is supposed to be known. The term $\xi : \mathbb{R}^{n+1} \to \mathbb{R}^n$ represents either parameter variations, external perturbations, unmodeled dynamics, etc. We propose an important assumption: the uncertainties $\xi\left(x,t\right)$

satisfy the inequality

$$\|\xi(x,t)\|^2 \leq \gamma_0 + \gamma_1 \|x\|^2, \;\; \gamma_0, \gamma_1 \in \mathbb{R}^+, \forall t \geq 0 \tag{5.2}$$

Then if we consider the space domain of x can be partitioned in $\mathcal{N}$ subregions then Eq. (5.1) can be expressed for each region as follows

$$\begin{gathered} \frac{d}{dt}x_a(t) = x_b(t) \\ \frac{d}{dt}x_b(t) = f^{[i]}(x(t)) + g(x_a(t))\,u(t) + \xi^{[i]}(x(t),t) \\ i = 1,\ldots,\mathcal{N} \end{gathered} \tag{5.3}$$

Therefore, the system dynamics in each region (Eq. (5.3)) may be captured by a set of fuzzy implications that characterizes local relations in the state space using the T-S inference method [Tanaka and Wang, 2001] as follows:

$$\begin{gathered} \mathrm{R}_j^i : \text{IF } x_1 \text{ is } M_{1,q_j}^{[i]} \text{ and IF } x_2 \text{ is } M_{2,q_j}^{[i]} \text{ and } \ldots \text{ and IF } x_n \text{ is } M_{n,q_j}^{[i]} \\ \text{THEN } \frac{d}{dt}x_a(t) = x_b(t) \\ \frac{d}{dt}x_b(t) = f^{[i,j]}(x(t)) \\ j = 1,\ldots,R \end{gathered} \tag{5.4}$$

where R_j^i is the j-th fuzzy rule, R is the number of inference rules, i determines the subregion, $x_a = [x_1, x_2, \ldots, x_n]^T$ are the premise variables (position vector), $M_{r,q_j}^{[i]}$ ($r = 1 \ldots n$) are the fuzzy sets for the premise variables x_j, q_j is the membership function number for each premise variable r.

Remark 11 *In the case treated here due to the assumption that $g(\cdot)$ is known, it is not necessary to approximate it.*

The system description presented in Eq. (5.4) is a class of system interpolator. This interpolation is run by the state values, x_a, and determine the contribution of each subsystem in the final state dynamics. Therefore, a system constructed as the weighted

contribution of all subsystems $f^{[i,j]}(x)$ (some of which will not contribute all the time) is derived. The individual functions $f^{[i,j]}(x)$ can be any of the elements included in the set $f^{[i,j]}(x) \in F(x)$, where $F\left(x^{[i]}\right)$ contains a maximum of R selectable systems (in general, there are much fewer systems than segmentations produced by the space partition $\left[M_{1,q_j}^{[i]}, M_{2,q_j}^{[i]}, \ldots, M_{n,q_j}^{[i]}\right]$). Most existing results regarding this class of fuzzy model have been used to express the local information of each fuzzy implication (rule) by a linear system. The overall fuzzy model of the system is achieved by fuzzy blending of the linear models as

$$f^{[i,j]}(x) = A_a^{[i,j]} x_a + A_b^{[i,j]} x_b + \tilde{f}^{[i,j]}(x) \tag{5.5}$$

where $\tilde{f}^{[i,j]}(x) = f^{[i,j]}(x) - A_a^{[i,j]} x_a - A_b^{[i,j]} x_b$. The matrices $A_a^{[i,j]}$, $A_b^{[i,j]} \in \mathbb{R}^{n \times n}$ are selected in such a way that they are within a subspace $X^{[j]}$ defined by $X^{[j]} := M_{1,q_j}^{[i]} \cap M_{2,q_j}^{[i]} \cap \ldots \cap M_{n,q_j}^{[i]}$. Therefore, the trajectories belonging to submanifold $X^{[j]}$ are $X^{[j]} := \left\{ x \in \mathbb{R}^n | x_l \in M_{l,q_j}^{[i]} \right\}$, where x_l is the lth component of x. The fuzzy sets $M_{r,q_j}^{[i]}$, $r = \overline{1,n}$ define the membership functions. If we consider the usual linear system decomposition in Eq. (5.5), the representation given in the last equation yields to the following multi-model system or T-S system for Eq. (5.3):

$$\begin{aligned} \frac{d}{dt} x_a(t) &= \sum_{j=1}^{R} \alpha^{[i,j]}(t)\, x_b(t) \\ \frac{d}{dt} x_b(t) &= \sum_{j=1}^{R} \alpha^{[i,j]}(t) \left[A_a^{[i,j]} x_a(t) + A_b^{[i,j]} x_b(t) \right] + g(x_a(t))\, u(t) + \\ &\sum_{j=1}^{R} \alpha^{[i,j]}(t)\, \tilde{f}^{[i,j]}(x(t), u(t)) + \sum_{j=1}^{R} \alpha^{[i,j]}(t)\, \xi^{[i,j]}(x(t), t) \end{aligned} \tag{5.6}$$

where $\sum_{j=1}^{R} \alpha^{[i,j]}(t)\, \tilde{f}^{[i,j]}(x,u)$ is the modeling error produced by the fuzzy approximation. The value of $\alpha^{[i,j]}$ depends on the construction method selected for the fuzzy system. For example, if a singleton fuzzifier with a product inference and a weighted average

deffuzifier is used, we have

$$\alpha^{[i,j]} = \mu^{[i,j]} \left(\sum_{k=1}^{R} \mu^{[i,k]} \right)^{-1}, \quad \mu^{[i,j]} = \prod_{p=1}^{R} \mu_p^{[i,j]}, \quad \mu_p^{[i,j]} := \mu_p^{[i,j]} (x_p) \tag{5.7}$$

where $\mu_p^{[i,j]}$ is the membership degree of x_p in the fuzzy set $M_{p,q_j}^{[i]}$ $(j = 1, \ldots, R)$. In this area, two important elements have not been discussed in depth: (a) how to select the matrices $A_a^{[i,j]}$ and $A_b^{[i,j]}$ in such a way that the system approximation within each subspace $X^{[j]}$ is acceptable (the error is small or even zero); and (b) what happens in the interface between $X^{[j]}$ and $X^{[k]}$ (for $j \neq k$). In many references there are small jumps in the frontier between subspaces. This effect is observed when linear controllers or observers are used for the class of general T-S systems of the form given in Eq. (5.6).

Based on these natural weakness in classical T-S fuzzy systems, truly adaptive algorithms can be applied to achieve a good approximation of Eq. (5.3). Therefore, applying a combined scheme composed by a T-S decomposition with a set of R DNNs approximating each subsystem $f^{[i,j]}(x_a, x_b)$ seems to be a promising alternative for a better approximation of the uncertain system. This construction based on several continuous neural networks is an interesting method for improving the approximation produced by the adaptive scheme presented here. This methodology covers the classic single DNN approximation, but also increases the class of nonlinear systems that can be analysed using the DNN scheme.

5.1.1 Neuro-fuzzy identifier using DNN approximation

Considering the neural network approximation capability stated in the Stone-Weierstrass and Kolmogorov theorems [Cotter, 1990] the nonlinear functions $f(\cdot,\cdot)$ in Eq. (5.3) can always be represented as a composition of nominal systems $f_0^{[i,j]}:\mathbb{R}^{2n}\to\mathbb{R}^n$ and their corresponding modeling errors $\tilde{f}^{[i,j]}:\mathbb{R}^{2n}\to\mathbb{R}^n$. Then, Eq. (5.3) can be expressed as

$$\begin{gathered}\frac{d}{dt}x_a(t)=\sum_{j=1}^{R}\alpha^{[i,j]}(t)\,x_b(t)\\ \frac{d}{dt}x_b(t)=\sum_{j=1}^{R}\alpha^{[i,j]}(t)\,f_0^{[i,j]}\left(x(t)\,|W_0^{[i,j]}\right)+g(x_a(t))\,u(t)+\sum_{j=1}^{R}\alpha^{[i,j]}(t)\,\tilde{f}^{[i,j]}(x(t))+\\ \sum_{j=1}^{R}\alpha^{[i,j]}(t)\,\xi^{[i,j]}(x(t),t)\end{gathered}\tag{5.8}$$

where

$$\tilde{f}^{[i,j]}(x)=f^{[i,j]}(x)-f_0^{[i,j]}\left(x|W_0^{[i,j]}\right)$$

In this case the so-called nominal dynamics is selected as a DNN dynamics. Here, the set of parameters $W_0^{[i,j]}$ should be adjusted to obtain the best possible matching between the nominal dynamics $f_0^{[i,j]}$ and nonlinear dynamics $f^{[i,j]}$.

Considering that each individual nonlinear dynamic $f_0^{[i,j]}\left(x|W_0^{[i,j]}\right)$ is locally Lipschitz within each subsystem and under that class of admissible controls u, the following upper bound for modeling error $\tilde{f}^{[i,j]}(x)$ can be derived:

$$\left\|\tilde{f}^{[i,j]}(x)\right\|^2\leq\tilde{f}_0^{[i,j]}+\tilde{f}_1^{[i,j]}\|x\|^2,\quad \tilde{f}_0^{[i,j]},\tilde{f}_1^{[i,j]}\in\mathbb{R}^+,\quad \tilde{f}_0^{[i,j]},\tilde{f}_1^{[i,j]}<\infty,\tag{5.9}$$

Then,

$$\left\|\tilde{f}^{[i,j]}(x)\right\|^2\leq\tilde{f}_0^{[i,j]}+2\tilde{f}_1^{[i,j]}\|x_a\|^2+2\tilde{f}_1^{[i,j]}\|x_b\|^2\tag{5.10}$$

Remark 12 *The external disturbances can be associated only to the term $\xi(x,t)$ and the unmodeled dynamics and uncertainties can be introduced in the modeling error term $\tilde{f}(x,u)$ which satisfies a sector boundary condition.*

According to the DNN approach [Poznyak et al., 2001], the nominal dynamics in Eq. (5.8) for each subsystem is selected as

$$f_0^{[i,j]}\left(x|W_0^{[i,j]}\right) := A_1^{[i,j]}x_a + A_2^{[i,j]}x_b + W_0^{[i,j]}\sigma\left(x\right) \tag{5.11}$$

where $A_1^{[i,j]}, A_2^{[i,j]} \in \mathbb{R}^{n\times n}$, $W_0^{[i,j]} \in \mathbb{R}^{n\times p}$, $\sigma\left(x\right) \in \mathbb{R}^p$. This structure has been tested for the design of adaptive observers and controllers [Chairez, 2009]. In Eq. (5.11) the vector of parameters $W_0^{[i,j]}$ is assumed to be unknown but constant. Therefore, the problem of approximation can be understood in the sense of finding the structure of $\hat{f}^{[i,j]}\left(\hat{x}\left(t\right)|W^{[i,j]}\left(t\right)\right)$ working together with a special adaptive law for $W^{[i,j]}\left(t\right)$. Here, $\hat{x} \in \mathbb{R}^{2n}$, $\hat{x} = \left[\hat{x}_a^\top, \hat{x}_b^\top\right]^\top$, $\hat{x}_a, \hat{x}_b \in \mathbb{R}^n$ represents the state vector of the dynamic approximation, namely the adaptive identifier. The special law for $W^{[i,j]}\left(t\right)$ should depend on the identification error, that is the difference between the uncertain system and the adaptive identifier. The structure of such an approximation can be presented in a general form as

$$\begin{aligned}
\frac{d}{dt}\hat{x}_a\left(t\right) &= \sum_{j=1}^{R}\alpha^{[i,j]}\left(t\right)\hat{x}_b\left(t\right)\\
\frac{d}{dt}\hat{x}_b\left(t\right) &= \sum_{j=1}^{R}\alpha^{[i,j]}\left(t\right)\hat{f}^{[i,j]}\left(\hat{x}\left(t\right)|W^{[i,j]}\left(t\right)\right) + g\left(x_a\left(t\right)\right)u\left(t\right)\\
\frac{d}{dt}W^{[i,j]}\left(t\right) &= \Theta^{[i,j]}\left(W^{[i,j]}\left(t\right), x\left(t\right), \hat{x}\left(t\right)\right)
\end{aligned} \tag{5.12}$$

Remark 13 *Many DNNs are used to locally approximate the uncertain nonlinear system because using only one DNN makes difficult to approximate the entire nonlinear system behaviour including fast changes in the nonlinear system, which can generate oscillations during the identification process.*

Remark 14 *It is possible to consider $g(x)$ is uncertain in order and identify it using a DNN as well. However, during the identification process of this function, it is possible this approximation can reach values near to zero leading to a loss of controllability of the system. So, it would be necessary to apply certain restrictions in the synaptic weights of the DNN to avoid this situation.*

The set of functions $\Theta^{[i,j]}(\cdot)$ are called the learning or adaptive algorithms for adjusting the DNN weights and are designed using the second Lyapunov method. Following the nominal structure introduced in Eq. (5.11), the set of nonlinear functions $\hat{f}^{[i,j]}\left(\hat{x}|W^{[i,j]}\right)$ may be defined as an off-line system composed of the control independent dynamic part by a combination of Hurwitz fixed matrices $A_1^{[i,j]}, A_2^{[i,j]} \in \mathbb{R}^{n\times n}$ (selected by the designer) and a nonlinear part approximated by time-varying parameters $W^{[i,j]}$ with a sigmoid multiplier. The complete structure of the approximation system is

$$\hat{f}^{[i,j]}\left(\hat{x}^{[i]}|W^{[i,j]}\right) := A_1^{[i,j]}\hat{x}_a^{[i]} + A_2^{[i,j]}\hat{x}_b^{[i]} + W^{[i,j]}\sigma\left(\hat{x}^{[i]}\right) \tag{5.13}$$

In reality, the control actions are used just to develop a well-posed identification scheme. Therefore, without loss of generality, the admissible set of controls can be defined as

$$U_{adm} := \left\{u : \|u\|^2 \leq \gamma_{u1} + \gamma_{u2}\|\Delta_{id}\|^2\right\}. \tag{5.14}$$

where $\Delta_{id} := x - \hat{x}$ is the identification error.

The control functions that we proposed must satisfy the restriction in Eq. (5.14), e.g., feedback controllers based on the identified states. It is clear that the class of external functions must be useful to fulfil the persistent excitation condition required to solve the identification problem. This assumption implies the possibility of using a DNN for each domain and to obtain enough information to achieve a good non-parametric approximation.

The activation sector function $\sigma(\cdot)$ are usually constructed as a sigmoid function,

$$\sigma_k(x) := a_k \left(1 + b_k e^{-C^\top x}\right)^{-1}, \quad k = \overline{1,p} \tag{5.15}$$

where the parameters a_k, b_k and $C = [c_1 \dots c_{2n}]^\top$ are positive. There are some alternatives for adjusting these parameters, but for simplicity they were adjusted by trial and error. This function satisfy the following sector condition:

$$\|\tilde{\sigma}(x, \hat{x})\|^2 \leq L_\sigma \|\Delta_{id}\|^2_{\Lambda_\sigma} \tag{5.16}$$

where

$$\tilde{\sigma}(x, \hat{x}) = \sigma(x) - \sigma(\hat{x}) \tag{5.17}$$

and is globally bounded on $\mathbb{R}^n$, that is, $\|\sigma(\cdot)\| \leq \sigma^+$. L_σ is a known positive constant and $\Lambda_\sigma \in \mathbb{R}^{n\times n}$, $\Lambda_\sigma = (\Lambda_\sigma)^\top > 0$. In Eq. (5.13), the constant parameters $A_1^{[i,j]}$, $A_2^{[i,j]}$ and the time-varying parameters $W^{[i,j]}$ should be properly adjusted to guarantee a good state approximation.

The function $\sigma(\cdot) : \mathbb{R}^n \to \mathbb{R}^p$ is nonlinear and Lipschitz, and considering $\sigma(0) = 0$, the following inequality is satisfied

$$\|\sigma(\hat{x})\|^2 \leq \bar{L}_\sigma \|\hat{x}\|^2 \tag{5.18}$$

where $\bar{L}_\sigma > 0$. Then,

$$\|\sigma(\hat{x})\|^2 \leq 2\bar{L}_\sigma \|\hat{x}_a\|^2 + 2\bar{L}_\sigma \|\hat{x}_b\|^2 \tag{5.19}$$

5.1.2 Identifier structure

For the identifier structure described in Eq. (5.13), the dynamics may be expressed as

$$\frac{d}{dt}\hat{x}_a(t) = \sum_{j=1}^{R} \alpha^{[i,j]}(t)\,\hat{x}_b(t)$$
$$\frac{d}{dt}\hat{x}_b(t) = \sum_{j=1}^{R} \alpha^{[i,j]}(t)\left[A_1^{[i,j]}\hat{x}_a(t) + A_2^{[i,j]}\hat{x}_b(t) + W^{[i,j]}(t)\,\sigma(\hat{x}(t))\right] + g(x_a(t))\,u(t) \tag{5.20}$$

The main goal behind application of this identifier can be stated in the following manner.

Problem. For the uncertain nonlinear system of Eq. (5.3), the value of matrices $A_1^{[i,j]}$, $A_2^{[i,j]}$ must be selected and a set of nonlinear adaptive producers $\Theta^{[i,j]}$ must be designed to adjust the time-varying parameters $W^{[i,j]}(t)$,

$$\frac{d}{dt}W^{[i,j]}(t) = \Theta^{[i,j]}\left(W^{[i,j]}(t), \Delta_{id}(t)\right), \quad W^{[i,j]}(0) \text{ is fixed} \tag{5.21}$$

are fixed in such a way that estimation of the upper bound of the identification error Δ_{id} do not diverge. We use a practical stability framework to show that $\limsup_{t\to\infty} \|\Delta_{id}(t)\| \leq \rho$. Moreover, we have to demonstrate that in the absence of external signals considered as noise and of modeling inaccuracies, the error Δ_{id} must converge to zero asymptotically. The proposed identifier requires a set of assumptions introduced here.

The class of functions $f^{[i,j]} : \mathbb{R}^{2n} \to \mathbb{R}^n$ and $g^{[i,j]} : \mathbb{R}^{2n} \to \mathbb{R}^{n\times n}$ are Lipschitz continuous in $x \in X$; that is, for all $x, y \in X$ there exist constants $L_f^{[i]}$, $L_g^{[i]}$ such that

$$\left\|f^{[i,j]}(x) - f^{[i,j]}(y)\right\| \leq L_f^{[i,j]}\|x-y\|, \quad \left\|g^{[i]}(x) - g^{[i]}(y)\right\| \leq L_g^{[i]}\|x-y\| \tag{5.22}$$

where $x, y \in \mathbb{R}^{2n}$, $0 < L_f^{[i]}, L_g^{[i]} < \infty$. The signals

$$\left\|\xi^{[i,j]}(x,t)\right\|^2 \leq \gamma_\xi,\ \gamma_\xi \in \mathbb{R}^+,\ \forall i \in [1,M],\ j \in [1,R],\ \forall t \geq 0 \tag{5.23}$$

In this work one level training strategy of DNN identifiers is implemented. In this case we suppose that the matrix $W_0^{[i,j]}$ of the nominal system in Eq. (5.11) can be obtained by an off-line training through a new weight matrix $W_{to}^{[i,j]}(t)$, for example using the learning process proposed in [Chairez, 2009]. We suppose that $W_0^{[i,j]}$ is well characterized by $W_{to}^{[i,j]}(t)$ such that the error $W_0^{[i,j]} - W_{to}^{[i,j]}(t)$ is bounded by some scalar ε. Considering that $W_{to}^{[i,j]}(t)$ is known an on-line training of the weight matrix $W^{[i,j]}(t)$ is developed. This on-line training is used to identify the dynamic of the uncertain system (5.8) by the identifier in Eq. (5.20).

5.2 Trajectory tracking problem

This section states the trajectory tracking problem of desired signals by the uncertain nonlinear system using the information provided by the identifier proposed in the previous section as well as the conditions of the desired signals need to fulfil.

Statement. For the uncertain nonlinear system the goal is to force its states to track desired signals using the estimated states provided by the neuro-fuzzy identifier proposed in Section 2, i.e., starting from any reachable local arbitrary point in the space, the system must asymptotically converge to the desired trajectory. In other words, the identifier trajectory should coincide with the desired one as close as it is possible, i.e., the tracking errors Δ_{tr} between the identifier trajectories and desired positions should be zero when possible but if not, the tracking error should be bounded with an upper bound characterized by the effect of perturbations and uncertainties, namely $\limsup_{t\to\infty} \|\Delta_{tr}\| \leq \beta$, $\Delta_{tr} = \hat{x} - x_{ref}$ where x_{ref} is the desired trajectory.

The nonlinear reference model is given by

$$\begin{aligned} \frac{d}{dt} x_{ref,a}(t) &= x_{ref,b}(t), \\ \frac{d}{dt} x_{ref,b}(t) &= s_b(x_{ref,b}(t), t), \ \forall t \geq 0 \end{aligned} \tag{5.24}$$

where $x_{ref,a}, x_{ref,b} \in \mathbb{R}^n$ and the function $s_b(\cdot,\cdot) : \mathbb{R}^{n+1} \to \mathbb{R}^n$ is nonlinear and Lipschitz,

satisfying

$$\|s_b(x_{ref,b})\|^2 \leq L_{s,b}\|x_{ref,a}\|^2, \quad L_{s,b} > 0 \tag{5.25}$$

The references $x_{ref,a}$, $x_{ref,b}$ are bounded by design

$$\|x_{ref,a}\|^2 \leq \gamma_{ref,a}, \quad \|x_{ref,b}\|^2 \leq \gamma_{ref,b}, \quad \gamma_{ref,a}, \gamma_{ref,b} > 0 \tag{5.26}$$

5.3 Identification and trajectory tracking convergence

The following theorem describes the performance of the identification algorithm and the trajectory tracking based on DNN methodology. Also, in order to assure the T-S system do not turn unstable the following must be satisfied:

Theorem 15 *(Stability of the identification and trajectory tracking errors). Assume that the upper bounds given in Eqs. (5.16) and (5.23) are satisfied. Consider the application of the DNN identifier presented in (Eq. (5.13)) adjusted by the adaptive law presented in (5.32). If there exist a positive scalar* α_B *and matrices* $\Lambda_i = (\Lambda_i)^\top > 0$, $r = 1 \ldots 9$, Λ_1, $\Lambda_3 \in \mathbb{R}^{2n\times 2n}$, Λ_4, Λ_5, Λ_6, $\Lambda_7, \Lambda_8, \Lambda_9 \in \mathbb{R}^{n\times n}$, $\Lambda_2 \in \mathbb{R}^{p\times p}$ *and* $|\min_t\{\lambda_{min}(\mathcal{A}(t))\}| > max(\alpha_B)$ *such that the following Riccati differential equations (RDE) [Kilicaslan and Banks, 2010] have symmetric positive solutions:*

$$Ric(P_1(t)) = \frac{d}{dt}P_1(t) + P_1(t)\bar{\mathcal{A}}_1(t) + \bar{\mathcal{A}}_1^\top(t)P_1(t) + P_1(t)\bar{\mathcal{R}}_1(t)P_1(t) + \bar{\mathcal{Q}}_1(t) \tag{5.27}$$

$$Ric(P_2(t)) = \frac{d}{dt}P_2(t) + P_2(t)\bar{\mathcal{A}}_2(t) + \bar{\mathcal{A}}_2^\top(t)P_2(t) + P_2(t)\bar{\mathcal{R}}_2(t)P_2(t) + \bar{\mathcal{Q}}_2(t) \tag{5.28}$$

where

$$\bar{\mathcal{A}}_1(t) = \mathcal{A}(t) + \frac{\alpha_B}{2}I_{2n\times 2n}, \quad \bar{\mathcal{A}}_2(t) = \mathcal{A}(t) - \mathcal{B}_1 K_{tr} + \frac{\alpha_B}{2}I_{2n\times 2n}$$

$$\mathcal{A}(t)=\begin{bmatrix} 0_{n\times n} & \sum_{j=1}^{R}\alpha^{[i,j]}(t)\,I_{n\times n} \\ \sum_{j=1}^{R}\alpha^{[i,j]}(t)\,A_1^{[i,j]} & \sum_{j=1}^{R}\alpha^{[i,j]}(t)\,A_2^{[i,j]} \end{bmatrix},\ \mathcal{B}_1=\begin{bmatrix} 0_{n\times n} \\ I_{n\times n} \end{bmatrix},\ \mathcal{B}_2=\begin{bmatrix} I_{n\times n} \\ 0_{n\times n} \end{bmatrix}$$

$$\bar{\mathcal{R}}_1=\mathcal{B}_1\sum_{j=1}^{R}\alpha_B^{[i,j]}(t)\,W_0^{[i,j]}\Lambda_2\sum_{s=1}^{R}\alpha_B^{[i,s]}(t)\left[W_0^{[i,s]}\right]_1^{\top}\mathcal{B}_1^{T}+\Lambda_3+\mathcal{B}_1\Lambda_4\mathcal{B}_1^{\top}+\mathcal{B}_1\Lambda_5(t)\,\mathcal{B}_1^{\top}$$

$$\bar{\mathcal{R}}_2=\Lambda_1+\mathcal{B}_2(\Lambda_6+\Lambda_7)\,\mathcal{B}_2^{\top}+\mathcal{B}_1\sum_{j=1}^{R}\alpha^{[i,j]}(t)\,A_1^{[i,j]}\Lambda_8\sum_{j=1}^{R}\alpha^{[i,j]}(t)\left(A_1^{[i,j]}\right)^{\top}\mathcal{B}_1^{\top}+$$
$$\mathcal{B}_1\sum_{j=1}^{R}\alpha^{[i,j]}(t)\,A_2^{[i,j]}\Lambda_8\sum_{j=1}^{R}\alpha^{[i,j]}(t)\left(A_2^{[i,j]}\right)^{\top}\mathcal{B}_1^{\top}+\mathcal{B}_1\Lambda_9\mathcal{B}_1^{\top}$$

$$\bar{\mathcal{Q}}_1=K_{id}^{\top}\mathcal{B}_1^{T}\Lambda_1^{-1}\mathcal{B}_1K_{id}+\lambda_{\max}\left(\Lambda_2^{-1}\right)L_\sigma\Lambda_\sigma+2\sum_{j=1}^{R}\alpha^{[i,j]}(t)\sum_{s=1}^{R}\alpha^{[i,s]}(t)\,\lambda_{\max}\left\{\left(\Lambda_4^{j,s}\right)^{-1}\right\}\tilde{f}_1^{[i,j]}I_{2n\times 2n}$$

$$\bar{\mathcal{Q}}_2=\sum_{j=1}^{R}\alpha^{[i,j]}(t)\sum_{s=1}^{R}\alpha^{[i,s]}(t)\left(2\varepsilon_1\lambda_{\max}\left(\Lambda_3^{-1}\right)\bar{L}_\sigma+4\tilde{f}_1^{[i,j]}\lambda_{\max}\left\{\left(\Lambda_4^{j,s}\right)^{-1}\right\}\right)I_{2n\times 2n}$$

Then the control law

$$u(t)=g^{\top}(x_a(t))\left(g(x_a(t))\,g^{\top}(x_a(t))\right)^{-1}\times$$
$$\left(-\sum_{j=1}^{R}\alpha^{[i,j]}(t)\,W^{[i,j]}(t)\,\sigma(\hat{x}(t))-K_{id}\Delta_{id}(t)-K_{tr}\Delta_{tr}(t)\right),$$

$$K_{id}=[K_{p,id},\ K_{d,id}]\in\mathbb{R}^{n\times 2n},K_{tr}=[K_{p,tr},\ K_{d,tr}]\in\mathbb{R}^{n\times 2n},\ K_{p,id},K_{d,id},K_{p,tr},K_{d,tr}\in\mathbb{R}^{n\times n} \tag{5.29}$$

forces that:

a) The identification error $\Delta_{id}:=x-\hat{x}$ is ultimate bounded [Khalil, 2002] in the following sense

$$\lim_{t\to\infty}\sup\|\Delta_{id}(t)\|^2\leq\frac{\delta}{\min\limits_{t\geq 0}\{\lambda_{\min}(P_1(t))\}} \tag{5.30}$$

and

b) The trajectory tracking error $\Delta_{tr} := \hat{x} - x_{ref}$ *is also ultimate bounded, with a bound given by*

$$\limsup_{t\to\infty} \|\Delta_{tr}(t)\|^2 \leq \frac{\delta}{\min\limits_{t\geq 0}\{\lambda_{\min}(P_2(t))\}} \tag{5.31}$$

where $\delta = \left(2\sum_{j=1}^{R}\left(k^j\right)^{-1}\varepsilon + \frac{\beta}{\alpha_B}\right)$, α_B *is a positive scalar and*

$$\beta = \sum_{j=1}^{R}\alpha^{[i,j]}(t)\sum_{s=1}^{R}\alpha^{[i,s]}(t)\left(2\varepsilon_1\lambda_{\max}\left(\Lambda_3^{-1}\right)\bar{L}_\sigma^\top\gamma_{ref} + \tilde{f}_0^{[i,j]}\lambda_{\max}\left\{\left(\Lambda_4^{j,s}\right)^{-1}\right\} + 4\left(\lambda_{\max}\left\{\left(\Lambda_4^{j,s}\right)^{-1}\right\}\tilde{f}_1^{[i,j]}\gamma_{ref} + \lambda_{\max}\left\{\left(\Lambda_5^{j,s}\right)^{-1}\right\}\gamma_\xi\right) + \lambda_{\max}\left\{\Lambda_6^{-1}\right\}\gamma_{ref,b}\right) + \lambda_{\max}\left\{\Lambda_7^{-1}\right\}\gamma_{ref,b} + \lambda_{\max}\left\{\Lambda_8^{-1}\right\}\gamma_{ref,a} + \lambda_{\max}\left\{\Lambda_8^{-1}\right\}\gamma_{ref,b} + \lambda_{\max}\left\{\Lambda_9^{-1}\right\}L_{s,b}\gamma_{ref,b}$$

$I_{n\times n}$ *and* $I_{2n\times 2n}$ *are identity matrices of* $n\times n$ *and* $2n\times 2n$.

Here $\min\limits_t\{\lambda_{\min}(P_1(t))\}$ *and* $\min\limits_t\{\lambda_{\min}(P_2(t))\}$ *are the minimum eigenvalues of the matrices* $P_1(t)$ *and* $P_2(t)$ *along the time, respectively.*

Proof. The full proof is given in Appendix C. ■

Necessary conditions that ensure the solution of the RDEs (5.27) and (5.28) are presented in Section 5.

Remark 16 *The size of the region of convergence for the errors is determined by the solution of Eq. (5.27) for the identification and the solution of Eq. (5.27) for the trajectory tracking, respectively.*

Remark 17 *The RDE structure proposed in this work make use of a more general concept than the one presented in optimal control theory. There exist literature that introduce the concept of RDEs as a general problem [Reid, 1972], [Crouch and Pavon, 1987], [Kilicaslan and Banks, 2010] with some particular applications as: transmission line phenomena, theory of noise and random processes, variational theory, optimal control theory, diffusion problems and invariant embedding. The following theorem make use of two RDE based on the work presented by [Kilicaslan and Banks, 2010].*

5.4 Learning laws for the identifier

This section describes the learning laws structure as well as the identification. The quality of the identification algorithm is characterized by the region where the identification error converges. The theorem described in this section gives sufficient conditions and depends on the existence of the positive definite matrix as solution of a Riccati Differential Equation (RDE). The last subsection discusses the conditions for ensuring the existence of such positive definite matrix.

For this class of adaptive identifier, the following nonlinear weight-updating law is suggested. The structure given in the following equations was derived using the Lyapunov method for practical stability analysis. These laws are:

$$\begin{gathered}\frac{d}{dt}W^{[i,j]}(t)=\Theta^{[i,j]}\left(\tilde{W}^{[i,j]}(t),\Delta_b(t),P_2(t)\right),\\ \Theta^{[i,j]}\left(\tilde{W}^{[i,j]}(t),\Delta_{id}(t),P_2(t)\right)=\frac{1}{2}k^j\alpha^{[i,j]}(t)\,\mathcal{B}_1^{\top}P_1(t)\,\Delta_{id}(t)\,\sigma^{\top}(\hat{x}(t))+\frac{\alpha_B}{2}\tilde{W}^{[i,j]}(t),\\ P_2(t)=P_2^{\top}(t)>0,\ \tilde{W}^{[i,j]}(t):=W_{to}^{[i,j]}(t)-W^{[i,j]}(t),\ k^j\in\mathbb{R}^+.\end{gathered}\tag{5.32}$$

Here $P_1(t)$ is the positive definite solution matrix of the RDE defined in Theorem 1 (Eq. (5.27)).

5.5 On the Riccati Differential Equation solution

In order to guarantee the existence of the positive definite solution of the RDEs (5.27) and (5.28) we use the lemmas presented in Section 3 in Chapter 5. This lemma presents the necessary conditions to ensure the existence of positive definite and continuous solution for the class of Riccati equation such as the one obtained in the chapter.

Once the RDEs matrices considered in this study have fulfilled the existence conditions they can be solved on-line by using the information from the system that is needed in the time varying piecewise continuous functions included in the chapter and defined by the matrices $\bar{\mathcal{Q}}_1$, $\bar{\mathcal{Q}}_2$, $\bar{\mathcal{R}}_1$ and , $\bar{\mathcal{R}}_2$. One may notice that $\bar{\mathcal{A}}_1$ and $\bar{\mathcal{A}}_2$ depend

only fuzzy membership values and the proposed matrices A_1 and A_2, then they can be calculated on-line. Similar conditions arise when the matrices$\bar{\mathcal{Q}}_1$ and $\bar{\mathcal{Q}}_2$ are evaluated but the upper bounds for perturbations/uncertainties should be calculated a priori. Lambda matrices can also be determined a priori and they can be used in the on-line evaluation of $\bar{\mathcal{Q}}_1$, $\bar{\mathcal{Q}}_2$. In the case of $\bar{\mathcal{R}}_1$ and $\bar{\mathcal{R}}_2$, there is the necessity of introducing $W_0^{[i,s]}$ but instead of th ese matrices, one may use their corresponding upper values that were assumed to be known. Maybe this is the most challenging issue in evaluating the controller proposed in this study but similar problems have been solved using a numerical strategy equivalent to the one considered in this study. For example In view of parameters $W_0^{[i,s]}$ is a linear term multiplying the activation functions, the matrix leastmean square algorithm [Ljung, 1999], [Kunusch, 2003], [Poznyak et al.,] can be applied as an off-line training stage.

5.6 Implementation issues

In order to implement the identification and trajectory tracking tasks the following process needs to be carried out. The schematic in Fig. 5.1 shows the architecture of the closed-loop system.

1.- Integrating the RDE in Eq. (5.27) to obtain $P_1(t)$,

2.- Substitute $P_1(t)$ on the learning laws (5.32) of the DNNs to obtain $W^{[i,j]}(t)$.

3.- Implement the neuro-fuzzy identifier using the weights $W^{[i,j]}(t)$ and identification error Δ_{id}.

4.- Compute the neuro-fuzzy control law using the weights $W^{[i,j]}(t)$, the identification error Δ_{id} and the tracking error Δ_{tr}.

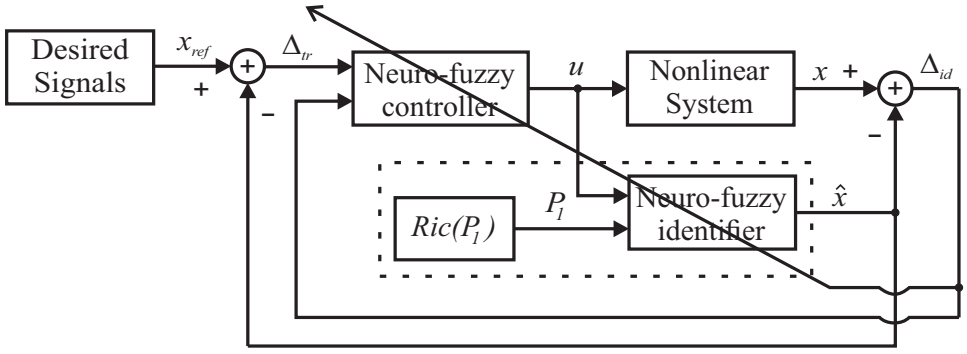

Figure 5.1: Closed-loop system architecture with learning capability and neuro-fuzzy controller.

5.7 Numerical results

In order to validate the effectiveness of the controller proposed in this chapter we use the model of a fully actuated AUV presented in Section 2.4. Considering the state variables $x_1 = x$, $x_2 = y$, $x_3 = z$, $x_4 = \psi$, $x_5 = \frac{d}{dt}x$, $x_6 = \frac{d}{dt}y$,$x_7 = \frac{d}{dt}z$, $x_8 = \frac{d}{dt}\psi$ the system (2.10)-(2.9) can be rewritten with the structure of Eq. (5.1), that is

$$\begin{aligned} \frac{d}{dt}\eta_a(t) &= \eta_b(t) \\ \frac{d}{dt}\eta_b(t) &= f(\eta(t)) + g(\eta_a(t))\,u(t) + \xi(\eta(t), t) \end{aligned} \tag{5.33}$$

where $\eta_a = \begin{bmatrix} x_1 & x_2 & x_3 & x_4 \end{bmatrix}^\top$, $\eta_b = \begin{bmatrix} x_5 & x_6 & x_7 & x_8 \end{bmatrix}^\top$, $\eta = \left[\eta_a^\top, \eta_b^\top\right]^\top$,

$u = \begin{bmatrix} X & Y & Z & N \end{bmatrix}^\top$, $f(\eta) = \begin{bmatrix} f_1(\eta) & f_2(\eta) & f_3(\eta) & f_4(\eta) \end{bmatrix}^\top$,

$$\begin{aligned} f_1(\eta) = \{c_1\cos^2 x_4 + c_2\sin^2 x_4\}x_5 + \{c_1\cos x_4\sin x_4 - c_2\sin x_4\cos x_4 - x_8\}x_6 + \\ \{c_3\left[x_5\sin x_4\cos x_4 - x_6\cos^2 x_4\right] + c_4\left[x_5\sin x_4\cos x_4 + x_6\sin^2 x_4\right]\}x_8 + \end{aligned},$$

$$\begin{aligned} f_2(\eta) = \{x_8 + c_1\sin x_4\cos x_4 - c_2\cos x_4\sin x_4\}x_5 + \{c_1\sin^2 x_4 + c_2\cos^2 x_4\}x_6 + \\ \{c_3\left[x_5\sin^2 x_4 - x_6\sin x_4\cos x_4\right] - c_4\left[x_6\sin x_4\cos x_4 + x_5\cos^2 x_4\right]\}x_8 \end{aligned},$$

$$f_3(\eta) = c_7 x_7 + c_8,$$

$$f_4(\eta) = \{c_{10}\left[x_5 \sin x_4 \cos x_4 - x_6 \cos^2 x_4 + x_7\right] + c_{11}\left[x_5 \sin x_4 \cos x_4 + x_6 \sin^2 x_4\right]\}x_5 + \{c_{10}\left[x_5 \sin^2 x_4 - x_6 \sin x_4 \cos x_4\right] - c_{11}\left[x_6 \sin x_4 \cos x_4 + x_5 \cos^2 x_4\right]\}x_6 + c_{12}x_8,$$

$$g(\eta_a) = \begin{bmatrix} c_5 \cos x_4 & -c_6 \sin x_4 & 0 & 0 \\ c_5 \sin x_4 & c_6 \cos x_4 & 0 & 0 \\ 0 & 0 & c_9 & 0 \\ 0 & 0 & 0 & c_{13} \end{bmatrix},$$

$$\xi(\eta_a, t) = \begin{bmatrix} c_5 \cos x_4 \tau_{E_1}(t) - c_6 \sin x_4 \tau_{E_2}(t) \\ c_5 \sin x_4 \tau_{E_1}(t) + c_6 \cos x_4 \tau_{E_2}(t) \\ c_9 \tau_{E_3}(t) \\ c_{13} \tau_{E_6}(t) \end{bmatrix}$$

It may be noticed that the AUV system considered here is fully actuated ($m = n$), so it represents a particular case of the nonlinear system in Eq. (5.1). Also, in order to known the complete structure of $g(\eta_a(t))$ the parameters c_5, c_6, c_9 and c_{13} are supposed to be known.

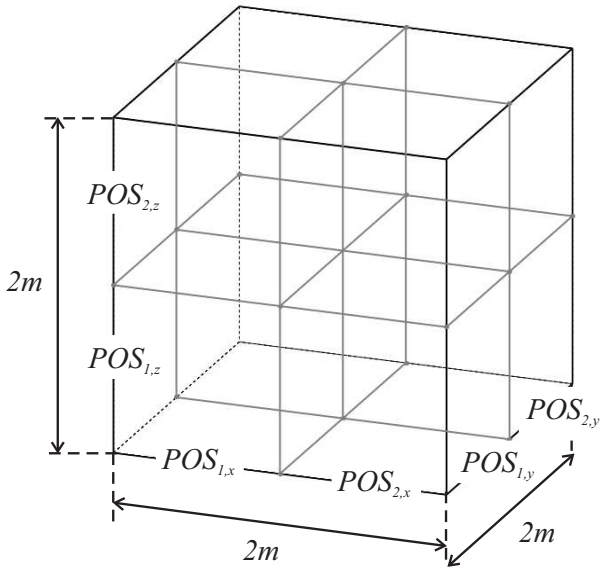

Figure 5.2: Partition of the AUV movement space.

In order to represent the dynamics of the AUV using the T-S structure, it is considered that the AUV moves inside a three dimension space represented by a cube of 2 meters $\times$ 2 meters. This space is partitioned in eight cubes as is shown in Fig. 5.2. Then, for the fuzzification stage the position vector $x_a = [x_1, x_2, x_3]^\top$ is chosen as the fuzzy set, and the following two partitions corresponding to each cube are proposed: Position 1 (POS_1) and Position 2 (POS_2). The membership functions structure of POS_1, POS_2 are selected as in Fig. 6.10 by trial and error. In consequence, it is necessary to propose eight rules to represent the AUV dynamics when it is located in each cube, as follows:

$$\begin{gathered} \mathrm{R}^j : \text{IF } x_1 \text{ is } POS_{s,x_1} \text{ and IF } x_2 \text{ is } POS_{s,x_2} \text{ and IF } x_3 \text{ is } POS_{s,x_3} \\ \text{THEN } \frac{d}{dt}\hat{x}_a(t) = \hat{x}_b(t) \\ \frac{d}{dt}\hat{x}_b(t) = A_1^{[j]}\hat{x}_a(t) + A_2^{[j]}\hat{x}_b(t) + W^{[j]}(t)\,\sigma(\hat{x}(t)) \\ j = 1 \ldots 8,\ s = 1, 2 \end{gathered} \quad , \tag{5.34}$$

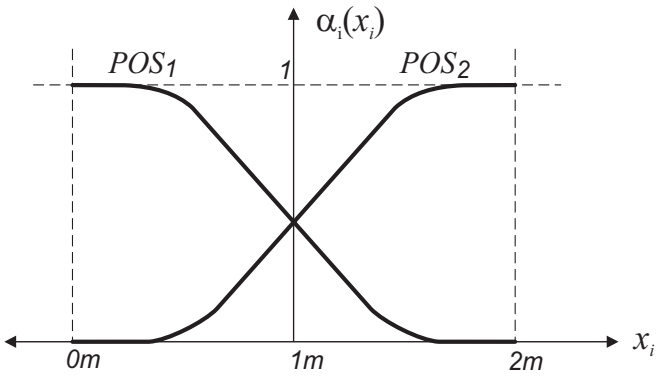

Figure 5.3: Membership functions structure.

The system parameters for a typical AUV, used for simulation purposes, are given by $m = 4.28\ kg$, $X_{\dot{u}} = 0.5\ kg/s$, $Y_{\dot{v}} = 0.22\ kg/s$, $Z_{\dot{w}} = 0.3\ kg/s$, $N_{\dot{r}} = 0.4\ kgm^2/s$, $\tau_{D_x} = \tau_{D_y} = \tau_{D_z} = \tau_{D_\psi} = -0.05$, $I_z = 0.04$, $F_{WB} = 0$.

The environmental disturbances are proposed as the following wave profile [Perez, 2005]:

$$\tau_{E_1} = \tau_{E_2} = \tau_{E_3} = \tau_{E_6} = \sin(0.1t) + 3\sin\left(0.8t + \frac{\pi}{2}\right) + 1.5\sin(0.5t) + 0.8\sin(0.4t)\,.$$

The desired three dimension (X-Y-Z) path to solve for the trajectory tracking problem is the one shown in Fig. 5.4. First, the AUV immerses from the water surface (blue point) performing a constant velocity circular path of radius 1 meter (blue arrows) to reach 0.5 meters depth staying there approximately 20 seconds (magenta point). Then, the AUV returns to the surface following the same circular path (green arrows) until reaching the water surface (green point). In order to describe the path in Fig. 5.4, the desired paths for each state must be:

$$\begin{gathered} \mathrm{x}_{ref}(t) = \sin(0.5t)\,,\ \mathrm{y}_{ref}(t) = \cos(0.5t)\,, \\ \mathrm{z}_{ref}(t) = 0.5\left(\frac{1}{1+e^{-(t-6)}} - 1\right) - 0.5\left(\frac{1}{1+e^{-(t-24)}} - 1\right). \end{gathered} \tag{5.35}$$

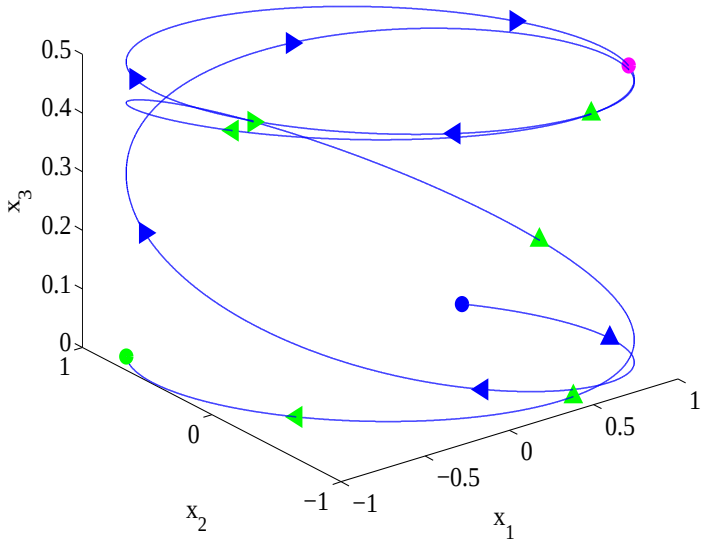

Figure 5.4: Three dimension desired path.

The initial conditions are: $x\left(0\right)=0$, $y\left(0\right)=1$, $z\left(0\right)=0$, $\psi\left(0\right)=0$.

The controller gains used are:

$K_{p,tr}=diag\left(19680,16400,13119,2880\right)$,

$K_{d,tr}=diag\left(0.0196,0.0164,0.013119,0.0028\right)$,

$K_{p,id}=K_{d,id}=diag\left(65.595,49.195,98.395,-24.005\right)$.

The inference matrices used to define the contribution given by the first three DNN identifiers are:

$A_1^{[1]}=diag\left(-50,-75,-100,-150\right)$, $A_2^{[1]}=diag\left(-150,-100,-50,-125\right)$,

$A_1^{[2]}=diag\left(-50,-75,-100,-200\right)$, $A_2^{[2]}=diag\left(-150,-100,-50,-225\right)$,

$A_1^{[3]}=diag\left(-50,-75,-100,-125\right)$, $A_2^{[3]}=diag\left(-150,-100,-50,-65\right)$.

These matrices were defined using previous knowledge on the system dynamics. For the other identifiers, similar matrices were calculated using a similar procedure. The sigmoid function considered is: $\sigma_l\left(x_l\right)=2/(1+exp(-2x_l))-0.5$, where x_l is the l-th component of x_b. The gains for the learning laws of the eight DNNs are: $k_1=\ldots=k_8=50$. The off-line weight matrices considered are: $W_{to}^{[1]}=\ldots=W_{to}^{[8]}=I_{4\times4}$.

The values of the constants used to solve the RDE stated in Eq. (28) used in the control algorithm are the following

$$L_\sigma=0.000001,\ \tilde{f}_1^{[i,j]}=0.000001 \tag{5.36}$$

The values of the constants that participates in the boundary term β (page 12) are the following:

$$\gamma_{ref,a}=2.25,\ L_{s,b}=0 \tag{5.37}$$

and are obtained as follows. In view of the reference vector satisfies

$$x_{ref,a}=\left[\begin{array}{cccc}\mathrm{x}_{ref}, & \mathrm{y}_{ref}, & \mathrm{z}_{ref}\end{array}\right] \tag{5.38}$$

We know that $|\sin(0.5t)| \leq 1$, $|\cos(0.5t)| \leq 1$,

$\left|[0.5/(1+e^{-(t-6)}) - 0.5 - \left(0.5/(1+e^{-(t-24)}) - 0.5\right)\right| \leq 0.5$.

Then, $\|x_{ref,a}(t)\|^2 \leq 1 + 1 + 0.25 \leq 2.25$. That is, $\gamma_{ref,a} = 2.25$. On the other hand, in the particular case of the AUV simulation the function $s_b(\cdot)$ in Eq. (26) does not depend explicitly on $x_{ref,b}(t)$ only depends on time, so the boundary defined in Eq. (26) is $L_{s,b} \equiv 0$.

Concerning the constant values ϵ_1, $\bar{L}_\sigma$and $\tilde{f}_1^{[i,j]}$, they participate in the RDE in Eq. (29). It is important to note that is not necessary to solve this equation for the simulation implementation. This equation is part of the theoretical proof that ensures the convergence of the trajectory tracking error. Even so, this equation was solved using the following constant values:

$$\epsilon_1 = 1, \qquad \bar{L}_\sigma = 0.000001, \qquad \tilde{f}_1^{[i,j]} = 0.000001 \tag{5.39}$$

In order to proposed a challenging comparison between a classical controller such as the T-S form and the controller proposed in this study, the stable matrices $\bar{A}^{[j]}$ were determined by trial and error in order to approximate as much as possible the behaviour of the nonlinear uncertain system. Then, any knowledge of the nonlinear system are being used which is a less restrictive condition than the one assumed in this study.

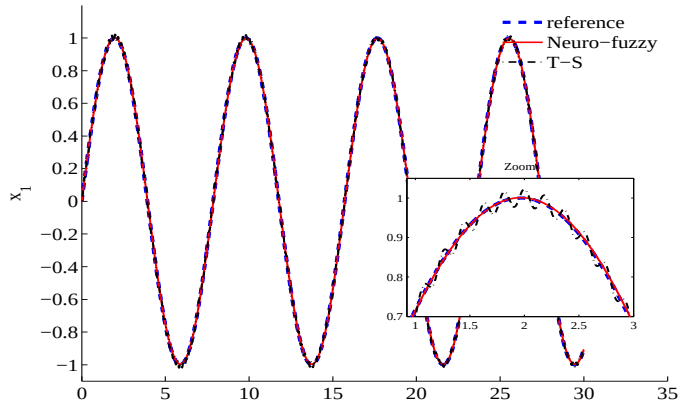

(a)

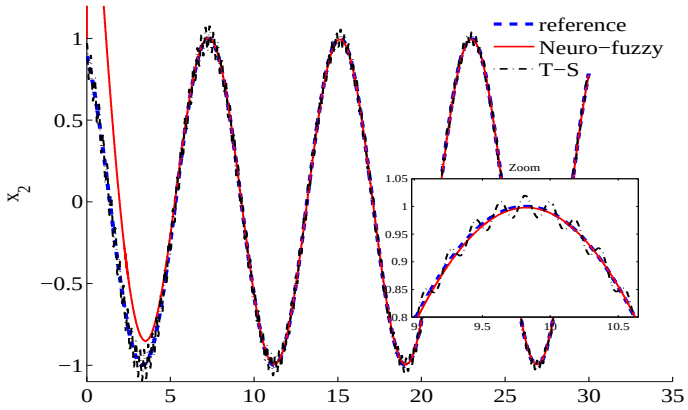

(b)

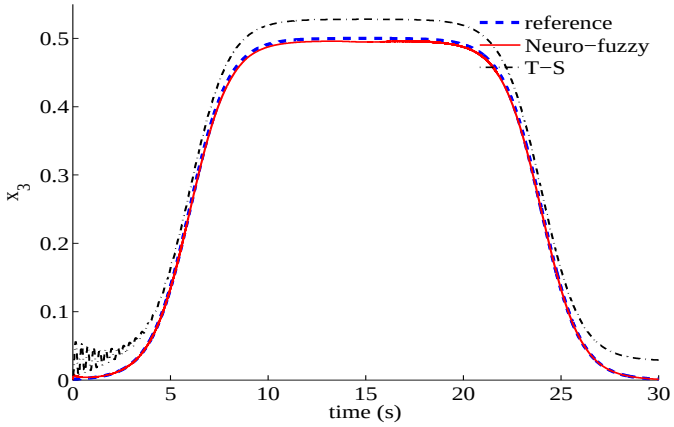

(c)

Figure 5.5: Comparison of states trajectories obtained when PDC controller compared with the adaptive controller proposed in this study

The matrix $B^{[j]}$ was obtained by linearising the nonlinear section associated to the input $g(x_a)$ around the operating point $x_4 = 0$. Then a feedback control that stabilizes each linear system is calculated using the pole placement technique. Now with these gains, we can construct a Parallel Distributed Compensator (PDC) [Takagi and Sugeno, 1985] based on the T-S fuzzy modeling strategy. The PDC has the following form

$$u(t) = K(t)\,\Delta_{tr}(t), \quad K(t) = \sum_{i=1}^{8} \alpha_i(t)\,K_i \tag{5.40}$$

where Δ_{tr} is the tracking error. Based on the PDC design, we proposed a comparison between the trajectories produced by implementing the controller proposed in our study and the one proposed in Eq. (5.40). An additional comparison was done considering the energy needed to enforce the tracking of the three individual coordinates. The figure 5.5-a demonstrates the tracking comparison between the proposed neuro-fuzzy controller and a common PDC fuzzy controller in the coordinate x while figure 5.5-b demonstrates the same comparison considering the coordinate y.

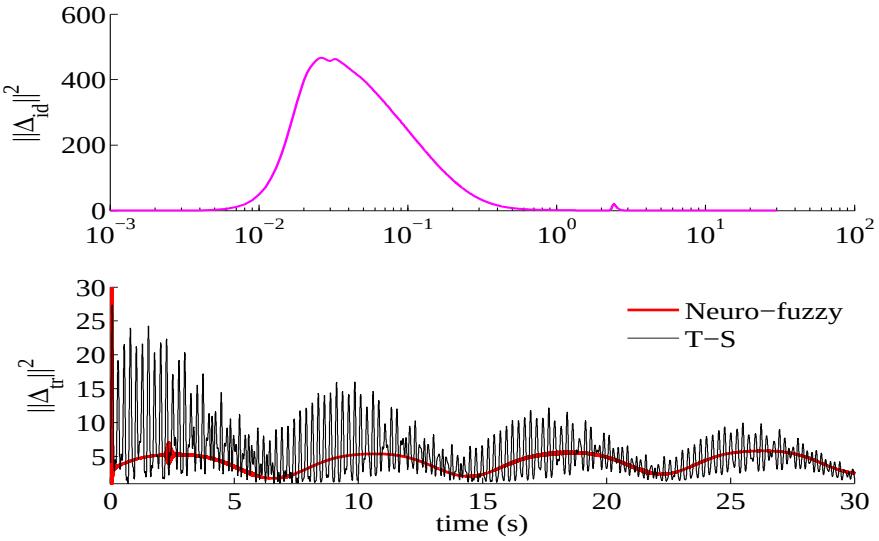

Figure 5.6: Identification error (top) and Trajectory tracking error (bottom).

These comparisons showed that the neuro-fuzzy controller proposed in our study tracks smoothly the reference trajectories with less relevant oscillations around the references. In comparison the common fuzzy controller follows the references but with a greater oscillation obtaining a worse tracking result. The effect of this oscillations promotes a relevant miss tracking of the reference trajectory in z coordinate by using the fuzzy controller as shown in figure 5.5-c.

In Fig. 5.6, the norm of the identification and trajectory tracking errors are shown. It is important to emphasize that the identification error converges almost to the origin in approximately 7 seconds. The approximated trajectories are suitable to define a trajectory tracking for the AUV. It can be seen that the tracking error converge to region of acceptable size near to the origin, that is, the identified trajectories reach the desired signals. An additional comparison was done considering the energy needed to enforce the tracking of the three individual coordinates. Figure 5.7 demonstrates the effective controller needed to enforce the tracking. One may notice that bigger energy is needed in the PDC and worse tracking performance was attained.

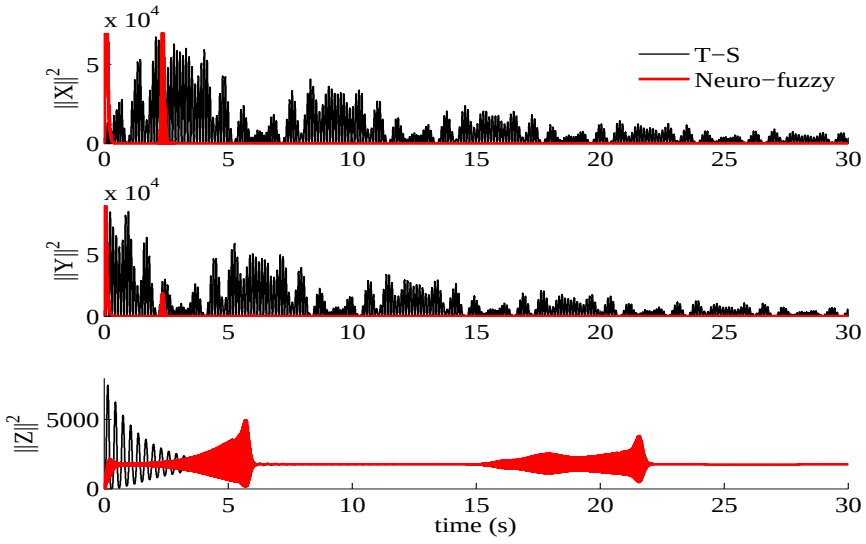

Figure 5.7: Forces in surge (top), sway (midst) and heave (bottom) direction.

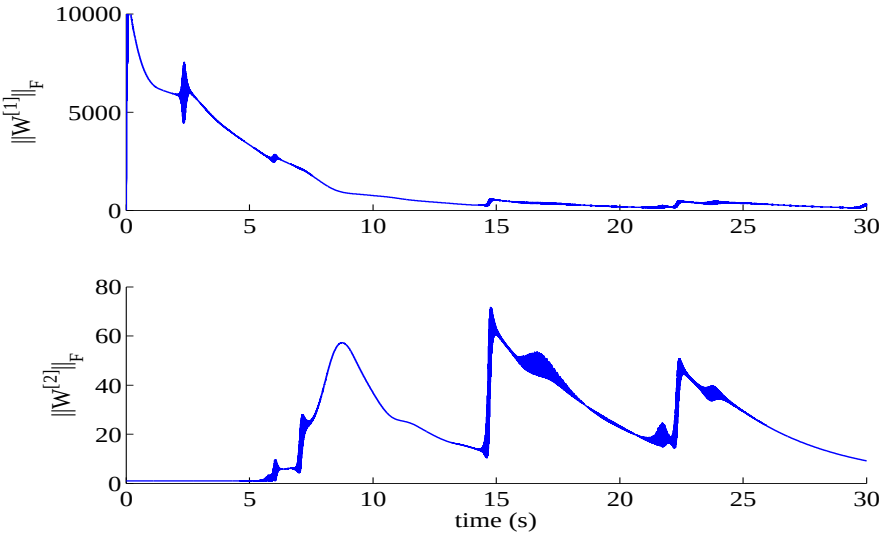

Figure 5.8: Performance of the Frobenius norm of the weigth matrices $W^{[1]}$ of the DNN_1 (top) and $W^{[2]}$ of the DNN_2 (bottom).

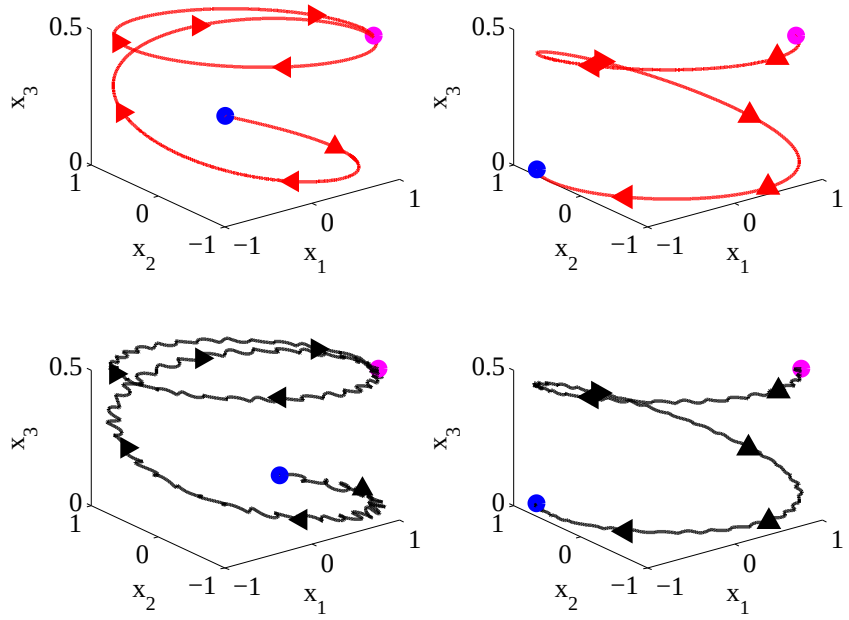

Figure 5.9: Stage 1: The AUV immerses (left side). Stage 2: The AUV returns to the water surface (rigth side).

From the results showed in Fig. 5.7, it is found that the controller proposed in this study (defined by the forces in surge, sway and heave directions) solves the tracking trajectory problem using the identified states of the AUV nonlinear system under the presence of disturbances. Also, the same figure shows the comparison of the norm for tracking errors gotten in each coordinate (x, y, z). This last result confirms the better result enforced by the controller developed in this study.

In Fig. 5.8 shows the performance of the Frobenius norm of the first two weight matrices. These weight matrices can be able to adapt according to the AUV behavior changes during the on-line learning process.

An integral comparison of controllers performance for the three dimension desired path tracking realized by the AUV was depicted in Fig. 5.9. For visualization purposes the AUV movement is separated in two stages. This comparison confirmed that better tracking using the controller designed in this study than the common T-S fuzzy controller was obtained even when the AUV system modified its z coordinate in two different directions (form top to bottom and bottom to high). Moreover, no high frequency oscillations were observed on the trajectories executed by the AUV system.

A number of simulation results have shown that the proposed control scheme performs well in terms of smooth transient response, quick convergence of tracking errors near to the origin, and robustness, even in the case of disturbed conditions.

5.8 Conclusions of the chapter

In this work a neuro-fuzzy scheme was developed to accomplish two goals: identification and control of uncertain nonlinear systems. This scheme mixed the use of DNNs to approximate the local dynamics of the nonlinear system in a certain region determined by a set of T-S rules. This two goals was solved using the solution of two RDEs calculated on-line. This fact differs from the existing works that solve AREs. The main contribution of this study was to propose a methodology to design an adaptive

parallel distributed controller used to solve a trajectory tracking problem. A set of continuous neural networks was used to approximate the dynamics of each subsystem needed in the controller. The rule needed to select what subset of systems approximated by the neural networks must be considered in the controller execution. A controlled Lyapunov function was proposed to prove the existence of an ultimate bounded stable equilibrium point for the tracking error dynamics. The same Lyapunov function was used to design the laws that adjusted the weights in each neural network. This kind of solution has been rarely explored and the solution attained in this study offered superior performance that usual linear PDC working without adaptation. In summary, the identification and control algorithm sre designed for running on-line to makes it adaptable in the sense of the system dynamics changes allowing to obtain a suitable identification for the trajectory tracking purpose. Simulation results using an AUV system validate the algorithm designed by tracking a three-dimension desired path.

5.9 Future work

We can propose a methodology based on a separation of the AUV's model into two parts: the first one is a known nominal model and the second one is a model with parameter uncertainties. A similar procedure developed in this chapter can be implemented to deal with this problem. Also, in order to have a complete control system a neuro-fuzzy observer can be designed. This observer has the aim to estimate the state information from the AUV system output. In consequence, we may have a closed-loop control system composed by an identification, estimation and trajectory control parts.

The neuro-fuzzy observer approximates the right hand side of the uncertain nonlinear system, and at the same time estimates the unmeasurable states of this approximation. So these two tasks, estimation and identification, need to be carried out during an on-line process in order to calculate the stabilizing control law. This closed-loop system structure represents a more challenging problem.

Alternatively, we can use a robust exact differentiator to estimate the unmeasurable states of a nonlinear identified system using the neuro-fuzzy identification process. Then, identification and estimation are performed using two different structures. Moreover, it is known that an sliding mode observer converges in finite time horizon. The previous considerations leads us to think that the implementation of this algorithm seems to be easier than the neuro-fuzzy observer for control purposes.

6

Trajectory tracking of a real AUV

6.1 AUV platform

To demonstrate the feasibility of the developed controller in Chapter 5, it was applied to an experimental platform shown in Figs. 6.1 and 6.2, this is an AUV developed at UMI-LAFMIA Laboratory at the Research and Advanced Studies Center of the National Polytechnic Institute in Mexico (CINVESTAV). The AUV measures 430mm x 230mm x 200mm and approximately weights 4.22 kg. Two battery tubes are attached to its bottom. An acrylic tube to contain the electronic system is located at the forefront of the structure. The platform includes an internal computer system connected to an external computer, this configuration is shown in Fig. 6.6. The external computer is a laptop with Microsoft Windows operating system. The internal computer system consists of an electronic (controller) board (Fig. 6.4) that integrates: power stages, an electronic speed controller (ESC) for each thruster, and an ATmega2560 AVR microcontroller. The AUV is equipped with three T100 Blue Robotics brushless thrusters (Fig. 6.3): port and starboard thrusters located at the bottom of the vehicle and a vertical thruster located at the center of gravity of the vehicle as shown in Fig. 6.2. The AUV is

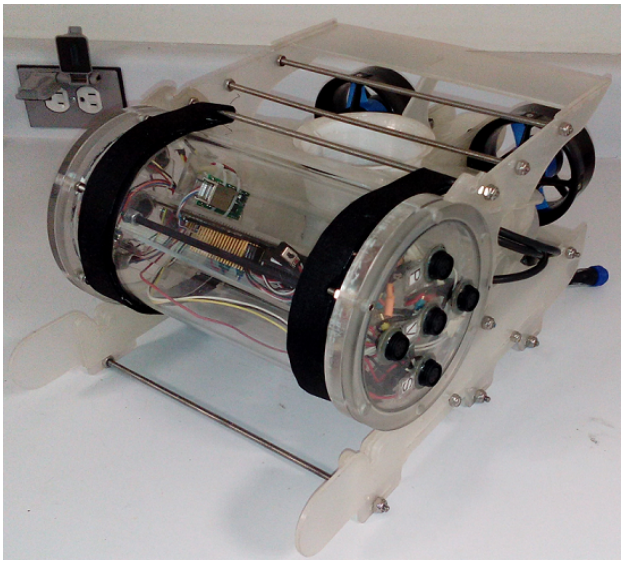

Figure 6.1: Experimental platform.

equipped with two sensors: An inertial measurement unit (IMU) Invesense MPU-9150 to measure the orientation (heading) of the AUV and a pressure sensor Measurement Specialities MS5803-14B to measure the depth the vehicle is located underwater (Fig. 6.5).

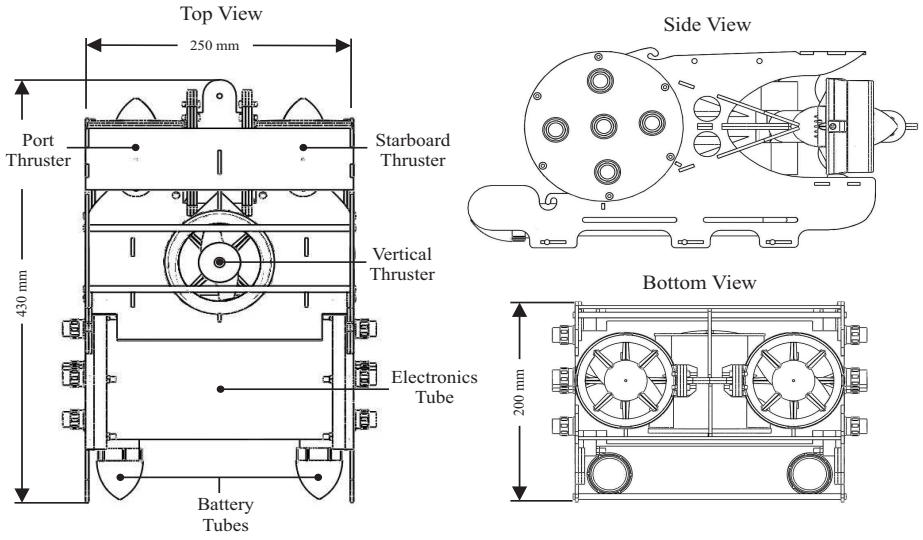

Figure 6.2: Mechanical structure of the AUV.

Figure 6.3: Thruster T100.

The ATmega2560 carries out the data aquisition from the sensors via I2C communication protocol and provides PWM signals to move the thrusters. In the external computer we use a real-time interface developed on MATLAB-Simulink. The external computer communicates with the electronic board via a full duplex serial communication protocol (using the same serial port). That is, MATLAB receives the sensor data from the Arduino Mega and sends the control signal converted as cycle duties to the thrusters.

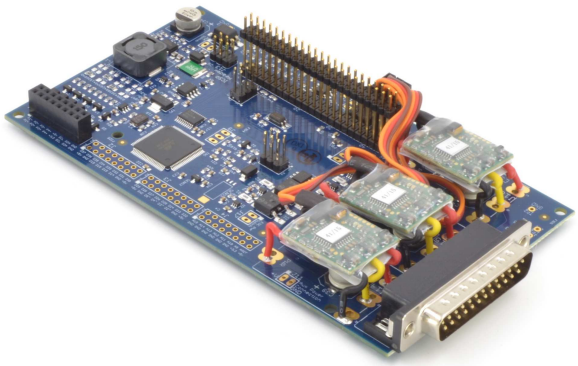

Figure 6.4: Controller board.

Figure 6.5: IMU (left) and pressure (right) sensors.

In order to extend the communication distance and use a lightweight communication cable between the external and internal computers two communication protocol conversion stages are implemented to convert from serial protocol (15 meters) to Ethernet protocol (100 meters) and then to a power line communication (PLC) protocol (300 meters). The PLC protocol uses electrical wiring (two cables) to simultaneously carry both data and direct current (DC) electric power. The devices implemented are: a serial UART to Ethernet converter USR-TCP232-T and a powerline mini adapter Tenda P200.

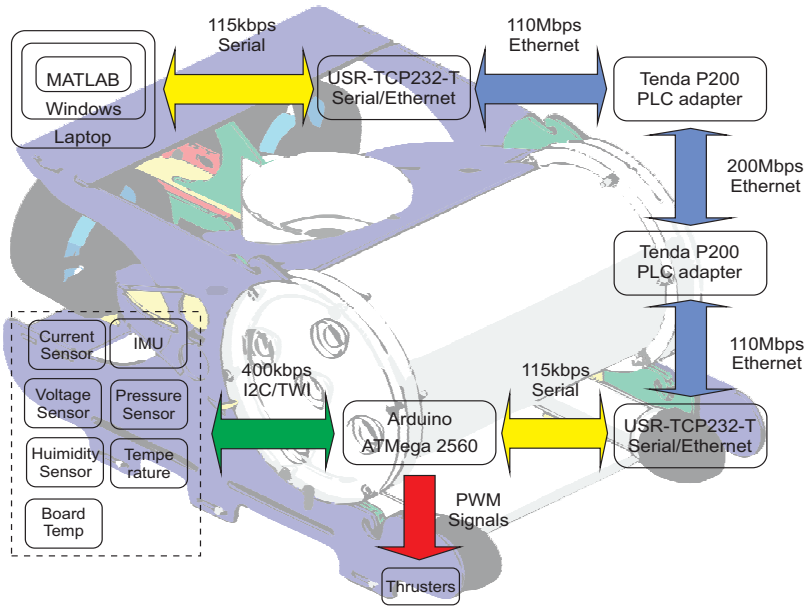

Figure 6.6: System configuration of the AUV platform.

6.2 Real-time experimentation interface

In order to realize the experimentation tests with the AUV platform a real-time interface shown in Fig. 6.7 was developed using MATLAB-Simulink. This interface implements a serial send-receive communication and the computation of the control signal. In the "Serial Receive" block we acquire the sensor data frame (depth and heading) from the ATmega. The sensor data is used to compute the control signal traduced as a PMW cycle duty. In the "Serial Send" block we send the PWM cycle duty frame to move the thrusters to the ATmega. A camera is used to visualize the movement of the AUV inside the tank (top-right). Also a plot of the vehicle trajectory and the desired signal is shown (bottom-right).

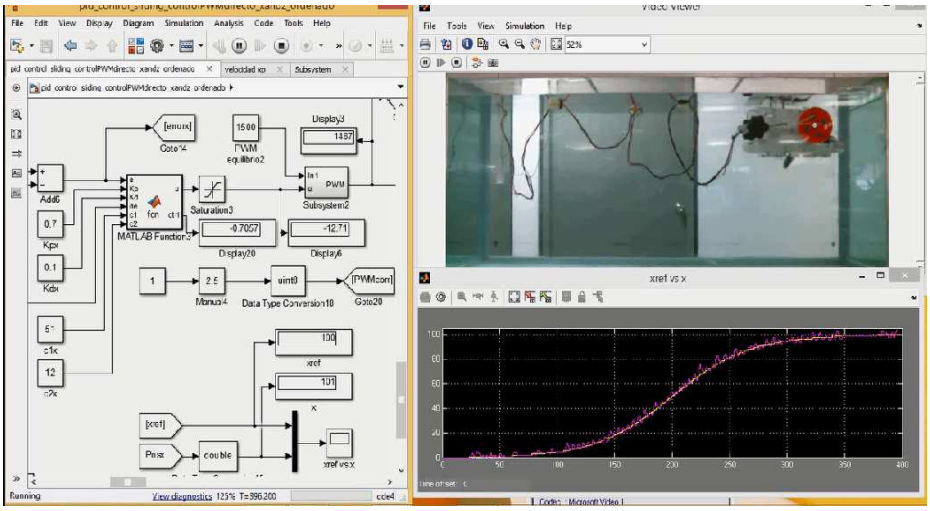

Figure 6.7: Real-time interface in MATLAB-Simulink.

6.3 Problem statement

This section is focused in the application of the controller developed in Chapter 5 in order to control the movement of the experimental AUV platform described in Section 5.1. The objective is to move the AUV inside a tank of dimensions 180 cm x 80 cm x 50 cm. However, due to the movement restrictions given by the limited space of the tank the vehicle is not be able to move in y axis only in x and z axes. Then, the problem is reduced to track a smooth trajectory in the $x-z$ plane by the AUV. Also, the position of the center of gravity of the vehicle cannot reach the entire space in the tank because the dimensions of its structure, so the real movement space in the x-z plane is 132 cm x 52 cm as is shown in Fig. 6.8.

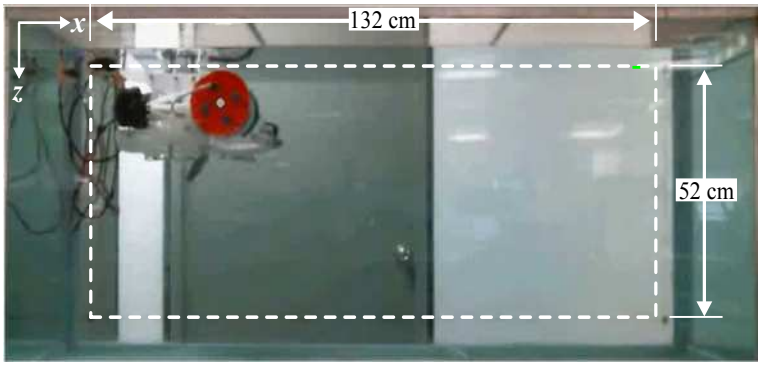

Figure 6.8: AUV movement space inside the tank.

In order to describe the model that characterizes the AUV lateral movement (x-z) dynamics the 6-DOF AUV model is reduced to obtain a 2-DOF model described in Section 2.5 in Chapter 2. Considering the state variables $x_1 = x$, $x_2 = z$, $x_3 = \dfrac{d}{dt}x$, $x_4 = \dfrac{d}{dt}z$ the system (**??**)-(**??**) can be rewritten as follows

$$\frac{d}{dt}\eta_a(t) = \eta_b(t)$$
$$\frac{d}{dt}\eta_b(t) = f(\eta(t)) + g(\eta_a(t))\tau_0(t) + \xi_E(\eta_a(t), t)$$

where

$$\eta_a = [x_1\ x_2]^\top, \eta_b = [x_3\ x_4]^\top, \eta = \left[\eta_a^\top\ \eta_b^\top\right]^\top, \tau_0 = [X\ Z]^\top,$$

$$f(\eta) = [f_1(\eta) \;\; f_2(\eta)]^\top, \;\; f_1(\eta) = c_1 x_3, \;\; f_2(\eta) = c_7 x_4 + c_8$$

$$g(\eta_a) = diag(c_5, c_9), \;\; \xi_E(\eta_a, t) = [c_5 \tau_{E_1}(t) \;\; c_9 \tau_{E_2}(t)]^\top$$

It may be noticed that the AUV system considered here is fully actuated ($m = n$), so it represents a particular case of the nonlinear system in Eq. (5.1). Also, in order to known the complete structure of $g(\eta_a)$ the parameters c_5 and c_9 are supposed to be known.

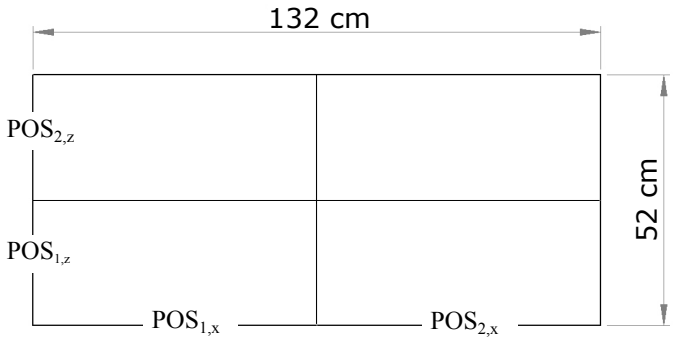

Figure 6.9: Partition of the tank space.

In order to represent the dynamics of the AUV using the T-S structure, it is considered that the AUV moves inside the region previously described. This space is partitioned in four squares as shown in Fig. 6.9. Then, for the fuzzification stage the

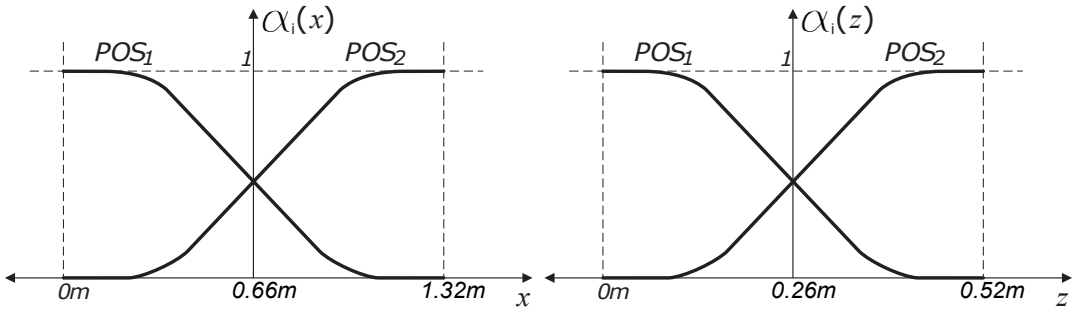

(a) Functions for x axis (b) Functions for z axis

Figure 6.10: Membership functions structure.

position vector $x_a = [x_1, x_2]^\top$ is chosen as the fuzzy set, and the following two partitions corresponding to each square are proposed: Position 1 (POS_1) and Position 2 (POS_2).

The membership functions structure of POS_1, POS_2 are selected by trial and error as in Fig. 6.10 (a) for x-axis and Fig. 6.10 (b) for z-axis. In consequence, it is necessary to propose four rules to represent the AUV dynamics when it is located in each square, as follows:

$$\begin{gathered} \mathrm{R}^j : \text{IF } x_1 \text{ is } POS_{s,x_1} \text{ and IF } x_2 \text{ is } POS_{s,x_2} \\ \text{THEN } \frac{d}{dt}\hat{x}_a(t) = \hat{x}_b(t) \\ \frac{d}{dt}\hat{x}_b(t) = A_1^{[j]}\hat{x}_a(t) + A_2^{[j]}\hat{x}_b(t) + W^{[j]}(t)\,\sigma(\hat{x}(t)) \\ j = 1 \ldots 4,\ s = 1, 2 \end{gathered} \quad , \tag{6.1}$$

The system parameters and the environmental disturbances are proposed as in Section 5.7.

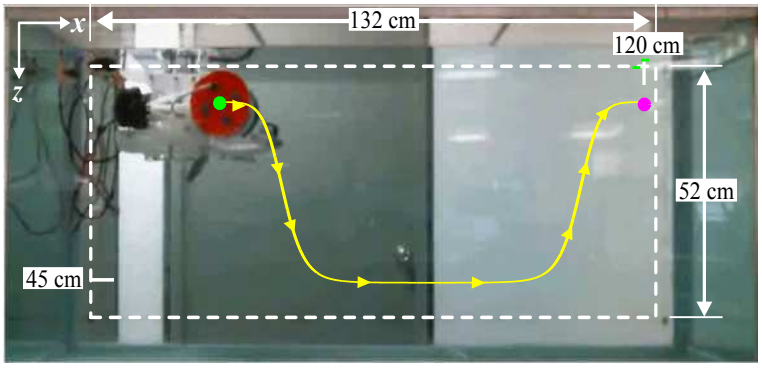

Figure 6.11: Two dimension desired path inside the tank.

The desired two dimension (x-z) path to solve for the trajectory tracking problem is the one shown in Fig. 6.11. First, the AUV immerses from the water surface (green point) following a sigmoid reference (blue arrows) to reach 0.4 meters depth staying in this reference approximately 15 seconds. Then, the AUV returns to the surface following the same sigmoid path until reaching the water surface (magenta point). In order to describe the path in Fig. 6.11, the desired trajectory are proposed as a composition of sigmoid functions [Cruz et al., 2014].

The references signals for each state are:

$$\begin{aligned} \mathrm{x}_{ref}(t) &= 1.2\left(\frac{1}{1+e^{-0.15(t-20)}}-1\right), \\ \mathrm{z}_{ref}(t) &= 0.4\left(\frac{1}{1+e^{-(t-10)}}-1\right)-0.4\left(\frac{1}{1+e^{-(t-30)}}-1\right). \end{aligned} \tag{6.2}$$

6.4 On the controller realization

The main drawback of the proposed controller designed in Chapter 5 is the necessity of measuring linear velocities of the AUV. This vehicle is not equipped with a sensor that can measure these velocities. Therefore, a sliding mode super-twisting algorithm (STA) is applied as a robust exact differentiator (RED) to estimate $\frac{d}{dt}x$, $\frac{d}{dt}z$ velocities from given AUV positions x and z. This estimator is used due to the well-known characteristic that a robust exact differentiator (RED) based on STA converges in finite time. This property allow us to use the estimated states in the controller structure without the necessity of solving a controller-observer system, i.e., the separation principle holds. The STA implemented in this work has a different structure to the one presented in [Levant, 2002, Levant, 2007, Davila et al., 2005], because it uses a sigmoid function instead of a sign function. This STA has the following structure [Chairez, 2015]:

$$\begin{aligned} \dot{\gamma}_1(t) &= \gamma_2(t) + k_1 \left|e_\gamma(t)\right|^{1/2} s\left(e_\gamma(t)\right) \\ \dot{\gamma}_2(t) &= k_2 s\left(e_\gamma(t)\right) \end{aligned} \tag{6.3}$$

where $e_\gamma = x_{mes} - \gamma_1$, x_{mes} is the measurable variable (in this case the linear positions x and z), $s(e_\gamma)$ is a sigmoid function defined as $s(e_\gamma) = \left(2/\left(1+e^{-be_\gamma}\right)\right) - 1$, and k_1, k_2 are positive constants.

6.5 Numerical results

The initial conditions are:

$x(0), z(0) = 0,\ \frac{d}{dt}x(0), \frac{d}{dt}z(0) = 0,\ \hat{x}(0), \hat{z}(0) = 0,\ \frac{d}{dt}\hat{x}(0), \frac{d}{dt}\hat{z}(0) = 0.$

The controller gains used are:

$K_{p,tr} = diag(17712, 41000),\ K_{d,tr} = diag(19.68, 16.40),$

$K_{p,id} = diag(500, 500),\ K_{d,id} = diag(60, 60).$

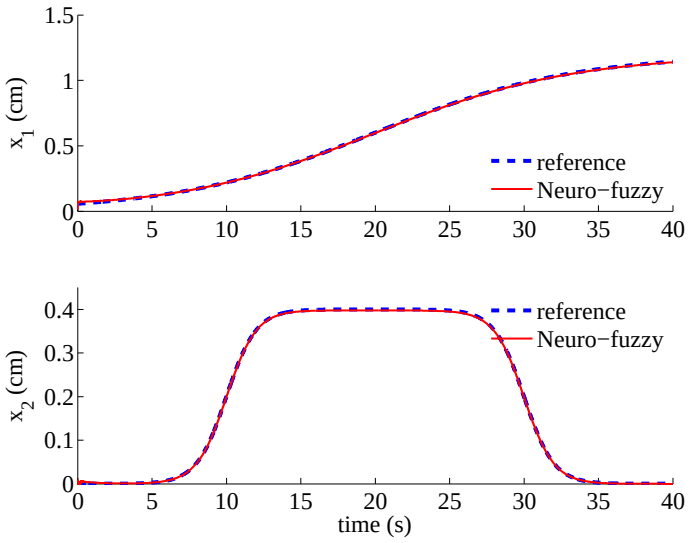

Figure 6.12: Tracking in x-axis (top) and z-axis (bottom) obtained with the adaptive controller.

The inference matrices used to define the contribution given by the four DNN identifiers are: $A_1^{[1]} = diag(-50, -75),\ A_2^{[1]} = diag(-150, -100),\ A_1^{[2]} = diag(-75, -125),$ $A_2^{[2]} = diag(-100, -25),\ A_1^{[3]} = diag(-100, -65),\ A_2^{[3]} = diag(-150, -110),$ $A_1^{[4]} = diag(-100, -25),\ A_2^{[4]} = diag(-150, -110)$. The sigmoid activation function considered is: $\sigma_l(x_l) = 2/(1 + exp(-2x_l)) - 0.5$, where x_l is the l-th component of velocity vector x_b.

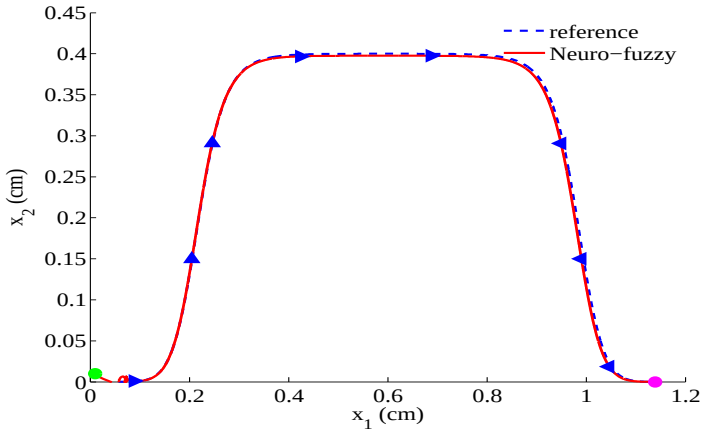

Figure 6.13: Two dimension trajectory performed by the controlled AUV system.

The initial conditions for the learning laws are: $W_o^{[i]} = diag\{300, 300\},\ i = 1 \ldots 4$. The gains for the learning laws are: $k_1 = \ldots = k_4 = 500$. The off-line weight matrices considered are: $W_{to}^{[i]} = diag\{30, 30\},\ i = 1 \ldots 4$. The values of the constants used to solve the corresponding RDE are the same as in Section 5.7. The values of the gains of the super-twisting REDs are: $k_{1,x} = k_{1,z} = 85$, $k_{2,x} = k_{2,z} = 60$.

In Fig. 6.12, the tracking of the desired position by the controlled AUV system in each axis x and z is depicted. It can be seen that the AUV trajectories in the x and z axis reach the reference ones in approximately 5 seconds for the x position and almost instantly for the z position, performing an acceptable convergence behaviour.

In Fig. 6.13, the trajectories of the controlled AUV in the $x - z$ plane is depicted.

The identification result of the AUV system can be observed by means of analysing the converge of the square norm of the identification error to a region near to the origin shown in Fig. 6.23 (top). Also the square norm of the tracking error converges to a region near to the origin that is depicted in Fig. 6.23 (bottom), confirming that the system have an acceptable response tracking the desired position .

The square norm of the control laws applied to the system are shown in Fig. 6.24. This control laws represent the forces in the surge X and heave Z directions.

In Fig. 6.16 the performance of the Frobenius norm of the first two weight matrices

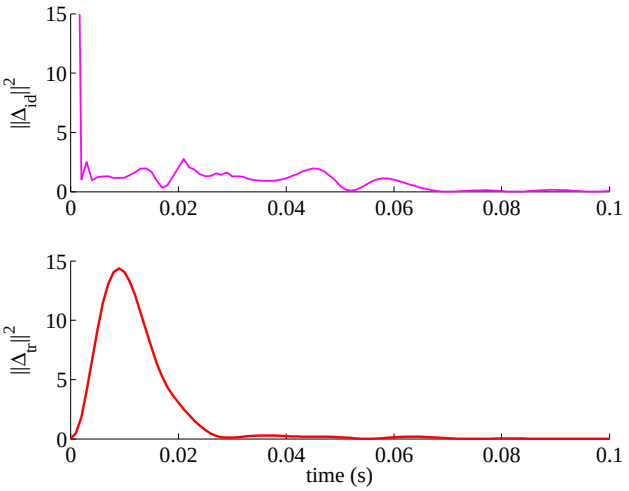

Figure 6.14: Identification error (top) and Trajectory tracking error (bottom).

is shown. These weight matrices can be able to adapt according to the AUV behavior changes during the on-line learning process.

The linear velocities in x and y axis estimated using the super-twisting algorithm are shown in Figs. 6.17 and 6.18. It can be seen that the velocity estimates converges very fast to the real velocities in approximately 0.01 seconds.

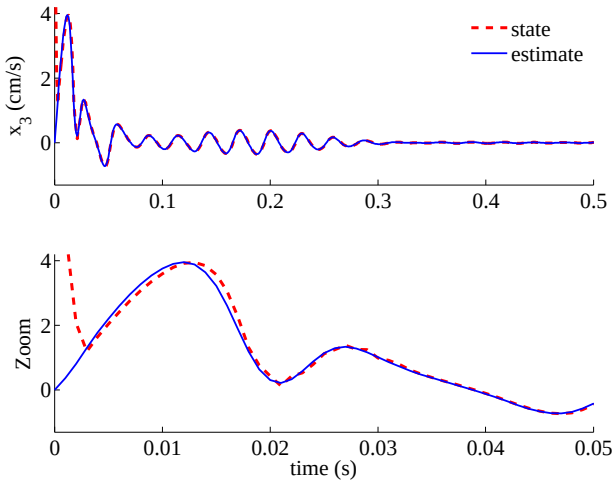

Figure 6.17: Estimation of linear velocity in x-axis by the STA.

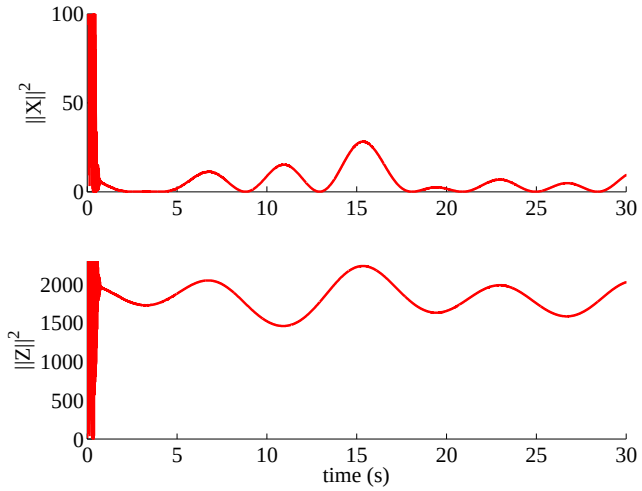

Figure 6.15: Forces in surge (top) and heave (bottom) direction.

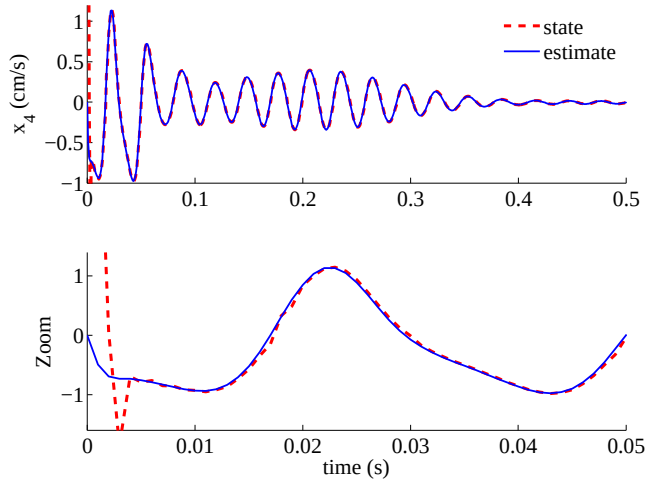

Figure 6.18: Estimation of linear velocity in z-axis by the STA.

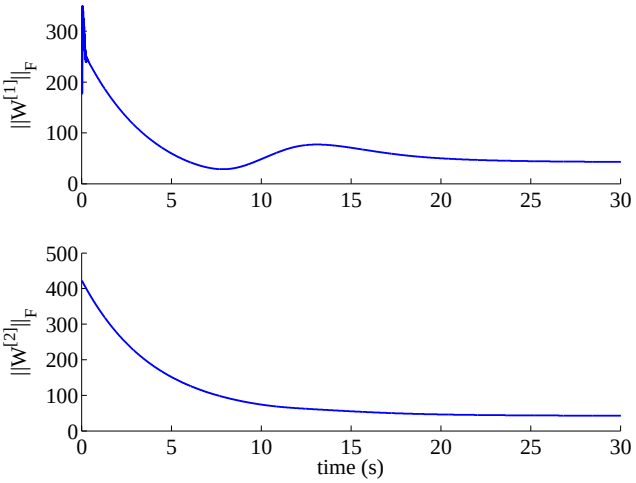

Figure 6.16: Frobenius norm of the weight matrices $W^{[1]}$ of the DNN_1 (top) and $W^{[2]}$ of the DNN_2 (bottom).

6.6 Experimental results

In this section the trajectory tracking problem proposed in section 6.2 is solved by applying a proportional derivative (PD) controller for the real AUV platform. These controllers have the form:

$$X = K_{p,x}\Delta_x + K_{p,x}\frac{d}{dt}\Delta_x \tag{6.4}$$

$$Z = K_{p,z}\Delta_z + K_{p,z}\frac{d}{dt}\Delta_z \tag{6.5}$$

where $\Delta_x = x_{ref} - x$ and $\Delta_z = z_{ref} - z$. The controller uses in the proportional part the AUV x and z positions. The z position is obtained from the pressure sensor, however the AUV is not equipped with any sensor to measure the x position. In general the problem to determine the AUV position underwater represents a great challenge. 7

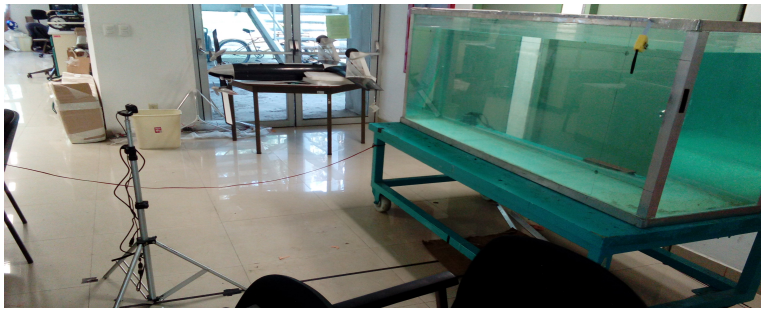

Figure 6.19: Location of the camera.

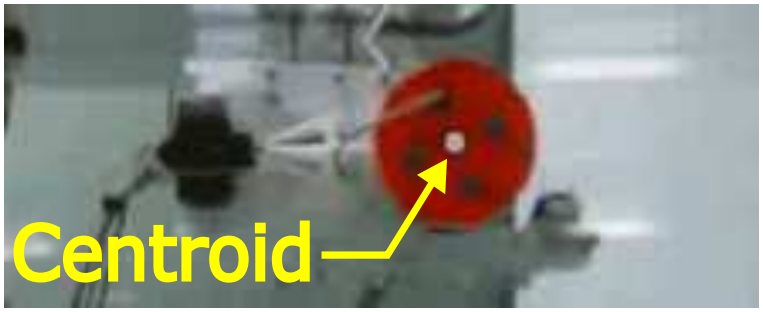

Figure 6.20: Centroid of the red area in the AUV.

In order to overcome this problem a vision algorithm in MATLAB-Simulink using a camera located in front of the tank was implemented to determine the AUV x position as shown in Fig. 6.19. This algorithm detects a red area in the AUV and calculate the centroid position of this area as shown in Fig. 6.20. On the other hand, the linear velocities $\frac{d}{dt}x$ and $\frac{d}{dt}z$ used in the derivative part was obtained by differentiating the x and z positions obtained from the sensors using a second order STA structure.

The experimentation procedure was divided in two stages:

- The first experiment consist of controlling each one of the axis (x and z) separately without the influence of the other in order to perform a 1-D trajectory by the AUV.
- In the second part both controllers acting in each axis was applied to the AUV to perform a 2-D trajectory

6.6.1 Independent tracking control of x and z axes

In this subsection are described the AUV experiments when the vehicle perform 1-D trajectory in the x and z axis separately. The gains of the PD controllers used in the experiment selected by trial and error was: $K_{p,x} = 0.7$, $K_{d,x} = 0.1$ for the x axis and $K_{p,z} = 2.7$, $K_{d,x} = 0.05$ for the z axis.

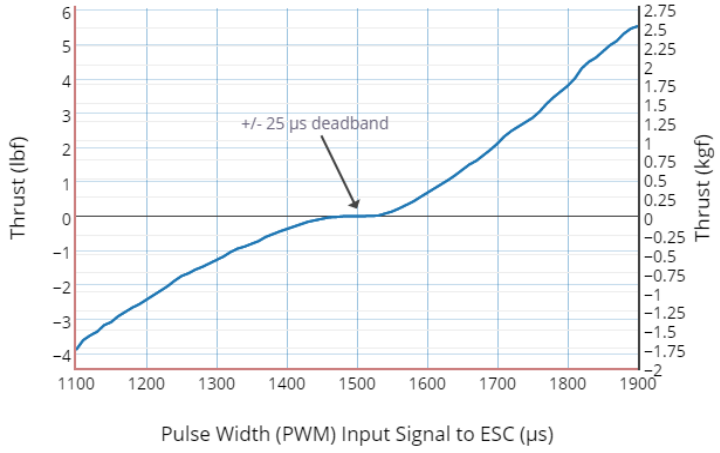

Figure 6.21: Thrust versus PWM input to ESC.

The controller provides a duty cycle in microseconds necessary to move the brushless thrusters used in the vehicle. A graph that relates the thrust versus the PWM input applied to the ESC is shown in Fig. 6.21. From this graph the following can be implied:

- Values above 1500 make the motor to turn rigth (submerge).
- Values below 1500 make the motor to turn left (surface).
- A value of 1500 makes the motor to stop.

As can be seen in Fig. 6.21 the thrusters present a dead-zone nonlinerity that impact tha way the thruster behave when a PMW is applied to it. This dead-zone is approximately between of 1498 and 1550 PWM values where the thrusters do not move. In consequence some constants determined experimentally was added to the

PWM signals provided by the controller to overcome this phenomena in order to have an effective PWM signal to move the thrusters. These constants was selected as $c_{1,x} = 51$ and $c_{2,x} = 12$ for the tracking in x axis and $c_{1,z} = 55$ and $c_{2,z} = 2$ for the tracking in z axis.

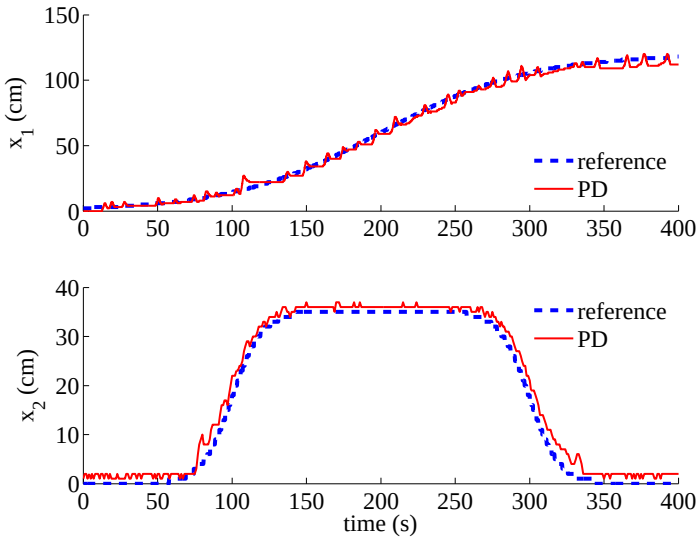

Figure 6.22: Real-time tracking in x-axis (top) and z-axis (bottom) obtained with the PD controller.

The values of the gains of the super-twisting REDs was: $k_{1,x} = k_{1,z} = c$, $k_{2,x} = k_{2,z} = 1.5c^{1/2}$, $c = 2.5$. The gains was selected comparing the linear velocities provided by the STA with those provided by an Euler differentiator. The desired paths are the same as those considered in the Section 6.5.

In Fig. 6.22, the real-time trajectories in x and z axes described by the AUV are shown. It can be seen that the real AUV trajectory oscillates around the desired signals. This oscillations generated are due to the perturbations the AUV is subject. (the source cable attached to the AUV, the water waves inside the tank and the vehicle making contact with the tank walls).

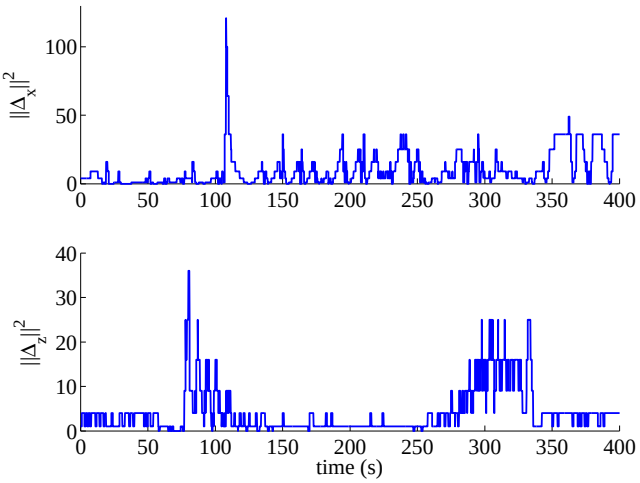

Figure 6.23: Mean-square errors in the x axis (top) and z axis (bottom).

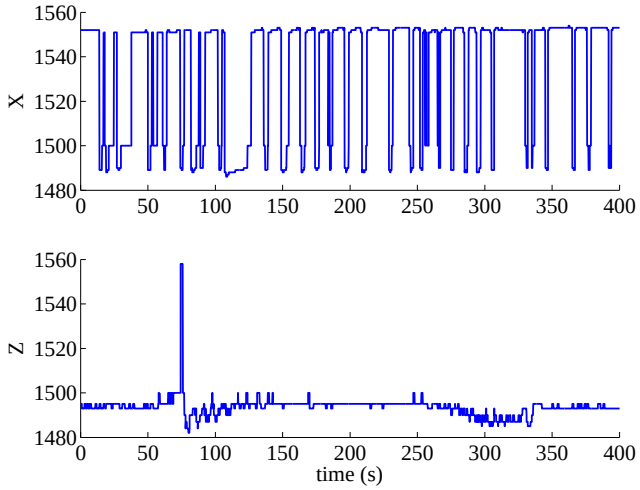

Figure 6.24: PWM control signals applied to the horizontal (top) and vertical (bottom) thrusters.

The errors remains in a region near to zero due the disturbances affecting the vehicle movement as shown in Fig. 6.23. The main disturbances in the experiment was the source cable attached to the vehicle (acting as a spring), the water waves produced by the thrusters and the vehicle making contact with the tank walls.

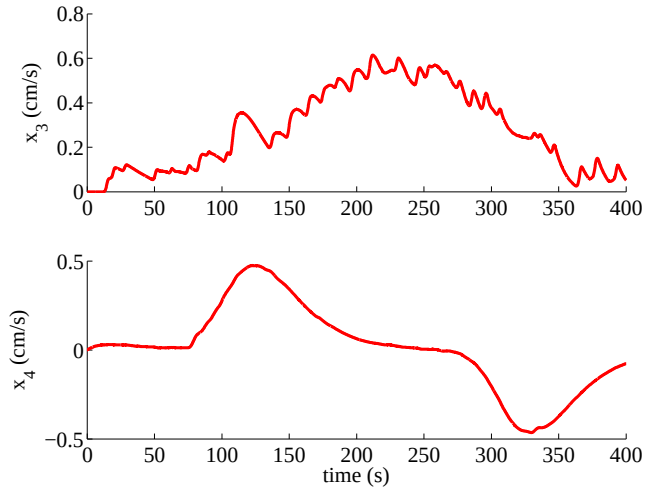

Figure 6.25: Estimation of linear velocities in the x-axis (top) and in the z-axis (bottom) by the STA.

On the other hand, the control signal represent the PWM signals applied to the thrusters in order to move the vehicle to follow the desired trajectory. In Fig. 6.24, it can be seen that the values of the PWM signals necessary to correct the error position represent PWM value variations in a small interval.

In Fig. 6.25, the linear velocities obtained by the STA are shown. These velocities was obtained by filtering the x and z position measurements before applying the RDE and then applying a second filtering in the output of the RDE.

6.6.2 Dependent tracking control of x and z axes

Unlike the previous subsection here we consider the control of the AUV in the x-z plane to perform a 2-D trajectory. The gains of the PD controllers used in this part was: $K_{p,x} = 0.1$, $K_{d,x} = 0.5$ for the x axis and $K_{p,z} = 3.5$, $K_{d,x} = 0.05$ for the z axis. The constants to to avoid the thrusters dead-zone was selected as $c_{1,x} = 51$ and $c_{2,x} = 12$ for the x axis and $c_{1,z} = 55$ and $c_{2,z} = 2$ for the z axis.

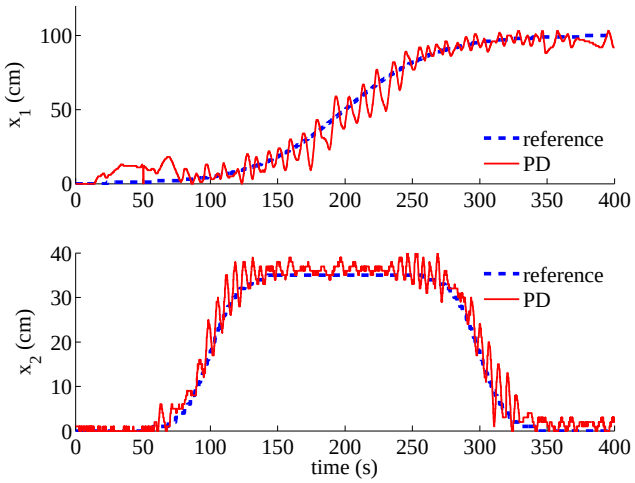

Figure 6.26: Real-time tracking in x-axis (top) and z-axis (bottom) obtained with the PD controller.

In Fig. 6.26 the real-time trajectories in x and z axes described by the AUV acting at the same time are shown. It can be seen that both AUV trajectories present a greater deviation to the desired signal unlike the AUV tracking in Fig. 6.22.

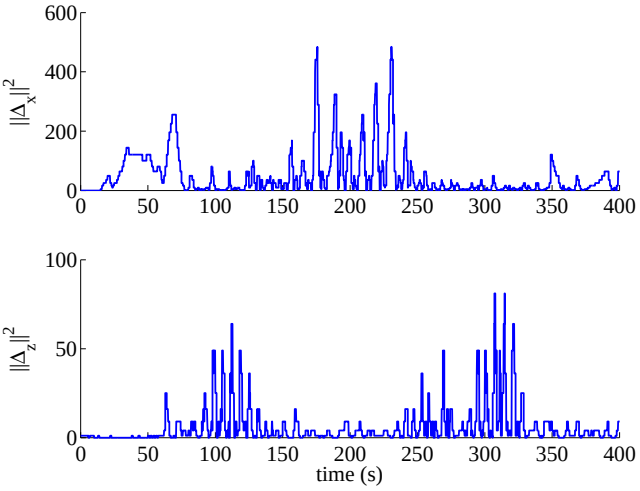

Figure 6.27: Mean-square errors in the x axis (top) and z axis (bottom).

This due to the x and z axes present a coupled behaviour, that is when the vehicle moves forward or backward there exist small displacements upwards or downwards, also when the vehicle moves upward or downward there exist displacements forwards or downwards. Despite this phenomena the vehicle performs an acceptable trajectory tracking.

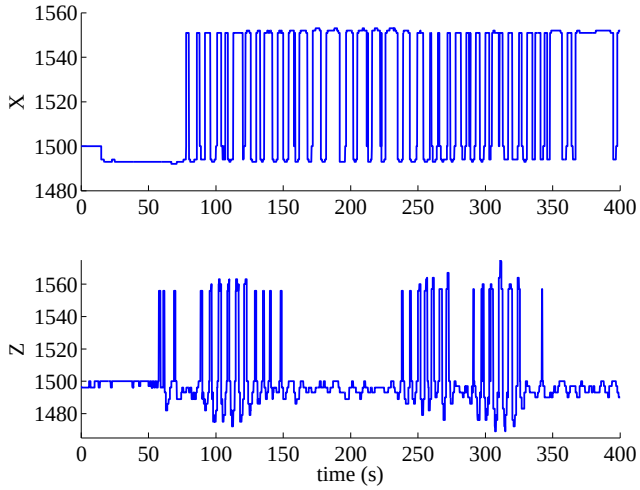

Figure 6.28: PWM control signals applied to the horizontal (top) and vertical (bottom) thrusters.

In consequence of the greater deviation of the AUV trajectories to the desired ones the mean square error is greater than the error depicted in Fig. 6.23, even so the error remains bounded but in a greater region.

The controllers signals in Fig. 6.28 required to correct the position error of the AUV in x and z are still small variations of the PWM signal.

Also the STA provides a similar estimation of the linear velocities as the ones obtained in the previous subsection.

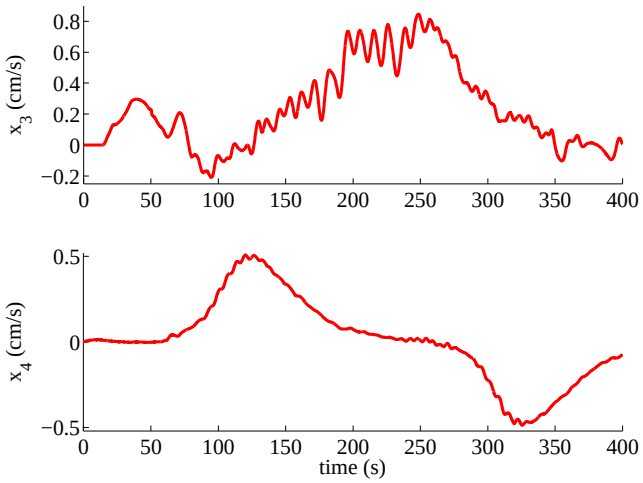

Figure 6.29: Estimation of linear velocities in the x-axis (top) and in the z-axis (bottom) by the STA.

6.7 Conclusions of the chapter

In this chapter the problem of tracking a desired trajectory using the neuro-fuzzy controller designed in Chapter 5 was solved for a particular case of an AUV moving inside a tank of limited space. Due to this fact the problem was reduced to follow a trajectory in the x-z plane by considering a lateral AUV model. The linear velocities used in the controller was provided by a set of RDEs based on the STA. Some numerical results showed the controller is capable to stabilize the tracking errors in a region near to the origin obtaining as a result a good tracking of the desired sigmoid-based functions proposed as desired signals. Also, experimental results was obtained using the real AUV platform described in Section 6.1 implementing a real-time interface designed on MATLAB-Simulink. The experiments was divided in two stages. First, a PD controller to control each axis in one dimension was used. Then, the PD controllers in both axis was implemented at the same time to perform a 2-D trajectory tracking. The z position was determined by a pressure sensor. However determine the x position represent

a problem even more difficult to resolve. To overcome this problem implementing a vision algorithm was implemented to obtain the x position. This task was done by acquiring an image from a camera in front of the tank. The linear velocities in x-z axis used in the controller was provided by the STA since the x and z positions. The same sigmoid functions used in the numerical results was proposed as desired signals. The PD controller showed an acceptable performance tracking x and z desired positions, separately. On the other hand, when both controllers were applied to the AUV at the same time to perform a 2-D trajectory the position error increases in each axis because of the interaction of both controllers acting together. However, the controller objective was reached despite of all the perturbations affecting the real AUV while is moving underwater.

7

General conclusions

In this thesis work a state feedback control and an state observer were designed in this study based on the Lyapunov stability analysis for a T-S fuzzy system. A Lyapunov time-varying function was used to prove the ultimate boundedness of the tracking error. The controller design was supported on the existence of two time-varying matrix RDEs. Numerical simulations showed the superiority of the result obtained compared to the regular control design based on LMIs.

A neuro-fuzzy scheme was developed to identify and control the AUV uncertain nonlinear system. This scheme mixed the use of DNNs to approximate the local dynamics of the nonlinear system in a certain region determined by a set of T-S rules. This two goals was solved using the solution of two RDEs calculated on-line. A Lyapunov function was proposed to prove the existence of an ultimate bounded for the tracking error and to design the laws that adjusted the weights in each neural network. An control algorithms are adaptable in the sense of the system dynamics changes. Simulation results using an AUV system showed superiority compared to standard fuzzy control by tracking a three-dimension desired path.

The problem to follow a trajectory in the x-z plane by AUV model using the neuro-

fuzzy controller was carried out. The linear velocities was provided by a set of RDEs based on the STA. Numerical results showed a good tracking of the desired sigmoid-based functions. Experimental results applying a PD controller with STA showed an acceptable performance tracking x and z desired positions, separately. When x and z are controlled at the same time to perform the position error increases in each axis because of the interaction of both controllers acting together. The controller objective was reached despite of all the perturbations affecting AUV while is moving underwater.

8

Publications

Congress

- Wen Yu, Jorge Cervantes, Sergio Salazar, "Takagi-Sugeno Fuzzy Controller Design Using Riccati Differential Equation", *IEEE World Congress on Computational Intelligence*, Vancouver, 2016.

- Jorge Cervantes, Wen Yu, Sergio Salazar, Isaac Chairez, Rogelio Lozano, "Output Based Backstepping Control for Trajectory Tracking of an Autonomous Underwater Vehicle", *American Control Conference*, Boston, 2016.

Journals

- Jorge Cervantes, Wen Yu, Sergio Salazar, Isaac Chairez, "Takagi-Sugeno Dynamic Neuro-Fuzzy Controller of Uncertain Nonlinear Systems", *IEEE Transactions on Fuzzy Systems*, 2016. (accepted)

- Jorge Cervantes, Wen Yu, Sergio Salazar, Isaac Chairez, "On-line T-S Fuzzy Control Using Riccati Differential Equation", *International Journal of Fuzzy Systems*, 2016.
  (accepted)

- Jorge Cervantes, Wen Yu, Sergio Salazar, Isaac Chairez, "Output Based Takagi-Sugeno Fuzzy Controller of Uncertain Nonlinear Systems", *Fuzzy Optimization and Decision Making, Springer* (submitted)

- Fabrice Le Bars, Elba Antonio, Jorge Cervantes, Carlos De La Cruz, and Luc Jaulin "Estimating the trajectory of low-cost autonomous robots using interval analysis : application to the euRathlon competition", *Journal of Oceanic Engineering.* (submitted)

- Jorge Cervantes, Sergio Salazar, Isaac Chairez, "Adaptive Neuro-Fuzzy Controller-Observer of Uncertain Nonlinear Systems", *IEEE Transactions on Fuzzy Systems.* (in progress)

- Jorge Cervantes, Sergio Salazar, Isaac Chairez, "Adaptive Neuro-Fuzzy Controller of Nonlinear Systems with an Uncertain Part", *IEEE Transactions on Control Systems Technology.* (in progress)

Appendix A1

Proof. In order to prove the tracking error is bounded, we use the following Lyapunov function

$$V(\Delta, t) = \Delta^{\top} P(t) \Delta \tag{8.1}$$

where $P(t)$ is a time-variant positive definite matrix, $P(t) = P^{\top}(t) > 0$. From Eq. (3.10), Eq. (3.5) and Eq. (3.16), the dynamic of the tracking error Δ is

$$\begin{aligned} \frac{d}{dt}\Delta(t) = A(t)x(t) + B(t)[u(t) - v(t)] - B^{\perp}(t)r(t) + \\ \eta(x(t), u(t)) + \xi(x(t), t) \end{aligned} \tag{8.2}$$

Using Eq. (8.2), the derivative of the Lyapunov function in Eq. (8.1) is

$$\begin{aligned} \frac{d}{dt}V(t) = \Delta^{\top}(t)\frac{d}{dt}P(t)\Delta(t) + 2\Delta^{\top}(t)P(t)A(t)x(t) + \\ 2\Delta^{\top}(t)P(t)B(t)u(t) + 2\Delta^{\top}(t)P(t)\eta(x(t), u(t)) + \\ 2\Delta^{\top}(t)P(t)\xi(x(t), t) - 2\Delta^{\top}(t)P(t)B^{\perp}(t)r(t) \end{aligned} \tag{8.3}$$

Using $x = \Delta + x_{ref}$ and Eq. (3.19), Eq. (8.3) becomes

$$\begin{aligned} \frac{d}{dt}V(t) = \Delta^{\top}(t)\frac{d}{dt}P(t)\Delta(t) + \Delta^{\top}(t)\{P(t)[A(t) - B(t)K(t)] + \\ [A(t) - B(t)K(t)]^{\top}P(t)\}\Delta(t) + 2\Delta^{\top}(t)P(t)A(t)x_{ref}(t) + \\ 2\Delta^{\top}(t)P(t)\eta(x(t), u(t)) + 2\Delta^{\top}(t)P(t)\xi(x(t), t) - \\ 2\Delta^{\top}(t)P(t)B^{\perp}(t)r(t) \end{aligned} \tag{8.4}$$

For any matrices $X, Y \in \mathbb{R}^{m\times n}$, they satisfy the following inequality [Poznyak, 2008],

$$X^\top Y + Y^\top X \leq X^\top \Lambda X + Y^\top \Lambda^{-1} Y \tag{8.5}$$

where Λ is a positive definite matrix, $\Lambda = \Lambda^\top > 0$. Now we apply this inequality to the term $2\Delta^\top(t) P(t) A(t) x_{ref}(t)$,

$$\begin{gathered} 2\Delta^\top(t) P(t) A(t) x_{ref}(t) \leq \Delta^\top(t) P(t) A(t) \Lambda_1 A^\top(t) P(t) \Delta(t) + \\ \lambda_{\max}\left(\Lambda_1^{-1}\right) \gamma_{ref} \end{gathered} \tag{8.6}$$

The other cross terms have similar relations. The derivative of the Lyapunov function Eq. (8.4) becomes

$$\begin{gathered} \frac{d}{dt}V(t) \leq \Delta^\top(t)\{\frac{d}{dt}P(t) + P(t)[A(t) - B(t)K(t)] + \\ [A(t) - B(t)K(t)]^\top P(t)\}\Delta(t) + P(t)[A(t)\Lambda_1 A^\top(t) + \Lambda_2 + \Lambda_3]P(t) + \\ 2\lambda_{\max}\left(\Lambda_2^{-1}\right) f_1 * I_{n\times n}\}\Delta(t) + \lambda_{\max}\left(\Lambda_1^{-1}\right)\gamma_{ref} + \lambda_{\max}\left(\Lambda_2^{-1}\right) f_0 + \\ 2\lambda_{\max}\left(\Lambda_2^{-1}\right) f_1 \gamma_{ref} + \lambda_{\max}\left(\Lambda_3^{-1}\right)\gamma_\xi - 2\Delta^\top(t) P(t) B^\perp(t) r(t) \end{gathered} \tag{8.7}$$

Adding and subtracting the term $\alpha V = \alpha \Delta^\top P \Delta$ to Eq. (8.7), and using Eqs. (3.11), (8.7) becomes

$$\begin{gathered} \frac{d}{dt}V(t) \leq \Delta^\top(t)\{\frac{d}{dt}P(t) + P(t)[A(t) - B(t)K(t) + \frac{\alpha}{2}I] + \\ [A(t) - B(t)K(t) + \frac{\alpha}{2}I]^\top P(t)\}\Delta(t) + P(t)[A(t)\Lambda_1 A^\top(t) + \\ \Lambda_2 + \Lambda_3]P(t) + 2\lambda_{\max}\left(\Lambda_2^{-1}\right) f_1 * I_{n\times n}\}\Delta(t) - \alpha V(t) + \lambda_{\max}\left(\Lambda_1^{-1}\right)\gamma_{ref} + \\ \lambda_{\max}\left(\Lambda_2^{-1}\right) f_0 + 2\lambda_{\max}\left(\Lambda_2^{-1}\right) f_1 \gamma_{ref} + \lambda_{\max}\left(\Lambda_3^{-1}\right)\gamma_\xi - \\ 2\Delta^\top(t) P(t) S_1(t) s(x_{ref}(t)) \end{gathered} \tag{8.8}$$

where $S_1(t)$ is defined in theorem 1 statement. Applying Eq. (8.5) to $-2\Delta^\top(t) P(t) S_1(t) s(x_{ref}(t))$,

$$-2\Delta^\top(t) P(t) S_1(t) s(x_{ref}, t) \leq \Delta^\top(t) P(t) S_1 \Lambda_5 S_1^\top P(t) \Delta(t) + \lambda_{\max}\left(\Lambda_5^{-1}\right) L\gamma_{ref} \tag{8.9}$$

Under the assumption on $s(x_{ref}(t), t)$ in Eq. (3.8), and $s(x_{ref,0}, 0) = 0$,

$$\|s(x_{ref}(t), t)\|^2 \leq L_s \gamma_{ref} \tag{8.10}$$

So Eq. (8.8) becomes

$$\frac{d}{dt} V(t) \leq \Delta^\top(t) L(t) \Delta(t) - \alpha V + \beta \tag{8.11}$$

where $\alpha > 0$, $\beta > 0$,

$$L(t) = \frac{d}{dt} P(t) + P(t) A_1(t) + A_1^\top(t) P(t) + P(t) R_1(t) P(t) + Q_1(t) \tag{8.12}$$

where $A_1(t) = A(t) - B(t) K(t) + \frac{\alpha}{2}$, $R_1(t)$ and $Q_1(t)$ are defined in Eq. (3.18). In order to obtain feedback control in Eq. (3.19), the definition $\bar{A}_1(t) = A(t) + \frac{\alpha}{2} I$ is used,

$$L_t = \frac{d}{dt} P(t) + P(t) \bar{A}_1(t) + \bar{A}_1^\top(t) P(t) - P(t) R_1(t) P(t) + Q_1(t) - P(t) B(t) K(t) - K^\top(t) B^\top(t) P(t) + 2P(t) R_1(t) P(t) \tag{8.13}$$

Eq. (8.13) can be formed into the following form

$$L(t) = \bar{L}(t) + \left(\sqrt{2} P(t) B(t) \bar{R}_1^{1/2}(t) - G(t)\right) \left(\sqrt{2} P(t) B(t) \bar{R}_1^{1/2}(t) - G(t)\right)^\top \tag{8.14}$$

where $G(t) = \dfrac{K^{\top}(t)\,\bar{R}_1^{-1/2}}{\sqrt{2}}$ and

$$\bar{L}(t) = \frac{d}{dt}P(t) + P(t)\,\bar{A}_1 + \bar{A}_1^{\top}P(t) - P(t)\,R_1(t)\,P(t) + Q_1(t) - \frac{K^{\top}(t)\,\bar{R}_1^{-1}(t)\,K(t)}{2} \tag{8.15}$$

where $R_1(t) = B(t)\,\bar{R}_1 B^{\top}(t)$. To assure $L(t) = 0$, $\bar{L}(t) = 0$ is needed and

$$K(t) = 2\bar{R}_1(t)\,B^{\top}(t)\,P(t) \tag{8.16}$$

Substitute (8.16) into (8.15) and use $R_1(t) = B(t)\,\bar{R}_1 B^{\top}(t)$ to get

$$\bar{L}(t) = \frac{d}{dt}P(t) + P(t)\,\bar{A}_1 + \bar{A}_1^{\top}P(t) - P(t)\,\hat{R}_1(t)\,P(t) + Q_1(t) \tag{8.17}$$

where $\hat{R}_1(t) = 3R_1(t)$. The conditions $L(t) = 0$ and Eq. (3.9) are Eqs. (3.17) and (3.19). So $L(t) = 0\ \forall t \geq 0$, Eq. (8.11) becomes

$$V(t) \leq -\alpha V(t) + \beta \tag{8.18}$$

Using the comparison principle to solve the differential inequality in Eq. (8.18),

$$V(t) \leq e^{-\alpha t}V(0) + \frac{\beta}{\alpha}\left(1 - e^{-\alpha t}\right). \tag{8.19}$$

The inequality in Eq. (8.19) means

$$\lim_{t\to\infty} \sup V(t) \leq \frac{\beta}{\alpha}$$

According to the concept of ultimate boundedness (based on limit superior operation) theory [Khalil, 2002], after finite time t, the tracking error $\Delta(t)$ remains in a bounded region defined in Eq. (3.20). ■

Appendix A2

Let us define $e(t) = P(t) - P_2$. Using condition (3.23), the definition $H = \begin{bmatrix} H_{11} & H_{12} \\ H_{21} & H_{22} \end{bmatrix}$ and rewriting Riccati equations (3.21) in the Hamiltonian form as

$$-\frac{d}{dt}P(t) = \begin{bmatrix} I & P(t) \end{bmatrix} H(t) \begin{bmatrix} I \\ P(t) \end{bmatrix}$$

$$0 = \begin{bmatrix} I & P_2 \end{bmatrix} H_2 \begin{bmatrix} I \\ P_2 \end{bmatrix}$$

the following can be derived:

$$-\frac{d}{dt}e(t) = \begin{bmatrix} I & e(t) + P_2 \end{bmatrix} H(t) \begin{bmatrix} I \\ e(t) + P_2 \end{bmatrix} \leq$$

$$\left[\begin{bmatrix} I & e(t) \end{bmatrix} + \begin{bmatrix} 0 & P_2 \end{bmatrix}\right] H_2 \left[\begin{bmatrix} I \\ e(t) \end{bmatrix} + \begin{bmatrix} I \\ P_2 \end{bmatrix}\right] =$$

$$\left(A^\top + P_2 R\right) e(t) + e(t)(A - RP_2) - e(t) Re(t) = L(t) - Q(0)$$

where

$$L(t) = \left(A^\top - P_2 R\right) e(t) + e(t)(A - RP_2) - e(t) Re(t) + Q(0)$$

Based on Theorem 3 of [Wimmer, 1985], the term $\left(A^{\top} - P_2 R\right)$ is stable when (A, R) is stabilizable. From (3.22), $e(0) > 0$. By Lemma 1 of [Wimmer, 1985], there exit $Q(0) > 0$ such that $L(0) = 0$. This leads to

$$\frac{d}{dt} e(t) \geq Q(0) > 0.$$

Taking into account that the solution of the RDE with time-varying parameters continuous in time is also a continuous function. The conclusion is that for time $t = 0$, there exists a $\varepsilon > 0$ such that

$$Q(\tau) > 0 \; \forall \tau \in [t, t + \varepsilon].$$

As a result,

$$e(t + \varepsilon) = e(t) + \int_t^{t+\varepsilon} \frac{d}{dt} e(\tau) \, d\tau \geq e(t) + \int_t^{t+\varepsilon} Q(0) \, d\tau \geq e(t) + Q(0) \, \varepsilon > 0$$

that yields to

$$P(\tau) > P_2 \; \forall \tau \in [0, \varepsilon]$$

Iterating this procedure for the next time interval $[\varepsilon, 2\varepsilon]$, the final result in (3.24) is obtained.

Appendix B

Proof. In order to prove the tracking error is bounded, the following Lyapunov function is used

$$V(\Delta_1, \Delta_2, t) = \Delta_1^\top P_1(t)\Delta_1 + \Delta_2^\top P_2(t)\Delta_2 \tag{8.20}$$

where $P_1(t)$, $P_2(t)$ are defined in Theorem 1 statement. From Eqs. (4.5), (4.11) and (4.16), the dynamic of the observation error Δ_1 is

$$\frac{d}{dt}\Delta_1(t) = [A(t) - L(t)C(t)]\Delta_1(t) + \eta(x(t), u(t)) + \xi(x(t), t) - L(t)\delta(x(t)) \tag{8.21}$$

Also from Eqs. (4.11), (4.14) and (4.15), the tracking error is governed by the following dynamics

$$\begin{aligned}\frac{d}{dt}\Delta_2(t) = [A(t) - L(t)C(t)]\hat{x}(t) + B(t)u(t) + L(t)C(t)x(t) + \\ L(t)\delta(x(t)) - T(t)v(t) - T^\perp(t)r(t)\end{aligned} \tag{8.22}$$

Using Eqs. (8.21) and (8.22), the derivative of the Lyapunov function in Eq. (8.20) is

$$\begin{aligned}\frac{d}{dt}V(t) = 2\Delta_1^\top P_1(t)[A(t) - L(t)C(t)]\Delta_1(t) + \\ 2\Delta_1^\top P_1(t)\eta(x(t), u(t)) + 2\Delta_1^\top P_1(t)\bar{\xi}(x(t), t) - 2\Delta_1^\top P_1(t)L(t)\delta(x(t)) + \\ 2\Delta_2^\top P_2(t)[A(t) - L(t)C(t)]\hat{x}(t) + 2\Delta_2^\top P_2(t)B(t)u(t) + \\ 2\Delta_2^\top P_2(t)L(t)C(t)x(t) - 2\Delta_2^\top P_2(t)T(t)v(t) + 2\Delta_2^\top P_2(t)L(t)\delta(x(t)) - \\ 2\Delta_2^\top P_2(t)T^\perp(t)r(t) + \Delta_1^\top(t)\frac{d}{dt}P_1(t)\Delta_1(t) + \Delta_2^\top(t)\frac{d}{dt}P_2(t)\Delta_2(t)\end{aligned} \tag{8.23}$$

Then, applying the time-varying gain feedback control of Eq. (4.21), using $x = \Delta_1 + \Delta_2 + x_{ref}$ and $\hat{x} = \Delta_2 + x_{ref}$, and substituting Eq. (4.6), the differential equation (8.23) becomes

$$\begin{aligned}
\frac{d}{dt}V(t) = \Delta_1^\top(t)\{\frac{d}{dt}P_1(t) + P_1(t)[A(t) - L(t)C(t)] + \\
[A(t) - L(t)C(t)]^\top P_1(t)\}\Delta_1(t) + \Delta_2^\top(t)\{\frac{d}{dt}P_2(t) + \\
P_2(t)[A(t) - B(t)K(t)] + [A(t) - B(t)K(t)]^\top P_2(t)\}\Delta_2(t) + \\
2\Delta_2^\top(t)P_2(t)L(t)C(t)\Delta_1(t) + 2\Delta_2^\top(t)P_2(t)A(t)x_{ref}(t) + \\
2\Delta_1^\top(t)P_1(t)\bar{\xi}(x(t),t) + 2\Delta_1^\top(t)P_1(t)\eta(x(t),u(t)) - \\
2\Delta_1^\top(t)P_1(t)L(t)\delta(x(t)) + 2\Delta_2^\top(t)P_2(t)L(t)\delta(x(t)) - \\
2\Delta_2^\top(t)P_2(t)T(t)\left[T^\top(t)T(t)\right]^{-1}T^\top(t)s(x_{ref},t) - \\
2\Delta_2^\top(t)P_2(t)T^\perp(t)\left[\left(T^\perp(t)\right)^\top T^\perp(t)\right]^{-1}\left(T^\perp(t)\right)^\top s(x_{ref},t)
\end{aligned} \tag{8.24}$$

Considering that for any matrices $X, Y \in \mathbb{R}^{m\times n}$, they satisfy the following inequality [Poznyak, 2008]

$$X^\top Y + Y^\top X \leq X^\top \Lambda X + Y^\top \Lambda^{-1} Y \tag{8.25}$$

where Λ is a positive definite matrix, $\Lambda = \Lambda^\top > 0$, $\Lambda \in \mathbb{R}^{n\times n}$.

Now the inequality in Eq. (8.25) is applied to the term, yielding to

$$-2\Delta_2^\top(t)P_2(t)T(t)\left[T^\top(t)T(t)\right]^{-1}T^\top(t)s(x_{ref}(t),t),$$

$$\begin{aligned}
-2\Delta_2^\top(t)P_2(t)T(t)\left[T^\top(t)T(t)\right]^{-1}T^\top(t)s(x_{ref}(t),t) \leq \\
\Delta_2^\top(t)P_2(t)S_2(t)\Lambda_7 S_2^\top(t)P_2(t)\Delta_2(t) + \lambda_{\max}\left(\Lambda_7^{-1}\right)\|s(x_{ref}(t),t)\|^2
\end{aligned} \tag{8.26}$$

where $S_2(t) = T(t)\left[T^\top(t)T(t)\right]^{-1}T^\top(t)$. Under the assumption that $s(x_{ref}(t),t)$ in Eq. (4.2) is Lipschitz and using Eq. (4.3) the following inequality is satisfied

$$\|s(x_{ref}(t),t)\|^2 \leq L_s\gamma_{ref} \tag{8.27}$$

Then, Eq. (8.26) results in

$$\begin{aligned} -2\Delta_2^\top(t) P_2(t) T(t) \left[T^\top(t) T(t)\right]^{-1} T^\top(t) s(x_{ref}(t), t) \leq \\ \Delta_2^\top(t) P_2(t) S_2(t) \Lambda_7 S_2^\top(t) P_2(t) \Delta_2(t) + \lambda_{\max}\left(\Lambda_7^{-1}\right) L_s \gamma_{ref} \end{aligned} \tag{8.28}$$

The other crossed terms have similar relations. Then, Eq. (8.24) results in

$$\begin{aligned} \frac{d}{dt}V(t) \leq \Delta_1^\top(t) \{\frac{d}{dt}P_1(t) + P_1(t)\left[A(t) - L(t) C(t)\right] + \\ \left[A(t) - L(t) C(t)\right]^\top P_1(t) + P_1(t)\left[L(t) \Lambda_4 L^\top(t) + \Lambda_3 + \Lambda_6\right] P_1(t) + \\ \Lambda_1^{-1} + 3\lambda_{\max}\left(\Lambda_4^{-1}\right)\delta_1 I_{n\times n} + 3\lambda_{\max}\left(\Lambda_6^{-1}\right)\eta_1 I_{n\times n} + \\ 3\lambda_{\max}\left(\Lambda_5^{-1}\right)\delta_1 I_{n\times n}\}\Delta_1(t) + \Delta_2^\top(t)\{\frac{d}{dt}P_2(t) + P_2(t)[A(t) - \\ B(t) K(t)] + \left[A(t) - B(t) K(t)\right]^\top P_2(t) + \\ P_2(t)[S_1(t) \Lambda_1 S_1^\top(t) + A(t) \Lambda_2 A^\top(t) + L(t) \Lambda_5 L^\top(t) + \\ S_2(t) \Lambda_7 S_2^\top(t) + S_3(t) \Lambda_8 S_3^\top(t)] P_2(t) + \\ 3\lambda_{\max}\left(\Lambda_4^{-1}\right)\delta_1 I_{n\times n} + 3\lambda_{\max}\left(\Lambda_6^{-1}\right)\eta_1 I_{n\times n} + \\ 3\lambda_{\max}\left(\Lambda_5^{-1}\right)\delta_1 I_{n\times n}\}\Delta_2(t) + \beta \end{aligned} \tag{8.29}$$

where β is defined in Eq. (7) Adding and subtracting the term αV, Eq. (8.29) becomes

$$\frac{d}{dt}V(t) \leq \Delta_1^\top(t) L_1(t) \Delta_1(t) + \Delta_2^\top(t) L_2(t) \Delta_2(t) - \alpha V(t) + \beta \tag{8.30}$$

where

$$L_1(t) = \frac{d}{dt}P_1(t) + P_1(t) A_1(t) + A_1^\top(t) P_1(t) + P_1(t) R_1(t) P_1(t) + Q_1(t) \tag{8.31}$$

$$L_2(t) = \frac{d}{dt}P_2(t) + P_2(t) A_2(t) + A_2^\top(t) P_2(t) + P_2(t) R_2(t) P_2(t) + Q_2(t) \tag{8.32}$$

where $A_1(t) = A(t) - L(t) C(t) + \frac{\alpha}{2} I_{n\times n}$, $A_2(t) = A(t) - B(t) K(t) + \frac{\alpha}{2} I_{n\times n}$, $R_1(t)$, $R_2(t)$, $Q_1(t)$, $Q_2(t)$ and α is defined in 4.17 and 4.18.

In order to obtain the feedback control gain and observer gain in Eqs. (4.21) and (4.22), the definition $\bar{A}(t) = A(t) + \frac{\alpha}{2} I_{n\times n}$ is used, then

$$\begin{aligned} L_1(t) = \frac{d}{dt}P_1(t) + P_1(t)\bar{A}(t) + \bar{A}^\top(t)P_1(t) - P_1(t)R_1(t)P_1(t) \\ +Q_1(t) - P_1(t)L(t)C(t) - C^\top(t)L^\top(t)P_1(t) + 2P_1(t)R_1(t)P_1(t) \end{aligned} \tag{8.33}$$

$$\begin{aligned} L_2(t) = \frac{d}{dt}P_2(t) + P_2(t)\bar{A}(t) + \bar{A}^\top(t)P_2(t) - P_2(t)R_2(t)P_2(t) + \\ Q_2(t) - P_2(t)B(t)K(t) - K^\top(t)B^\top(t)P_2(t) + 2P_2(t)R_2(t)P_2(t) \end{aligned} \tag{8.34}$$

Eqs. (8.33) and (8.34) can be rewritten into the following form

$$\begin{aligned} L_1(t) = \bar{L}_1(t) + \left(\sqrt{2}P_1(t)L(t)\bar{R}_1^{1/2}(t) - G_1(t)\right) \\ \left(\sqrt{2}P_1(t)L(t)\bar{R}_1^{1/2}(t) - G_1(t)\right)^\top \end{aligned} \tag{8.35}$$

$$\begin{aligned} L_2(t) = \bar{L}_2(t) + \left(\sqrt{2}P_2(t)B(t)\bar{R}_2^{1/2}(t) - G_2(t)\right) \\ \left(\sqrt{2}P_2(t)B(t)\bar{R}_2^{1/2}(t) - G_2(t)\right)^\top \end{aligned} \tag{8.36}$$

where $G_1(t) = \frac{C^\top(t)\bar{R}_2^{-1/2}(t)}{\sqrt{2}}$, $G_2(t) = \frac{K^\top(t)\bar{R}_2^{-1/2}(t)}{\sqrt{2}}$ and

$$\begin{aligned} \bar{L}_1(t) = \frac{d}{dt}P_1(t) + P_1(t)\bar{A}(t) + \bar{A}^\top(t)P_1(t) - P_1(t)R_1(t)P_1(t) + \\ Q_1(t) - \frac{C^\top(t)\bar{R}_1^{-1}(t)C(t)}{2} \end{aligned} \tag{8.37}$$

$$\begin{aligned} \bar{L}_2(t) = \frac{d}{dt}P_2(t) + P_2(t)\bar{A}(t) + \bar{A}^\top(t)P_2(t) - P_2(t)R_2(t)P_2(t) + \\ Q_2(t) - \frac{K^\top(t)\bar{R}_2^{-1}(t)K(t)}{2} \end{aligned} \tag{8.38}$$

where $R_1(t) = L(t)\bar{R}_1(t)L^\top(t)$ and $R_2(t) = B(t)\bar{R}_2(t)B^\top(t)$. To assure that $L_1(t) = 0$, the following must satisfy: $\bar{L}_1(t) = 0$ and $K(t)$ satisfying Eq. (4.22). Also to assure that $L_2(t) = 0$, the following must satisfy: $\bar{L}_2(t) = 0$ and $L(t)$ satisfying Eq. (4.22).

Therefore, if $L_1(t) = 0$, $L_2(t) = 0\ \forall t \geq 0$, then Eq. (8.30) becomes

$$\frac{d}{dt}V(t) \leq -\alpha V(t) + \beta \tag{8.39}$$

Using the comparison method [Khalil, 2002] to solve the differential inequality in Eq. (8.39), one gets

$$V(t) \leq e^{-\alpha t}V(0) + \frac{\beta}{\alpha}\left(1 - e^{-\alpha t}\right). \tag{8.40}$$

Then Eq. (8.40) means

$$\lim_{t\to\infty} \sup V(t) \leq \frac{\beta}{\alpha}$$

According to the concept of ultimate boundedness [Khalil, 2002], after some time t, the tracking error $\Delta_2(t)$ remains in a region defined in Eq. (4.23). □

Remark 18 *The ultimate boundedness concept [Khalil, 2002] considers that the origin* $x = 0$ *may not be an equilibrium point of the perturbed system (4.1), i.e.,* $\bar{\xi}(0,t) = 0$. *So we cannot study stability of the origin as an equilibrium point, nor should we expect the solution of the perturbed system to approach the origin as* $t \to \infty$. *The best we can hope for is that if the perturbation term* $\bar{\xi}(x,t)$ *is small in some sense, then* $x(t) - x_{ref}(t)$ *is ultimately bounded by a small bound; that is,* $\|x(t) - x_{ref}(t)\|$ *will be small for sufficiently large* t.

Remark 19 *In order to prove the stability of several linear systems (**??**) and (4.10) for T-S fuzzy control, there are two popular methods: common Lyapunov function and LMI method. Both of them try to find common stability conditions for all linear systems. This work combines all these linear systems as in Eq. (4.11). Then, it becomes into a linear time-varying system. RDE avoid the solution complexity when the common Lyapunov functions method and LMI method are used.*

■

Appendix C

Proof. Considering the following time-varying Lyapunov function

$$V\left(\Delta_{id}, \Delta_{tr}, \hat{x}, W_{err}^{[i,j]}, t\right) = \Delta_{id}^{\top} P_1(t)\,\Delta_{id} + \Delta_{tr}^{\top} P_2(t)\,\Delta_{tr} + \sum_{j=1}^{R} tr\left\{\left(k^j\right)^{-1}\left[W_{err}^{[i,j]}\right]^{\top} W_{err}^{[i,j]}\right\} \tag{8.41}$$

where $\Delta_{tr} = \hat{x} - x_{ref}$, $x_{ref} = \begin{bmatrix} x_{ref,a} & x_{ref,b} \end{bmatrix}^{\top}$, are the trajectory tracking errors, $W_{err}^{[i,j]}$ is the difference between the weight matrices $W_0^{[i,j]}$ of the nominal system and $W^{[i,j]}$ of the identifier system, i.e., $W_{err}^{[i,j]} = W_0^{[i,j]} - W^{[i,j]}$.

Analysing the term $\left[W_{err}^{[i,j]}\right]^{\top} W_{err}^{[i,j]}$ of Eq. (8.41) the following is obtained

$$\left[W_{err}^{[i,j]}\right]^{\top} W_{err}^{[i,j]} = \left(\left[W_0^{[i,j]} - W_{to}^{[i,j]}(t)\right] + \left[W_{to}^{[i,j]}(t) - W^{[i,j]}(t)\right]\right)^{\top} \left(\left[W_0^{[i,j]} - W_{to}^{[i,j]}(t)\right] + \left[W_{to}^{[i,j]}(t) - W^{[i,j]}(t)\right]\right) < 2\left[W_0^{[i,j]} - W_{to}^{[i,j]}(t)\right]^{\top}\left[W_0^{[i,j]} - W_{to}^{[i,j]}(t)\right] + 2\left[\tilde{W}^{[i,j]}(t)\right]^{\top}\tilde{W}^{[i,j]}(t)$$

where $\tilde{W}^{[i,j]} = W_{to}^{[i,j]} - W^{[i,j]}$ is the error between $W^{[i,j]}$ of the identifier and a known matrix $W_{to}^{[i,j]}$ obtained in the off-line training. Then,

$$tr\left\{(k^j)^{-1}\left[W_{err}^{[i,j]}\right]^{\top} W_{err}^{[i,j]}\right\} < 2tr\left\{(k^j)^{-1}\left[W_0^{[i,j]} - W_{to}^{[i,j]}(t)\right]^{\top}\left[W_0^{[i,j]} - W_{to}^{[i,j]}(t)\right]\right\} + 2tr\left\{(k^j)^{-1}\left[\tilde{W}^{[i,j]}(t)\right]^{\top}\tilde{W}^{[i,j]}(t)\right\}$$

Since $\left[W_0^{[i,j]} - W_{to}^{[i,j]}\right]^\top \left[W_0^{[i,j]} - W_{to}^{[i,j]}\right] \leq \varepsilon I_{p\times p}$, where $I_{p\times p}$ is an identity matrix of $p \times p$, then

$$tr\left\{\left(k^j\right)^{-1}\left[W_{err}^{[i,j]}\right]^\top W_{err}^{[i,j]}\right\} \leq 2\left(k^j\right)^{-1}\varepsilon + 2tr\left\{\left(k^j\right)^{-1}\left[\tilde{W}^{[i,j]}(t)\right]^\top \tilde{W}^{[i,j]}(t)\right\}$$

Then the Lyapunov function (Eq. (8.41)) can be bounded as

$$V\left(\Delta, \hat{x}, \tilde{W}^{[i,j]}, t\right) \leq 2\sum_{j=1}^{R}\left(k^j\right)^{-1}\varepsilon + V^{id}\left(\Delta, \hat{x}, \tilde{W}^{[i,j]}, t\right) \tag{8.42}$$

where

$$\begin{aligned} V^{id}\left(\Delta, \hat{x}, \tilde{W}^{[i,j]}, t\right) = \Delta_{id}^\top P_1(t)\,\Delta_{id} + \Delta_{tr}^\top P_2(t)\,\Delta_{tr} + \\ 2\sum_{j=1}^{R} tr\left\{\left(k^j\right)^{-1}\left[\tilde{W}^{[i,j]}\right]^\top \tilde{W}^{[i,j]}\right\} \end{aligned} \tag{8.43}$$

From Eqs. (5.8), (5.11) and (5.20), the dynamic of the state estimation errors $\Delta_{id,a} = x_a - \hat{x}_a$, $\Delta_{id,b} = x_b - \hat{x}_b$ are governed by the following ODEs:

$$\begin{aligned} \frac{d}{dt}\Delta_{id,a}(t) &= \sum_{j=1}^{R}\alpha^{[i,j]}(t)\left[x_b(t) - \hat{x}_b(t)\right] \\ \frac{d}{dt}\Delta_{id,b}(t) &= \sum_{j=1}^{R}\alpha^{[i,j]}(t)\left(A_1^{[i,j]}x_a(t) + A_2^{[i,j]}x_b(t) + W_0^{[i,j]}\sigma\left(x_a(t), x_b(t)\right)\right) + \\ &\sum_{j=1}^{R}\alpha^{[i,j]}(t)\,\tilde{f}^{[i,j]}(x(t)) + \sum_{j=1}^{R}\alpha^{[i,j]}(t)\,\xi^{[i,j]}(x(t), t) - \\ &\sum_{j=1}^{R}\alpha^{[i,j]}(t)\left[A_1^{[i,j]}\hat{x}_a(t) + A_2^{[i,j]}\hat{x}_b(t) + W^{[i,j]}(t)\,\sigma(\hat{x}(t))\right] \end{aligned} \tag{8.44}$$

Using $\Delta_{id,a} = x_a - \hat{x}_a$, $\Delta_{id,b} = x_b - \hat{x}_b$ as well as (5.17) and then adding the terms $\sum_{j=1}^{R} \alpha^{[i,j]}(t) W_0^{[i,j]} \sigma(\hat{x}(t)) - \sum_{j=1}^{R} \alpha^{[i,j]}(t) W_0^{[i,j]} \sigma(\hat{x}(t))$ and $-\sum_{j=1}^{R} W_{t_0}^{[i,j]}(t)\sigma(\hat{x}(t)) + \sum_{j=1}^{R} W_{t_0}^{[i,j]}(t)\sigma(\hat{x}(t))$. Eq. (8.44) results in

$$\begin{aligned}
\frac{d}{dt}\Delta_{id,a}(t) &= \sum_{j=1}^{R} \alpha^{[i,j]}(t) \Delta_{id,b}(t) \\
\frac{d}{dt}\Delta_{id,b}(t) &= \sum_{j=1}^{R} \alpha^{[i,j]}(t) A_1^{[i,j]} \Delta_{id,a}(t) + \sum_{j=1}^{R} \alpha^{[i,j]}(t) A_2^{[i,j]} \Delta_{id,b}(t) + \\
&\sum_{j=1}^{R} \alpha^{[i,j]}(t) W_0^{[i,j]}(t) \tilde{\sigma}(x(t), \hat{x}(t)) + \sum_{j=1}^{R} \alpha^{[i,j]}(t) \left[W_0^{[i,j]} - W_{to}^{[i,j]}(t)\right] \sigma(\hat{x}(t)) + \\
&\sum_{j=1}^{R} \alpha^{[i,j]}(t) \tilde{W}^{[i,j]}(t) \sigma(\hat{x}(t)) + \sum_{j=1}^{R} \alpha^{[i,j]}(t) \tilde{f}^{[i,j]}(x(t)) + \\
&\sum_{j=1}^{R} \alpha^{[i,j]}(t) \xi^{[i,j]}(x(t), t)
\end{aligned} \tag{8.45}$$

From Eqs. (5.8), (5.11) and (5.20), the dynamic of the state estimation errors $\Delta_{tr,a} = \hat{x}_a - x_{ref,a}$, $\Delta_{tr,b} = \hat{x}_b - x_{ref,b}$ is governed by the following ODEs:

$$\begin{aligned}
\frac{d}{dt}\Delta_{tr,a} &= \sum_{j=1}^{R} \alpha^{[i,j]}(t) \Delta_{tr,b}(t) + \sum_{j=1}^{R} \alpha^{[i,j]}(t) x_{ref,b}(t) - s_a(x_{ref}(t), t) \\
\frac{d}{dt}\Delta_{tr,b} &= \sum_{j=1}^{R} \alpha^{[i,j]}(t) \left[A_1^{[i,j]} \Delta_{tr,a}(t) + A_2^{[i,j]} \Delta_{tr,b}(t)\right] + \\
&\sum_{j=1}^{R} \alpha^{[i,j]}(t) W^{[i,j]}(t) \sigma(\hat{x}(t)) + g(x_a(t)) u(t) + \\
&\sum_{j=1}^{R} \alpha^{[i,j]}(t) \left[A_1^{[i,j]} x_{ref,a}(t) + A_2^{[i,j]} x_{ref,b}(t)\right] - s_b(x_{ref}(t), t)
\end{aligned} \tag{8.46}$$

Considering $\Delta_{id} = \left[\Delta_{id,a}^{\top}, \Delta_{id,b}^{\top}\right]^{\top}$, $\Delta_{tr} = \left[\Delta_{tr,a}^{\top}, \Delta_{tr,b}^{\top}\right]^{\top}$ Eqs. (8.45) and (8.46) can be rewritten as follows

$$\frac{d}{dt}\Delta_{id}(t) = \mathcal{A}(t)\,\Delta_{id}(t) + \mathcal{B}_1\Gamma_1\left(x(t), \hat{x}(t)\right) + \mathcal{B}_1\Xi_1\left(x(t), \hat{x}(t)\right) \tag{8.47}$$

$$\begin{aligned}\frac{d}{dt}\Delta_{tr}(t) = \mathcal{A}(t)\,\Delta_{tr}(t) + \mathcal{B}_1\Gamma_2\left(x(t), \hat{x}(t), u(t)\right) + \mathcal{B}_2\Xi_2\left(x(t), \hat{x}(t)\right) + \\ \mathcal{B}_1\Xi_3\left(x(t), \hat{x}(t)\right)\end{aligned} \tag{8.48}$$

where

$$\mathcal{A}(t) = \begin{bmatrix} 0_{n\times n} & \sum_{j=1}^{R}\alpha^{[i,j]}(t)\, I_{n\times n} \\ \sum_{j=1}^{R}\alpha^{[i,j]}(t)\, A_1^{[i,j]} & \sum_{j=1}^{R}\alpha^{[i,j]}(t)\, A_2^{[i,j]} \end{bmatrix},\ \mathcal{B}_1 = \begin{bmatrix} 0_{n\times n} \\ I_{n\times n} \end{bmatrix},\ \mathcal{B}_2 = \begin{bmatrix} I_{n\times n} \\ 0_{n\times n} \end{bmatrix}$$

$$\Gamma_1(x,\hat{x},t) = \sum_{j=1}^{R}\alpha^{[i,j]}(t)\, W_0^{[i,j]}(t)\,\tilde{\sigma}(x,\hat{x}) +$$

$$\sum_{j=1}^{R}\alpha^{[i,j]}(t)\left[W_0^{[i,j]} - W_{to}^{[i,j]}(t)\right]\sigma(\hat{x}) + \sum_{j=1}^{R}\alpha^{[i,j]}(t)\,\tilde{W}^{[i,j]}(t)\,\sigma(\hat{x}),$$

$$\Gamma_2(x,\hat{x},t) = \sum_{j=1}^{R}\alpha^{[i,j]}(t)\, W^{[i,j]}(t)\,\sigma(\hat{x}) + g(x_a)\,u(t),$$

$$\Xi_1(x,\hat{x},t) = \sum_{j=1}^{R}\alpha^{[i,j]}(t)\,\tilde{f}^{[i,j]}(x) + \sum_{j=1}^{R}\alpha^{[i,j]}(t)\,\xi^{[i,j]}(x,t)$$

$$\Xi_2(x,\hat{x},t) = \sum_{j=1}^{R}\alpha^{[i,j]}(t)\, x_{ref,b} - s_a(x_{ref},t)$$

$$\Xi_3(x,\hat{x},t) = \sum_{j=1}^{R}\alpha^{[i,j]}(t)\left[A_1^{[i,j]}x_{ref,a} + A_2^{[i,j]}x_{ref,b}\right] - s_b(x_{ref},t)$$

The time derivative of the Lyapunov function defined in Eq. (8.43) satisfies

$$\begin{aligned}\frac{d}{dt}V^{id}(t) = 2\Delta_{id}^{\top}(t)\,P_1(t)\,\frac{d}{dt}\Delta_{id}(t) + 2\Delta_{tr}^{\top}(t)\,P_2(t)\,\frac{d}{dt}\Delta_{tr}(t) + \\ \Delta_{id}^{\top}(t)\,\frac{d}{dt}P_1(t)\,\Delta_{id}(t) + \Delta_{tr}^{\top}(t)\,\frac{d}{dt}P_2(t)\,\Delta_{tr}(t) - \\ 4\sum_{j=1}^{R} tr\left\{\left(k^j\right)^{-1}\left[\tilde{W}^{[i,j]}(t)\right]^{\top}\frac{d}{dt}W^{[i,j]}(t)\right\}\end{aligned} \tag{8.49}$$

Substituting Eqs. (8.47) and (8.48) yields to

$$\begin{aligned}\frac{d}{dt}V^{id}(t) = 2\Delta_{id}^{\top}(t)\,P_1(t)\,\mathcal{A}(t)\,\Delta_{id}(t) + 2\Delta_{id}^{\top}(t)\,P_1(t)\,\mathcal{B}_1\Gamma_1(x(t),\hat{x}(t))+\\ 2\Delta_{id}^{\top}(t)\,P_1(t)\,\mathcal{B}_1\Xi_1(x(t),\hat{x}(t))+2\Delta_{tr}^{\top}(t)\,P_2(t)\,\mathcal{A}(t)\,\Delta_{tr}(t)+\\ 2\Delta_{tr}^{\top}(t)\,P_2(t)\,\mathcal{B}_1\Gamma_2(x(t),\hat{x}(t),u(t))+2\Delta_{tr}^{\top}(t)\,P_2(t)\,\mathcal{B}_2\Xi_2(x(t),\hat{x}(t))+\\ 2\Delta_{tr}^{\top}(t)\,P_2(t)\,\mathcal{B}_1\Xi_3(x(t),\hat{x}(t))+\Delta_{id}^{\top}(t)\,\frac{d}{dt}P_1(t)\,\Delta_{id}(t)+\\ \Delta_{tr}^{\top}(t)\,\frac{d}{dt}P_2(t)\,\Delta_{tr}(t) - 4\sum_{j=1}^{R} tr\left\{\left(k^j\right)^{-1}\left[\tilde{W}^{[i,j]}(t)\right]^{\top}\frac{d}{dt}W^{[i,j]}(t)\right\}\end{aligned} \tag{8.50}$$

In order to cancel the known terms and the uncertain system to track the reference states the control law in Eq. (5.29) is proposed. The control law in Eq. (5.29) is suggested with a structure to cancel the not invertible function $g(x_a(t))$. Substituting Eq. (5.29) to Eq. (8.50) we obtain

$$\begin{aligned}\frac{d}{dt}V^{id}(t) = 2\Delta_{id}^{\top}(t)\,P_1(t)\,\mathcal{A}(t)\,\Delta_{id}(t) + 2\Delta_{id}^{\top}(t)\,P_1(t)\,\mathcal{B}_1\Gamma_1(x(t),\hat{x}(t))\\ 2\Delta_{id}^{\top}(t)\,P_1(t)\,\mathcal{B}_1\Xi_1(x(t),\hat{x}(t))+2\Delta_{tr}^{\top}(t)\,P_2(t)\,(\mathcal{A}(t)-\mathcal{B}_1K_{tr})\,\Delta_{tr}(t)-\\ 2\Delta_{tr}^{\top}(t)\,P_2(t)\,\mathcal{B}_1K_{id}\Delta_{id}(t)+2\Delta_{tr}^{\top}(t)\,P_2(t)\,\mathcal{B}_2\Xi_2(x(t),\hat{x}(t))+\\ 2\Delta_{tr}^{\top}(t)\,P_2(t)\,\mathcal{B}_1\Xi_3(x(t),\hat{x}(t)) + \Delta_{id}^{\top}(t)\,\frac{d}{dt}P_1(t)\,\Delta_{id}(t)+\\ \Delta_{tr}^{\top}(t)\,\frac{d}{dt}P_2(t)\,\Delta_{tr}(t) - 4\sum_{j=1}^{R} tr\left\{\left(k^j\right)^{-1}\left[\tilde{W}^{[i,j]}(t)\right]^{\top}\frac{d}{dt}W^{[i,j]}(t)\right\}\end{aligned} \tag{8.51}$$

Considering that for any matrices $X, Y \in \mathbb{R}^{m\times n}$, they satisfy the following inequality [Poznyak, 2008]

$$X^{\top}Y + Y^{\top}X \leq X^{\top}\Lambda X + Y^{\top}\Lambda^{-1}Y \tag{8.52}$$

where Λ is a positive definite matrix, $\Lambda = \Lambda^{\top} > 0$, $\Lambda \in \mathbb{R}^{n\times n}$. Applying the inequality in (8.52) to one of the cross terms of Eq. (8.51) we have

$$\begin{aligned}-2\Delta_{tr}^{\top}(t)\,P_2(t)\,\mathcal{B}_1K_{id}\Delta_{id}(t) \leq \Delta_{tr}^{\top}(t)\,P_2(t)\,\Lambda_1P_2(t)\,\Delta_{tr}(t)+\\ \Delta_{id}^{\top}(t)\,K_{tr}^{\top}\mathcal{B}_1^{\top}\Lambda_1^{-1}\mathcal{B}_1K_{id}\Delta_{id}(t)\end{aligned} \tag{8.53}$$

where $\Lambda_1 \in \mathbb{R}^{2n\times 2n}$.

Applying the same procedure to the rest of the crossterms the Eq. (8.51) and adding and substracting the term $\alpha_B V^{id}$, Eq. (8.51) can be bounded as follows

$$\frac{d}{dt}V^{id}(t) \leq \Delta_{id}^{\top}(t)\, Ric(P_1(t))\Delta_{id}(t) + \Delta_{tr}^{\top}(t)\, Ric(P_2(t))\Delta_{tr}(t)$$
$$-\alpha_B V^{id}(t) + \beta + 2\Delta_{id}^{\top}(t)\, P_1(t)\, \mathcal{B}_1 \sum_{j=1}^{R} \alpha^{[i,j]}(t)\, \tilde{W}^{[i,j]}(t)\, \sigma(\hat{x}(t)) -$$
$$4\sum_{j=1}^{R} tr\left\{ \left(k^j\right)^{-1} \left[\tilde{W}^{[i,j]}(t)\right]^{\top} \frac{d}{dt} W^{[i,j]}(t) \right\} + 2\alpha_B \sum_{j=1}^{R} tr\left\{ \left(k^j\right)^{-1} \left[\tilde{W}^{[i,j]}\right]^{\top} \tilde{W}^{[i,j]} \right\}$$

where α_B is a known positive scalar and β is defined in Theorem 1. The RDEs $Ric(P_1(t))$ and $Ric(P_2(t))$ are defined in Theorem 1 (Eqs (5.27) and (5.28)).

Considering that $x^{\top}y = tr\left\{yx^{\top}\right\} = tr\left\{xy^{\top}\right\}$ where $x, y \in \mathbb{R}^n$, then the term $2\Delta_{id}^{\top}(t)\, P_1(t)\, \mathcal{B}_1 \sum_{j=1}^{R} \alpha^{[i,j]}(t)\, \tilde{W}^{[i,j]}(t)\, \sigma(\hat{x}(t))$ can be rewritten as

$$2\Delta_{id}^{\top}(t)\, P_1(t)\, \mathcal{B}_1 \sum_{j=1}^{R} \alpha^{[i,j]}(t)\, \tilde{W}^{[i,j]}(t)\, \sigma(\hat{x}(t)) =$$
$$2\sum_{j=1}^{R} tr\left\{ \left[\tilde{W}^{[i,j]}(t)\right]^{\top} \alpha^{[i,j]}(t)\, \mathcal{B}_1^{\top} P_1(t)\, \Delta_{id}(t)\, \sigma^{\top}(\hat{x}(t)) \right\}$$

Then,

$$\frac{d}{dt}V^{id}(t) \leq \Delta_{id}^{\top}(t)\, Ric(P_1(t))\Delta_{id}(t) + \Delta_{tr}^{\top}(t)\, Ric(P_2(t))\Delta_{tr}(t) - \alpha_B V^{id}(t) + \beta +$$
$$4\sum_{j=1}^{R} tr\{ \left[\tilde{W}^{[i,j]}(t)\right]^{\top} [\frac{1}{2}\alpha^{[i,j]}(t)\, \mathcal{B}_1^{\top} P_1(t)\, \Delta_{id}(t)\, \sigma^{\top}(\hat{x}(t)) -$$
$$\left(k^j\right)^{-1} \frac{d}{dt} W^{[i,j]}(t) + \frac{\alpha_B}{2}\left(k^j\right)^{-1} \tilde{W}^{[i,j]}(t)]\}$$

Taking equal zero the term

$$\frac{1}{2}\alpha^{[i,j]}(t)\,\mathcal{B}_1^{\top}P_1(t)\,\Delta_{id}(t)\,\sigma^{\top}(\hat{x}(t)) - \left(k^j\right)^{-1}\frac{d}{dt}W^{[i,j]}(t) + \frac{\alpha_B}{2}\left(k^j\right)^{-1}\tilde{W}^{[i,j]}(t) = 0$$

Therefore, the following learning law is obtained

$$\frac{d}{dt}W^{[i,j]}(t) = \frac{1}{2}k^j\alpha^{[i,j]}(t)\,\mathcal{B}_1^{\top}P_1(t)\,\Delta_{id}(t)\,\sigma^{\top}(\hat{x}(t)) + \frac{\alpha_B}{2}\tilde{W}^{[i,j]}(t)$$

Since both RDEs (5.27) and (5.28) admit positive definite solutions, $P_1(t)$ and $P_2(t)$, under adaptive weight adjustment law in Eq. (5.32) we obtain $\frac{d}{dt}V^{id}(t) \leq -\alpha_B V^{id}(t) + \beta$, then, $\lim_{t\to\infty}\sup V^{id}(t) \leq \frac{\beta}{\alpha_B}$. Considering the following

$$\lim_{t\to\infty}\sup V(t) \leq 2\sum_{j=1}^{R}\left(k^j\right)^{-1}\varepsilon + \lim_{t\to\infty}\sup V^{id}(t) \leq 2\sum_{j=1}^{R}\left(k^j\right)^{-1}\varepsilon + \frac{\beta}{\alpha_B} \tag{8.54}$$

It follows from the result presented in Eq. (8.54) that

$$\begin{gathered}\min_t\left\{\lambda_{\min}(P_1(t))\right\}\|\Delta_{id}(t)\|^2 \leq \\ \min_t\left\{\lambda_{\min}(P_1(t))\right\}\|\Delta_{id}(t)\|^2 + \min_t\left\{\lambda_{\min}(P_2(t))\right\}\|\Delta_{tr}(t)\|^2 + \\ \sum_{j=1}^{R} tr\left\{\left(k^j\right)^{-1}\left[W_{err}^{[i,j]}(t)\right]^{\top}W_{err}^{[i,j]}(t)\right\} \leq V(t) \leq 2\sum_{j=1}^{R}\left(k^j\right)^{-1}\varepsilon + V^{id}(t)\end{gathered} \tag{8.55}$$

Eq. (8.55) implies

$$\|\Delta_{id}(t)\|^2 \leq \frac{2\sum_{j=1}^{R}\left(k^j\right)^{-1}\varepsilon + V^{id}(t)}{\min_t\left\{\lambda_{\min}(P_1(t))\right\}}, \quad \|\Delta_{tr}(t)\|^2 \leq \frac{2\sum_{j=1}^{R}\left(k^j\right)^{-1}\varepsilon + V^{id}(t)}{\min_t\left\{\lambda_{\min}(P_2(t))\right\}}$$

Finally, applying the concept of ultimate boundedness [Khalil, 2002], the identification and tracking errors are bounded as in Theorem 1 (Eqs. (5.30) and (5.31)). ■

Appendix D

Output Feedback Tracking Controller Design using Backstepping

Also as a result of the doctorate work a paper that proposed a controller to follow a trajectory by an AUV was developed for the American Control Conference 2016.

Unlike other recent studies in the literature where it is common to use a backstepping algorithm directly on the nonlinear model of the AUV system, the strategy proposed in this work linearises the AUV dynamics applying a kind of nonlinear transformation and a subsystem decomposition. Particularly with regard to the methodology presented in [Repoulias and Papadopoulos, 2006], the work presented here differs in the way the linearisation is applied. In [Repoulias and Papadopoulos, 2006] a linearisation controller is design in order to obtain a quasi-linear AUV system and consequently a backstepping algorithm is implemented. On the other hand, in the present work we linearise the AUV system through the implementation of the backstepping concept in order to reduce the AUV system to a stable linear dynamics. Also, its important to note that most approaches used in the literature use the dynamic model with respect to Body-fixed reference frame, unlike the present work where the controller was designed with respect to the Earth-fixed reference frame. This condition makes possible to obtain a three dimensional location of the AUV. Therefore, the implementation of the common trajectory planning method is avoided.

In general, in order to find a feasible control law it is necessary to have the entire state vector available or at least an estimation. In the AUV control area this issue has been

treated in many different ways [Pettersen and Nijmeijer, 1999b], [Pettersen and Nijmeijer, 1999a], [Refsnes et al., 2006], [Pettersen and Egeland, 1996]. Additionally, in control theory the sliding mode super-twisting structure has been used as a state observer [Floquet and Barbot, 2005], [Salgado et al., 2011], [Davila et al., 2005]. In particular in [Benallegue et al., 2007], [Madani and Benallegue, 2007], a sliding mode observer to approximate unknown quadrotor linear velocities and disturbances is implemented. However, in the work presented here the unknown variables, i.e., the linear velocities of the AUV are estimated using a Robust Exact Differentiator (RED) [Chairez, 2015] where the usual sign function is substituted by a sigmoid one.

This work is organized accordingly to the following structure: Section II describes the class of AUV system used in this study. Section III present the problem statement where the objective of the automatic controller is stated. Section IV is devoted to the design of the aforementioned controller using the mixed output based backstepping form as well as the robust design. Section V shows the results of some numerical simulations where the controller proposed in this study was evaluated. Section VI closes the chapter with some final remarks.

Problem Statement

In this work, the main idea is to perform a trajectory tracking by an AUV, i.e., starting from any arbitrary point in the vehicle movement space, the AUV must asymptotically converge to the desired trajectory. In other words, the AUV trajectory should match with the desired route as close as possible, i.e., the tracking errors between the positions of the desired and actual trajectories should be bounded with an upper bound characterized by the effect of perturbations, namely

$$\limsup_{t\to\infty} \left\| \eta(t) - \eta^d(t) \right\| \leq \beta, \quad \beta > 0$$

$\eta^d = \left[\begin{array}{cccccc} x^d, & y^d, & z^d, & \phi^d, & \theta^d, & \psi^d \end{array} \right]^\top$ is the position and orientation vector of the de-

sired trajectory; x^d, y^d, z^d are the coordinates of the desired position, and ϕ^d, θ^d, ψ^d are orientations in the desired longitudinal, transversal and vertical axes, respectively. Also, η^d is assumed to be twice differentiable. It is important to note that for a real AUV the vector η can be measured using some specialized sensors, for example, the AUV can be equipped with echosounders or sonars to determine the x and y positions, a pressure sensor to determine the z position, and magnetometers to determine the ϕ, θ, ψ positions. The main problem here is to determine linear velocities $\dot{x}$, $\dot{y}$, $\dot{z}$, because, there is no sensor that provides these measurements easily and cheaply. So, the solution is to implement some kind of estimator to obtain these variables with the purpose of using them as part of the control algorithm. Despite de presence of non-holonomic constraints in the AUV movement the controller proposed in this study introduces a different scheme to solve the trajectory tracking problem, i.e., the non-holonomic constraints are considered in the AUV dynamic model.

Control Design

In this section, a methodology that combines a backstepping control and a feedback linearisation method is proposed. In addition, the unknown variables, i.e., the linear velocities of the AUV are estimated using a novel super-twisting sliding mode like structure.

Backstepping and feedback Linearisation Control Laws

To solve the control problem stated in Section II, a backstepping control strategy in combination with a feedback linearisation is used, that is, the nonlinear system is separated into three subsystems. The first one considers the specific dynamics of $x-y$ using $\dot{\psi}$ as virtual input, the second one considers the control of $\dot{\psi}$ to track the virtual controller obtained in the analysis of the first subsystem and finally, the third subsystem is formed only by the dynamic system of z.

Then, applying the concept of backstepping a virtual control is supposed to be available in order to use a feedback linearisation to stabilize the error dynamics of $x-y$

subsystem through the ψ dynamics. The methodology proposed below considers that the AUV model is not affected by disturbances and all the uncertainties are supposed to be known. Also, we consider the assumption of having the complete state vector available.

First, an analysis of the AUV system in the horizontal plane (See Fig. (2.1) presented in Section 2.1) is carried out. We omitted arguments of t to simplify the readability.

Rewriting the x and y dynamics of model presented in Eqs. (2.10) and (2.11) of Section 2.3, it follows

$$\begin{bmatrix} \ddot{x} \\ \ddot{y} \end{bmatrix} = \begin{bmatrix} f_1(\psi, \dot{x}, \dot{y}) \\ f_2(\psi, \dot{x}, \dot{y}) \end{bmatrix} + \begin{bmatrix} g_{1,\psi}(\psi, \dot{x}, \dot{y}) & g_{1,X}(\psi) \\ g_{2,\psi}(\psi, \dot{x}, \dot{y}) & g_{2,X}(\psi) \end{bmatrix} \begin{bmatrix} \dot{\psi} \\ X \end{bmatrix} \tag{8.56}$$

According to the problem statement described in Section III the trajectory tracking errors in x, y and z are defined as $e_x = x - x^d$, $e_y = y - y^d$ and $e_z = z - z^d$, respectively. Then, the tracking error dynamics of e_x and e_y, using the expression in Eq. (8.56), is governed by the following differential equations

$$\begin{bmatrix} \ddot{e}_x \\ \ddot{e}_y \end{bmatrix} = \begin{bmatrix} f_1(\psi, \dot{x}, \dot{y}) \\ f_2(\psi, \dot{x}, \dot{y}) \end{bmatrix} + \begin{bmatrix} g_{1,\psi}(\psi, \dot{x}, \dot{y}) & g_{1,X}(\psi) \\ g_{2,\psi}(\psi, \dot{x}, \dot{y}) & g_{2,X}(\psi) \end{bmatrix} \begin{bmatrix} \dot{\psi} \\ X \end{bmatrix} - \begin{bmatrix} \ddot{x}^d \\ \ddot{y}^d \end{bmatrix} \tag{8.57}$$

Next, using the idea of backstepping method [Khalil, 2002], the angular velocity $\dot{\psi}$ is considered as a virtual control V_1. So, the resultant control vector of the extended system is defined as $V = [V_1, X]^\top$. In order to stabilize the tracking error vector $e_{xy} = [e_x, e_y]^\top$ a control law via a partial (just for x and y dynamics) feedback linearisation [Khalil, 2002] can be implemented considering the assumption stated in Eqs. (2.7) and (2.8) presented in Section 2.3 are known, that is

$$V = G^{-1} \left(\begin{bmatrix} \ddot{x}^d - f_1(\psi, \dot{x}, \dot{y}) \\ \ddot{y}^d - f_2(\psi, \dot{x}, \dot{y}) \end{bmatrix} - K_{p,xy} \begin{bmatrix} e_x \\ e_y \end{bmatrix} - K_{d,xy} \begin{bmatrix} \dot{e}_x \\ \dot{e}_y \end{bmatrix} \right) \tag{8.58}$$

where the state dependent matrix G is given by

$$G := \begin{bmatrix} g_{1,\psi}\left(\psi, \dot{x}, \dot{y}\right) & g_{1,X}(\psi) \\ g_{2,\psi}\left(\psi, \dot{x}, \dot{y}\right) & g_{2,X}(\psi) \end{bmatrix},$$

The controller presented in Eq. (8.58) seems to be a kind of output-based active disturbance Proportional Derivative (PD) rejection form. Considering the specific structure of the elements included in the matrix G, it cannot be inverted only in the case when both velocities $\dot{x}$ and $\dot{y}$ are simultaneously zero. This situation only occurs when the AUV stops completely which is not a reachable situation (by the non-holonomic constrain) during the tracking trajectory problem. Both parameters $K_{p,xy}$, $K_{d,xy}$ are positive scalars and represent the proportional and derivative gains, respectively, of the PD controller. The closed-loop system for e_x and e_y are $\ddot{e}_x = -K_{p,xy}e_x - K_{d,xy}\dot{e}_x$, $\ddot{e}_y = -K_{p,xy}e_y - K_{d,xy}\dot{e}_x$ which are asymptotically stable, i.e., $e_x(t), e_y(t) \to 0$ as $t \to \infty$ by the gain selection proposed above. Finally, the next step of the control procedure is to introduce a new error defined as $e_{V1} = \dot{\psi} - V_1$. This error is introduced to force the angular velocity $\dot{\psi}$ to behave as the virtual control V_1. Its dynamic equation is described by

$$\dot{e}_{V1} = f_4\left(\psi, \dot{\psi}, \dot{x}, \dot{y}, \dot{z}\right) + g_{4,N}N - \dot{V}_1 \tag{8.59}$$

Then, the control input N to stabilize e_{V1} is proposed as follows

$$N = g_{4,N}^{-1}(\dot{V}_1 - f_4(\psi, \dot{\psi}, \dot{x}, \dot{y}, \dot{z}) - K_{V1}e_{V1}) \tag{8.60}$$

where $K_{V1} \in \mathbb{R}^+$ is the proportional gain of the stable dynamics. The term $g_{4,N}$ is a non-zero constant defined in Eq. (2.10) presented in Section 2.3, therefore it is invertible. The closed-loop system for e_{V1} is $\dot{e}_{V1} = -K_{V1}e_{V1}$, then, the error e_{V1} is asymptotically stable, i.e., $e_{V1}(t) \to 0$ as $t \to \infty$. This controller is realizable considering that $g_{4,N}$ is invertible because it is constant and different from zero. In this case the controlled

variable is the angular velocity $\dot{\psi}$.

On the other hand, since the z dynamics in Eq. (2.6) presented in Section 2.3 is partially decoupled from the other system dynamics it can be stabilized separately. The error dynamics e_z is described by

$$\ddot{e}_z = f_3(\dot{z}) + g_{3,Z} Z - \ddot{z}^d \tag{8.61}$$

So, the control input Z, representing the vertical thrust, is proposed as a common feedback linearisation as follows

$$Z = g_{3,Z}^{-1} \left(\ddot{z}^d - f_3(\dot{z}) - K_{p,z} e_z - K_{d,z} \dot{e}_z \right) \tag{8.62}$$

where $K_{p,z}$, $K_{d,z} \in \mathbb{R}^+$ are the proportional and derivative gains, respectively, of the stable dynamics. The term $g_{3,Z}$ is a non-zero constant defined in Eq. (2.9) presented in Section 2.3, therefore it is invertible. The closed-loop system is $\ddot{e}_z = -K_{p,z} e_z - K_{d,z} \dot{e}_z$, then the error e_z is asymptotically stable, i.e., $e_z(t) \to 0$ as $t \to \infty$. Finally, the vector $e = \begin{bmatrix} e_x & e_y & e_z \end{bmatrix}^\top$ converges to zero.

On the controller realization

The main drawback of the proposed controller designed in section IV is the necessity of measuring linear velocities of the AUV. This vehicle is not equipped with a sensor that can measure these velocities. Then, a sliding mode estimator with a super-twisting structure is applied to estimate $\dot{x}$, $\dot{y}$ and $\dot{z}$. This observer is used due to the well-known characteristic that a RED based on super-twisting like converges in finite time. This property allow us to use the estimated states in the controller designed in Section 4 without the necessity of solving a controller-observer system, i.e., the separation principle holds. The super-twisting estimator implemented in this work has a different structure to the one presented in [Levant, 2002, Levant, 2007], because it uses a sigmoid function instead of sign function. This sliding mode estimator has the following

structure [Chairez, 2015]:

$$\begin{aligned} \dot{\gamma}_1(t) &= \gamma_2(t) + k_1 |e_\gamma(t)|^{1/2} s(e_\gamma(t)) \\ \dot{\gamma}_2(t) &= k_2 s(e_\gamma(t)) \end{aligned} \tag{8.63}$$

where $e_\gamma = x_{mes} - \gamma_1$, x_{mes} is the measurable variable (in this case linear positions x, y and z) and $s(e_\gamma)$ is a sigmoid function defined as $s(e_\gamma) = \left(2/\left(1 + e^{-be_\gamma}\right)\right) - 1$. In the case of the angular velocity $\dot{\psi}$, it can be obtained by a gyroscope sensor integrated with the AUV.

Simulation Results

To demonstrate the performance of the proposed output based controller, the AUV model presented in Section 2.3 in Chapter 2 was used. The controller was also evaluated with different reference trajectories. In order to probe the effectiveness of the control law proposed in Eq. (8.58), it is applied to the AUV system in Eq. (8.56) that is affected by disturbances. The disturbed dynamic equations of trajectory tracking errors in the three coordinates are

$$\begin{aligned} \dot{e}_x &= -K_{p,xy}e_x - K_{d,xy}\dot{e}_x + g_{1,E1}(\psi)\tau_{E_1} + g_{1,E2}(\psi)\tau_{E_2} \\ \dot{e}_y &= -K_{p,xy}e_y - K_{d,xy}\dot{e}_y + g_{2,E1}(\psi)\tau_{E_1} + g_{2,E2}(\psi)\tau_{E_2} \\ \ddot{e}_z &= -K_{p,z}e_z - K_{d,z}\dot{e}_z + g_{3,E_3}\tau_{E_3} \end{aligned}$$

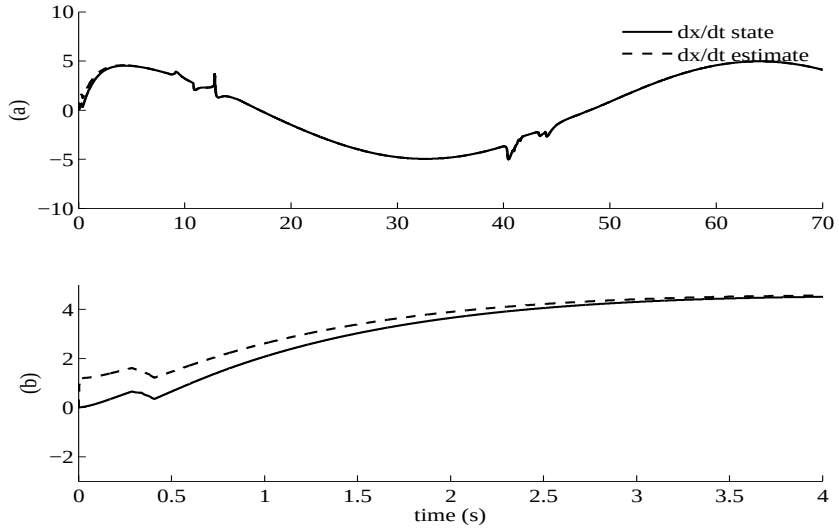

Figure 8.1: RED $\frac{d}{dt}x$ velocity estimation.

In the case of the virtual controller, the error dynamics satisfies the following non-linear differential equation $\dot{e}_{V1} = -K_{V1}e_{V1} + g_{4,E6}\tau_{E_6}$.

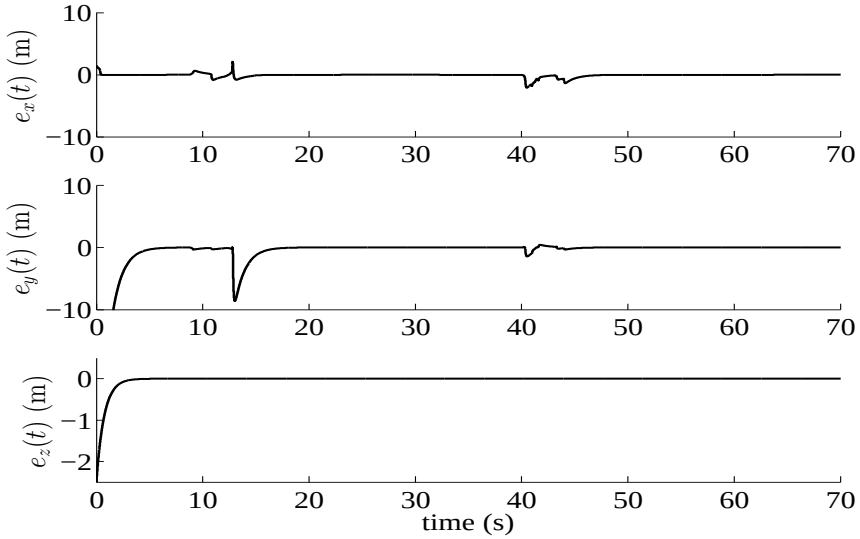

Figure 8.3: Tracking errors with disturbances for circular tracking.

The various system parameters for a typical AUV, used for simulation purposes, are given by $m = 4.28\ kg$, $X_{\dot{u}} = 0.5\ kg/s$, $Y_{\dot{v}} = 0.22\ kg/s$, $Z_{\dot{w}} = 0.3\ kg/s$, $N_{\dot{r}} = 0.4$

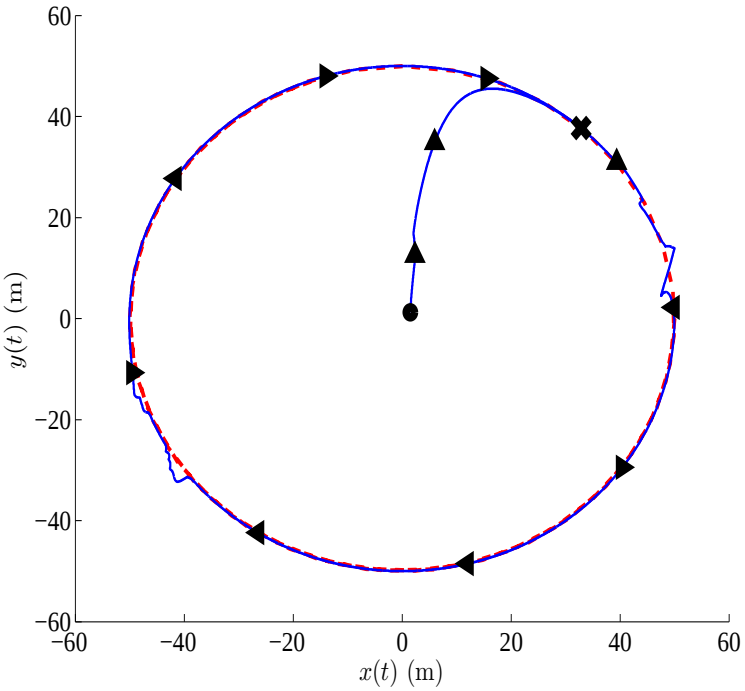

Figure 8.2: AUV reference (dotted line) and actual trayectory (solid line) with disturbances for circular tracking.

kgm^2/s,, $\tau_{D_x}, \tau_{D_y}, \tau_{D_z}, \tau_{D_\psi} = 0.3$, $I_z = 0.04$, $F_{WB} = 41.95$, and the disturbances are considered as $\tau_{E_1}, \tau_{E_2}, \tau_{E_3}, \tau_{E_6} = 0.001 \sin(0.1t)$. The desired trajectory considered here is a constant velocity circular trajectory, that is, $x^d = 50 \sin(0.1t)$, $y^d = 50 \cos(0.1t)$. The desired z position is a constant depth of $z^d = 2.5$. The initial conditions are: $x(0) = 1.5$, $y(0) = 1.2$, $z(0) = 0$, $\psi(0) = \pi/2$, $x_p(0) = 2$, $y_p(0) = 3$, $z_p(0) = 4$, $\psi(0) = 0.5$. It is ensured that the derivatives of at least second order of x^d, y^d, z^d, ψ^d exist. The controller gains used are: $K_{p,xy} = 15$, $K_{d,xy} = 16$, $K_{V1} = 1000$, $K_{p,z} = 20$, $K_{d,z} = 16$. From results depicted in Fig. 8.1, it can be seen the estimation of the linear velocity $\dot{x}$ by the RED proposed in Section IV. The circular tracking simulation results are presented in Fig. 8.2. In Figure 8.3, the trajectory tracking errors after 10 seconds are shown to converge to an acceptable region near the origin. And the z error position goes to zero at approximately 2 seconds. From the results showed in Figure 8.4, it is found that the control solves the tracking trajectory problem even in the disturbed

condition, that is under the presence of disturbances.

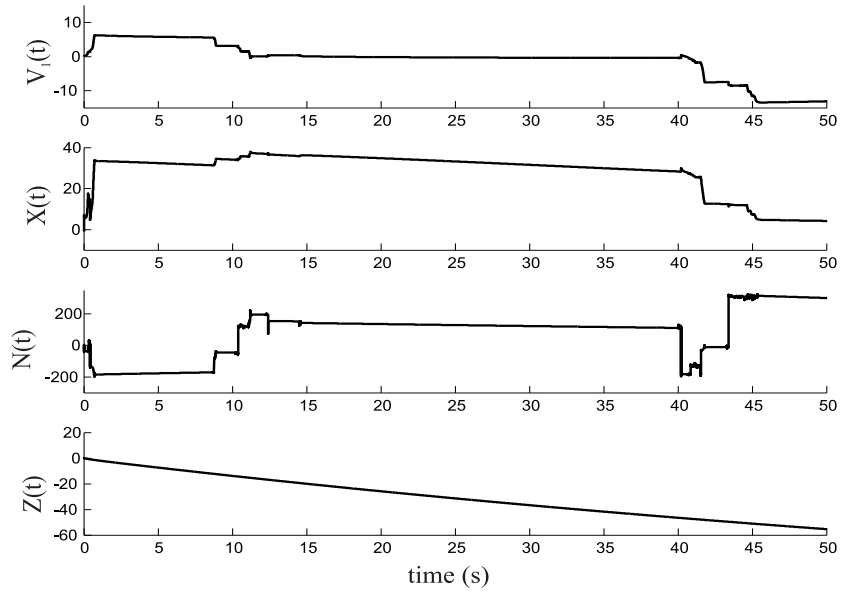

Figure 8.4: Control signals: Virtual control V_1, total surge thrust X, yaw torque N, heave thrust Z for circular tracking.

A number of simulation results have shown that the proposed control scheme performs well in terms of smooth transient response, quick convergence of tracking errors near to the origin, and robustness, even in the case of disturbed conditions. Figure 8.5 demonstrates the tracking between the spiral reference trajectories and the $x - y$ coordinates displayed in the phase-plane, that is, $x^d = t\sin(0.1t)$, $y^d = t\cos(0.1t)$. The initial conditions are: the same as in the circular reference. The controller gains used are: $K_{p,xy} = 10$, $K_{d,xy} = 8$, $K_{V1} = 1000$.

Conclusions

This study showed the design of an automatic control to solve the tracking trajectory problem of an AUV using only the output information. The AUV position was supplied to a set of RED to recover the displacement velocity. The information provided by these differentiators was injected into the controller structure that satisfied a backstepping-like form. Taking into account the finite-time convergence characteristic

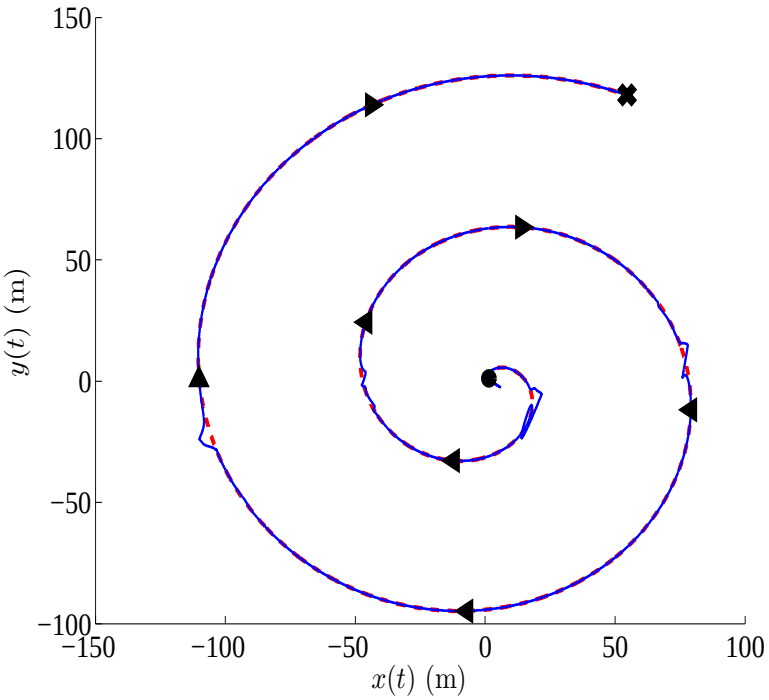

Figure 8.5: AUV reference (dotted line) and actual trajectory (solid line) with disturbances for spiral tracking.

of the super twisting algorithm, the separation principle is fulfilled and there is no the necessity to make a closed-loop stability analysis. The first element of the controller, the angular velocity with respect to the z-coordinate, is considered as virtual controller. Then, this velocity modify the $x - y$ displacement to track a given smooth reference path. The controller developed in this study showed acceptable performance compared to the regular solutions found in the literature accordingly to the numerical simulations developed in this study. This comparison was done assuming the same available information for reported controllers and one obtained in this study.

Bibliography

[Aguiar and Pascoal, 2007] Aguiar, A. P. and Pascoal, A. M. (2007). Dynamic positioning and way-point tracking of underactuated auvs in the presence of ocean currents. *International Journal of Control*, 80(7):1092–1108.

[Ballard, 1987] Ballard, R. (1987). *The Discovery of the Titanic*.

[Banks et al., 2007] Banks, H. T., Lewis, B. M., and Tran, H. T. (2007). Nonlinear feedback controllers and compensators: a state-dependent riccati equation approach. *Journal on Computational Optimization and Applications*, 37(2):177–218.

[Benallegue et al., 2007] Benallegue, A., Mokhtari, A., and Fridman, L. (2007). High-order sliding-mode observer for a quadrotor uav. *International Journal of Robust and Nonlinear Control*, 18(4):427 – 440.

[Bian et al., 2010] Bian, X., Qu, Y., Yan, Z., and Zhang, W. (2010). Nonlinear feedback control for trajectory tracking of an unmanned underwater vehicle. *IEEE International Conference on Information and Automation*, pages 1387–1392.

[Blidberg, 2001] Blidberg, D. (2001). The development of autonomous underwater vehicles (auv): a brief summary. *IEEE International Conference on Robotics and Automation*.

[Buciakowski et al., 2015] Buciakowski, M., Witczak, M., and Theilliol, D. (2015). Robust state estimation and control for nonlinear system with uncertain parameters. *Journal of Physics: Conference Series*, 659(1):012025.

[Cao et al., 1997] Cao, S., Rees, N., and Feng, G. (1997). Analysis and design for a class of complex control systems-part 1: Fuzzy modeling and identification. *Automatica*, 33:1017–1028.

[Chairez, 2009] Chairez, I. (2009). Wavelet differential neural network observer. *IEEE Transactions on Neural Networks*, 20(9):1439 – 1449.

[Chairez, 2013a] Chairez, I. (2013a). Differential neuro-fuzzy controller for uncertain nonlinear systems. *IEEE Transactions on Fuzzy Systems*, 21(2):369–384.

[Chairez, 2013b] Chairez, I. (2013b). Multiple dnn identifier for uncertain nonlinear systems based on takagi-sugeno inference. *Fuzzy Sets and Systems*, 237:118–135.

[Chairez, 2015] Chairez, I. (2015). Smooth approximation of finite-time robust exact differentiation based on sigmoidal functions. *Automatica(submitted)*.

[Chen and Ge, 2015] Chen, M. and Ge, S. (2015). Adaptive neural output feedback control of uncertain nonlinear systems with unknown hysteresis using disturbance observer. *IEEE Transactions on Industrial Electronics*, 62(12):7706–7716.

[Chen et al., 2016] Chen, Z., Li, Z., and Chen, C. L. P. (2016). Adaptive neural control of uncertain mimo nonlinear systems with state and input constraints. *IEEE Transactions on Neural Networks and Learning Systems*, PP(99):1 – 13.

[Cimen, 2008] Cimen, T. (2008). State-dependent riccati equation (sdre) control: A survey. *17th IFAC World Congress*.

[Cotter, 1990] Cotter, N. (1990). The stone-weierstrass theorem and its application to neural networks. *IEEE Transactions on Neural Networks*, 1:290–295.

[Crouch and Pavon, 1987] Crouch, P. E. and Pavon, M. (1987). On the existence of solutions of the riccati differential equation. *Systems and Control Letters*, 9:203–206.

[Cruz et al., 2014] Cruz, D., Luviano-Juarez, A., and Chairez, I. (2014). Output sliding mode controller to regulate the gait of gecko-inspired robot. *Congreso Latinoamericano de Control Automatico*, pages 558–563.

[Curtin and Bellingham, 2001] Curtin, T. and Bellingham, J. (2001). Autonomous ocean-sampling networks. *IEEE Journal of Oceanic Engineering*, 26:421–423.

[Davila et al., 2005] Davila, J., Fridman, L., and Levant, A. (2005). Second-order sliding-mode observer for mechanical systems. *IEEE Transactions on Automatic Control*, 50(11):1785 – 1789.

[Egeland and Dalsmo, 1996] Egeland, O. and Dalsmo, M. (1996). Feedback control of a nonholonomic underwater vehicle with constant desired configuration. *International Journal of Robotics Research*, 15(1):24 –35.

[Elmokadem et al., 2015] Elmokadem, T., Zribi, M., and Youcef-Toumi, K. (2015). *Trajectory tracking sliding mode control of underactuated AUVs*, volume 84.

[Esfandiari et al., 2015] Esfandiari, K., Abdollahi, F., and Talebi, H. A. (2015). Adaptive control of uncertain nonaffine nonlinear systems with input saturation using neural networks. *IEEE Transactions on Neural Networks and Learning Systems*, 26(10):2311–2322.

[Eski and Yildirim, 2014] Eski, I. and Yildirim, S. (2014). Design of neural network control system for controlling trajectory of autonomous underwater vehicles. *International Journal of Advanced Robotic Systems*, 11(7):1–17.

[Fantoni and Lozano, 2002] Fantoni, I. and Lozano, R. (2002). *Non-linear Control for Underactuated Mechanical Systems*. Springer-Verlag.

[Floquet and Barbot, 2005] Floquet, T. and Barbot, J. P. (2005). Super twisting algorithm based step-by-step sliding mode observers for nonlinear systems with unknown inputs. *International Journal of Systems Science*, 38(10):803–815.

[Fossen, 2002] Fossen, T. I. (2002). *Marine Control Systems*. Marine Cybernetics.

[Gaccia and Veruggio, 2000] Gaccia, M. and Veruggio, G. (2000). Guidance and control of a reconfigurable unmanned underwater vehicle. *Control Engineering Practice*, 8:21–37.

[Griffiths and Edwards, 2003] Griffiths, G. and Edwards, I. (2003). Auvs: designing and operating next generation vehicles. *Elsevier Oceanography Series*, 69:229–236.

[He-ming et al., 2012] He-ming, J., Wen-long, S., and Zi-yin, C. (2012). Nonlinear backstepping control of underactuated auv in diving plane. *Advances in information Sciences and Service Sciences*, 4(9):214–221.

[Hermann and Krener, 1977] Hermann, R. and Krener, A. (1977). Nonlinear controllability and observability. *IEEE Transactions on Automatic Control*, 22(5):728 – 740.

[Horgan and Toal, 2006] Horgan, J. and Toal, D. (2006). Review of machine vision applications in unmanned underwater vehicles. *9th International Conference on Control, Automation, Robotics and Vision*.

[Husa and Fossen, 1997] Husa, K. E. and Fossen, T. I. (1997). Backstepping designs for nonlinear way-point tracking of ships. *Proceedings of the 4th IFAC Conference on Manoeuvring and Control of Marine Craft*.

[Jain and Bhasin, 2015] Jain, A. K. and Bhasin, S. (2015). Adaptive tracking control of uncertain nonlinear systems with unknown input delay. In *2015 IEEE Conference on Control Applications (CCA)*, pages 1686–1691.

[Joe et al., 2014] Joe, H., Kim, M., and cheol Yu, S. (2014). Second-order sliding-mode controller for autonomous underwater vehicle in the presence of unknown disturbances. *Nonlinear Dynamics*, 78(1):183–196.

[Joh et al., 1998] Joh, J., Chen, Y.-H., and Langari, R. (1998). On the stability issues of linear takagi-sugeno fuzzy models. *IEEE Transactions Fuzzy Systems*, 6:402–410.

[Khalil, 2002] Khalil, H. K. (2002). *Nonlinear Systems.* Prentice Hall, third edition.

[Kilicaslan and Banks, 2010] Kilicaslan, S. and Banks, S. (2010). Existence of solutions of riccati differential equations for linear time varying systems. *Existence of solutions of riccati differential equations for linear time varying systems*, 134:1586–1590.

[Kilicaslan and Banks, 2012] Kilicaslan, S. and Banks, S. (2012). Existence of solutions of riccati differential equations. *Dynamical Systems Measurement and Control*, 134(3):031001–1 – 031001–11.

[Kim, 2015] Kim, D. (2015). Robust adaptive fuzzy output feedback control strategy for uncertain perturbed nonlinear system. In *2015 IEEE Conference on Control Applications (CCA)*, pages 101–106.

[Kinsey and Whitcomb, 2007] Kinsey, J. C. and Whitcomb, L. L. (2007). Model-based nonlinear observers for underwater vehicle navigation: Theory and preliminary experiments. *IEEE International Conference of Robotics and Automation.*

[Kondoa and Ura, 2004] Kondoa, H. and Ura, T. (2004). Navigation of an auv for investigation of underwater structures. *Control Engineering Practice*, 12:1551–1559.

[Kucera, 1972] Kucera, V. (1972). A contribution to matrix quadratic equations. *IEEE Transactions on Automatic Control*, 17(3):344–347.

[Kumar and Subudhi, 2014] Kumar, B. and Subudhi, S. B. (2014). Adaptive tracking control of an autonomous underwater vehicle. *International Journal of Automation and Computing*, 11(3):299–307.

[Kunusch, 2003] Kunusch, C. (2003). Identificacion de sistemas dinamicos. *Universidad Nacional de la Plata Tech Rep.*, La Plata Argentina.

[Lakhekar and Waghmare, 2015] Lakhekar, G. and Waghmare, L. (2015). Dynamic fuzzy sliding mode control of underwater vehicles. *Advances and Applications in Sliding Mode Control systems, Studies in Computational Intelligence*, 576:279–304.

[Latombe, 1991] Latombe, J.-C. (1991). *Robot Motion Planning*, volume 124 of *The Springer International Series in Engineering and Computer Science*. Springer US.

[Levant, 2002] Levant, A. (2002). *Sliding Mode Control in Engineering*, chapter High Order Sliding Modes. Marcel Dekker.

[Levant, 2007] Levant, A. (2007). Finite differences in homogeneous discontinuous control. *IEEE Transactions on Automatic Control*, 52(7):1208–1217.

[Li and Li, 2004] Li, N. and Li, S.-Y. (2004). Stability analysis and design of t-s fuzzy control system with simplified linear rule consequent. *IEEE Transactions Systems Science & Engineering, Human-Machine Systems, Cybernetics, B, Cybern.*, 34(1):799–795.

[Lin et al., 2004] Lin, C., Wang, Q.-G., and Lee, T.-H. (2004). Output tracking control for nonlinear systems via t-s fuzzy model approach. *IEEE Transactions Systems Science & Engineering, Human-Machine Systems, Cybernetics*, 36(2):450–457.

[Ljung, 1999] Ljung, L. (1999). *System Identification Theory For the User*. Prentice Hall.

[Lygouras et al., 1998] Lygouras, J., Lalakos, K., and Tsalides, P. (1998). Thetis: an underwater remotely operated vehicle for water pollution measurements. *Microprocessors and Microsystems*, 22(5):227–237.

[Madani and Benallegue, 2007] Madani, T. and Benallegue, A. (2007). Sliding mode observer and backstepping control for a quadrotor unmanned aerial vehicles. *American Control Conference*, pages 5887 – 5892.

[Nakamura and Savant, 1992] Nakamura, Y. and Savant, S. (1992). Nonlinear tracking control of autonomous underwater vehicle. *IEEE International Conference on Robotics and Automation*, pages A4 –A9.

[Osorio et al., 1997] Osorio, A., Poznyak, A. S., and Taksar, M. (1997). Robust deterministic filtering for linear uncertain time-varying systems. *American Control Conference*, pages 2526–2530.

[Perez, 2005] Perez, T. (2005). *Ship Motion Control*. Advances in Industrial Control. Springer-Verlag London, 1 edition.

[Pettersen and Egeland, 1996] Pettersen, K. and Egeland, O. (1996). Position and attitude control of an underactuated autonomous underwater vehicle. *IEEE Conference on Decision and Control*, 1:987 – 991.

[Pettersen, 1996] Pettersen, K. Y. (1996). *Exponential stabilization of underactuated vehides*. PhD thesis, Department of Engineering Cybernetics, Norwegian University of Science and Tecnology.

[Pettersen and Nijmeijer, 1998a] Pettersen, K. Y. and Nijmeijer, H. (1998a). Global practical stabilization and tracking for an underactuated ship - a combined averaging and backstepping approach. *In Proccedings IFAC Conference on System Struciure and Control*, pages 59–64.

[Pettersen and Nijmeijer, 1998b] Pettersen, K. Y. and Nijmeijer, H. (1998b). Tracking control of an underactuated surface vessel. in proccedings. *37th IEEE Conference on Decision and Control*, pages 4561–4566.

[Pettersen and Nijmeijer, 1999a] Pettersen, K. Y. and Nijmeijer, H. (1999a). *Output feedback tracking control for ships. In Lecture Notes in Control and Information Science 244, New Directions in Nonlinear Observer Design*. Springer.

[Pettersen and Nijmeijer, 1999b] Pettersen, K. Y. and Nijmeijer, H. (1999b). Passive nonlinear observer design for ships using lyapunov methods: Full scale experiments with a supply vessel. *Automatica*, 35(1).

[Polyakov and Poznyak, 2011] Polyakov, A. and Poznyak, A. (2011). Invariant ellipsoid method for minimization of unmatched disturbances effects in sliding mode control. *Automatica*, 47(7):1450–1454.

[Poznyak et al.,] Poznyak, A., Escobar, J., and Shtessel, Y. Stochastic sliding modes identification.

[Poznyak, 2008] Poznyak, A. S. (2008). *Advanced Mathematical Tools for Automatic Control Engineers, Volume 1: Deterministic Techniques*. 1st edition.

[Poznyak et al., 2004] Poznyak, A. S., Fridman, L., and Bejarano, F. J. (2004). Minimax integral sliding-mode control for multimodel linear uncertain systems. *IEEE Transactions on Automatic Control*, 49(1):97–102.

[Poznyak et al., 2001] Poznyak, A. S., Sanchez, E. N., and Yu, W. (2001). *Differential Neural Networks for Robust Nonlinear Control (Identification, State Estimation and Trajectory Tracking)*. World Scientific.

[Raimondi and Melluso, 2010] Raimondi, F. and Melluso, M. (2010). Hierarchical fuzzy/lyapunov control for horizontal plane trajectory tracking of underactuated auv. *IEEE International Symposium on Industrial Electronics (ISIE)*, pages 1875 – 1882.

[Refsnes et al., 2006] Refsnes, J. E., Pettersen, K. Y., and Sorensen, A. J. (2006). Observer design for underwater vehicles with angle and position measurement. *IFAC World Congress Manoeuvring and Control of Marine Craft*.

[Refsnes et al., 2008] Refsnes, J. E., Sorensen, A. J., and Pettersen, K. Y. (2008). Model-based output feedback control of slender-body underactuated auvs: Theory and experiments. *IEEE Transaction on Control System Technology*, 16(5):930–946.

[Reid, 1972] Reid, W. T. (1972). *Riccati Differential Equations*, volume 86 of *Mathematics in Science and Engineering*. Academic Press Inc.

[Repoulias and Papadopoulos, 2006] Repoulias, F. and Papadopoulos, E. (2006). Planar trajectory planning and tracking control design for underactuated auvs. *Ocean Engineering*, 34:1650–1667.

[Rezazadegan and Shojaei, 2013] Rezazadegan, F. and Shojaei, K. (2013). An adaptive control scheme for 6-dof control of an auv using saturation functions. *3rd International Conference on Intelligent Computational Systems*, pages 67–72.

[Rife and Rock, 2002] Rife, J. and Rock, S. (2002). Field experiments in the control of a jellyfish tracking rov. *MTS/IEEE Oceans*, 4:2031–2038.

[Salgado et al., 2011] Salgado, I., Chairez, I., Moreno, J., Fridman, L., and Poznyak, A. (2011). Generalized super-twisting observer for nonlinear systems. *IFAC World Congress*.

[Sasagawa, 1982] Sasagawa, T. (1982). On the finite escape phenomena for matrix riccati equations. *IEEE Transactions on Automatic Control*, 27:977–979.

[Smallwood et al., 1999] Smallwood, D., Bachmayer, R., and Whitecomd, L. (1999). A new remotely operated underwater vehicle for dynamics and control research. *Proceedings UUST*.

[Smallwood and Whitcomb, 2004] Smallwood, D. and Whitcomb, L. (2004). Model-based dynamic positioning of underwater robotic vehicles: theory and experiment. *IEEE Journal of Oceanic Engineering*, 29(1):169–186.

[Takagi and Sugeno, 1985] Takagi, T. and Sugeno, M. (1985). Fuzzy identification of systems and its applications to modeling and control. *IEEE Transactions on Systems, Man and Cybernetics*, SMC-15(1):116–132.

[Tanaka and Wang, 2001] Tanaka, K. and Wang, H. O. (2001). *Fuzzy Control Systems Design and Analysis: A Linear Matrix Inequality Approach.* Wiley.

[Teodorescu and Vandenplas, 2015] Teodorescu, C. S. and Vandenplas, S. (2015). A robust optimal nonlinear control for uncertain systems: Application to a robot manipulator. In *2015 IEEE Conference on Control Applications (CCA)*, pages 953–959.

[Tivey et al., 1998] Tivey, M., Johnson, H.; Bradley, A., and Yoerger, D. (1998). Thickness of a submarine lava flow determined from near-bottom magnetic field mapping by autonomous underwater vehicle. *Geophysical Research Letters*, 25:805–808.

[Tuan et al., 2001] Tuan, H. D., Apkarian, P., Narikiyo, T., and Yamamoto, Y. (2001). Parameterized linear matrix inequality techniques in fuzzy control system design. *IEEE Transactions Fuzzy Systems*, 9:324–332.

[Viana and Chairez, 2010] Viana, L. and Chairez, I. (2010). Improved dnn identifier based on takagi-sugeno fuzzy systems. *International Conference on Electrical Engineering, Computing Science and Automatic Control*, 1:122–127.

[von Alt, 2003] von Alt, C. (2003). Autonomous underwater vehicles. *Autonomous underwater Langrangian platforms and sensors workshop.*

[W. Yu, 2004] W. Yu, X. L. (2004). Fuzzy identification using fuzzy neural networks with stable learning algorithms. *IEEE Transactions on Fuzzy Systems*, 12(3):411–420.

[Wang and Wang, 2014] Wang, X. and Wang, J. (2014). Neurodynamics-based model predictive control for trajectory tracking of autonomous underwater vehicles. *Advances in Neural Networks*, 8866:184–191.

[Wernli, 2001] Wernli, R. (2001). Low cost auvs for military applications: Is the technology ready in pacific.

[Willcox et al., 2001] Willcox, S., Vaganay, J., Grieve, R., and Rish, J. (2001). The bluefin bpauv: An organic widearea bottom mapping and mine-hunting vehicle. *Proceedings UUST*.

[Willems, 1971] Willems, J. C. (1971). Least squares optimal control and algebraic riccati equations. *IEEE Transactions on Automatic Control*, 16:621–634.

[Williams, 2004] Williams, C. (2004). Auv systems research at the nrc-iot: an update. *International Symposium on Underwater Technology*, pages 59–73.

[Wilson and Bales, 2006] Wilson, R. and Bales, J. (2006). Development and experience of a practical pressure-tolerant, lithium battery for underwater use, ,. *Oceans*, pages 1–5.

[Wimmer, 1985] Wimmer, H. K. (1985). Monotonicity of maximal solutions of algebraic riccati equations. *System and Control Letters*, 5:317–319.

[Xie et al., 2013] Xie, D., Wang, Z., and Zhang, W. (2013). Attitude controller for reentry vehicles using state-dependent riccati equation method. *Journal of Central South University*, 20(7):1861–1867.